Fatigue Behaviour of Filled Polypropylene

Master Thesis

of

Markus Grinschgl, BSc

Institute of Materials Science and Testing of Plastics

Supervisors: Ao.Univ.-Prof. Dipl.-Ing. Dr.mont. Gerald Pinter

O.Univ.-Prof. Dipl.-Ing. Dr.mont. Reinhold W. Lang

Supervisor in Abu Dhabi: Univ.-Prof. Dr. Tahar Nabil Tarfa

Assessment: Ao.Univ.-Prof. Dipl.-Ing. Dr.mont. Gerald Pinter

DECLARATION OF AUTHORSHIP

I certify that the work presented here is, to the best of my knowledge and belief, original and the result of my own investigations, except as acknowledged.

Leoben, Nov. 2009 Markus Grinschgl

ACKNOWLEDGEMENT

I want to thank everyone who supported me during my work on this Master Thesis.

I especially want to thank:

Prof. Dipl.-Ing. Dr.mont. Gerald Pinter, for his kind supervision and support and for the possibility to write my final thesis at the Institute of Materials Science and Testing of Plastics, University of Leoben, Austria.

Univ.-Prof. Tahar Nabil Tarfa from the department of Mechanical Engineering of the Petroleum Institute of Abu Dhabi, who made it possible for me to do the main part of the work for this thesis at the Petroleum Institute of Abu Dhabi in the United Arab Emirates.

Prof. Dipl.-Ing. Dr.mont. Reinhold W. Lang for the assessment of the work as well as for the help with the organisation of this collaboration between the University of Leoben, the Petroleum Institute of Abu Dhabi and the Borealis Polyolefine GmbH Linz, Austria.

Michael Jerabek from the Borealis group and Borealis in general for providing the specimens and financial support.

Melina Mirales from the Petroleum Institute of Abu Dhabi, for help with the scanning electron microscope.

ABSTRACT

The goal of this work is the characterisation of polypropylene (PP) composites with different fillers (glass spheres, talc, olefin thermoplastic elastomer (TPO)) and different filler contents with regard to their fatigue behaviour. The specimens were provided by Borealis (Borealis Polyolefine GmbH Linz, Austria) and had previously been tested for their monotonic mechanical properties at the University of Leoben, Austria.

The development of the material damage and creep during a stress-controlled fatigue test was observed and evaluated by Wöhler curves (S-N curves), hysteresis measurements and isocyclic stress-strain diagrams. The isocyclic stress strain diagrams can provide information about irreversible damage accumulation caused by fatigue as well as reversible viscoelastic effects.

Pre-tests were run with a PP with 30 w% glass-spheres in order to evaluate the best testing parameters and the influence of the hysteretic heating on the fatigue behaviour. These tests already showed that hysteretic heating is a major problem and significantly influences the results. The specimens were cooled by air-ventilation during the tests to avoid this influence.

When compared to the talc and glass filled composites, the pure PP and the PP filled with thermoplastic elastomer showed a higher degree of hysteretic heating, caused by the lower modulus. This caused thermal fatigue, especially at higher load levels. These two materials also showed a ductile fracture (necking). Therefore their fatigue behaviour cannot be compared with that of the talc and glass filled materials, which showed a brittle fracture.

A big influence of the filler type and the content of filler (3.5 and 7 v%) on the fatigue behaviour between the talc filled materials and the materials filled with glass spheres could not be found in the S-N curves. However, differences could be found in the development of the dynamic modulus and the sacant modulus. These changes in the moduli, which were found by hysteresis measurement, indicate that both, creep and damage, occur in a significant range.

KURZFASSUNG

Ziel dieser Arbeit ist die Charakterisierung des Ermüdungsverhaltens von Polypropylen (PP) Composites mit verschiedenen Füllstoffen (Glaskugeln, Talk, Thermoplastisches Elastomer auf Olefinbasis (TPO)) und Füllstoffanteilen. Die Prüfkörper wurden von Borealis (Borealis Polyolefine GmbH Linz, Österreich) zur Verfügung gestellt und sind an der Montanuniversität Leoben, Österreich bezüglich ihrer mechanischen Eigenschaften in monotonen Zugversuchen geprüft worden.

In dieser Arbeit wurde das Ermüdungsverhalten der verschiedenen Composites anhand von Wöhlerkurven (S-N Diagrammen), Hysteresis-Messung und isozyklischen Spannungs-Dehnungs-Diagramme verglichen. Isozyklische Spannungs-Dehnungs-Diagramme können Auskunft über irreversible Schadensakkumulation (verursacht durch Ermüdung) aber auch über reversible viskoelastische Effekte geben.

Um geeignete Testparameter und Testbedingungen festzulegen und den Einfluss der hysteretischen Erwärmung auf das Ermüdungsverhalten festzustellen, wurden Vorversuche mit einem gefüllten Polypropylen (gefüllt mit 30 w% Glaskugeln) gemacht. Bei diesen Versuchen stellte sich bereits heraus, dass die hysteretische Erwärmung bei einer Prüffrequenz von 5 Hz die Prüfkörpertemperatur stark beeinflusst und somit einen großen Einfluss auf das Werkstoffverhalten während des Ermüdungsversuches hat. Um diesen Einfluss zu vermeiden wurden die Prüfkörper während der Versuche mit Ventilatoren gekühlt.

Im Vergleich zu den Materialien gefüllt mit Talk und Glas, zeigten das ungefüllte PP und das PP gefüllt mit TPO eine stärkere hysteretische Aufheizung. Diese beiden Materialien zeigten einen duktilen Bruch (mit Necking) wohingegen die mit Talk und Glas gefüllten Materialien Sprödbruch aufwiesen.

Bei den mit Talk und Glas gefüllten Typen konnten bezüglich der S-N Kurven kaum Unterschiede zwischen den verschieden Füllstoffen und den verschiedenen Füllstoffgehalten gefunden werden. Dagegen konnten klare Unterschiede in den Modulverläufen aufgezeigt werden.

CONTENT

1 INTRODUCTION AND AIMS

Since the advantages of commodity polymeric materials (e.g. of the polyolefins polyethylene (PE) and polypropylene (PP)) like the low price and the low weight, as well as easy processing and wide ranged possibilities of processing are obvious, the range to use this type of materials is unrivalled. A further advantage of these materials is the ease with which the properties can be increased or changed by filling them with small particles of other materials, e.g. talc, glass or other types of polymer. The addition of these small particles with a size of just a few micrometers has little or no influence on the processing, e.g. injection moulding. Compared with high performance composites like long fibre strengthened polymers, with their complicated and time consuming processing technologies, this is a big advantage.

With both the increasing knowledge of the properties of polymeric materials and the increasing range of properties due to the development of new materials and new composite materials, these materials have become more and more interesting for applications which had been occupied by metallic materials until very recently. The new materials show big advantages compared to metals, especially for modes of transport like planes and cars. The fact that the weight of a vehicle plays an important role in the fuel consumption in automotive applications is one of the main advantages of polymers and their composites. With their low density of up to one eighth of that of steel, a replacing of metallic materials in vehicles with polymers can contribute to a decrease in fuel costs and air pollution by reducing the overall weight of a vehicle (Talib et al., 2009; Sapuan et al. 2002). But the use in these areas brings new challenges. One of these is the exposure to vibrations, which are caused by the engine, acceleration, deceleration or a rough road (Ren 2001). The range of possibilities for PP and PP-composites is increasing rapidly due to the many new inventions in the area of fillers, modifiers and additives. The good UV-resistance and the good colourability mean they are also being used more and more often in automotive trims (Balow, 2003).

Polymeric materials are being used increasingly in the automotive industry. Because of their exposure to the vibrations that occur with this application, it is

important to have an idea of the behaviour and the change in the mechanical properties (e.g. the stiffness) of the materials used during a cyclic load.

The goal of this work was to compare the fatigue behaviour of different types of low performance polypropylene composites, depending on the type and content of filler particles. The data was evaluated by S-N-curves (S...stress level; N...cycle number at fracture) as well as by hysteresis measurement and the relatively new evaluation method of isocyclic stress-strain diagrams (ISSDs).

The results of the fatigue testing of materials with a relatively low modulus can easily be influenced by an increase of the temperature during the test. This is caused by thermal heating. In order to avoid this influence as far as possible, adequate testing parameters were determined with a series of pre-tests.

The data acquisition programs were written in Matlab to get the values needed (e.g., dynamic modulus, damping, ISSDs) from the data collected by the MTS-system.

2 BACKGROUND

2.1 Fillers

A good definition of fillers can be found in (Wypych, 1999). Fillers are described as a solid material that can change the properties (both chemical and physical properties) of a material by interactions with this material or by its own inherent properties.

Fillers are becoming more and more important for improving the properties of plastics as well as for reducing the costs. Filler materials can influence the mechanical properties (modulus, tensile-strength, etc) as well as other properties like material density, optical properties, colour, surface properties, product shape (shrinkage, warpage, etc.), thermal properties, electrical properties, magnetically properties, permeability, chemical reactivity, rheology and morphology (Wypych, 1999). Filled polymers find applications in different areas, e.g. pipes with cost saving filler (Calcium carbonate filled PE or PP), impact resistant window frames (elastomer filled polyvinyl chloride (PVC)), flame-resistant and flame-retardant polymers for applications in cars and in electronic equipment (e.g. magnesium-hydroxide filled PP) or improvement of the mechanical properties like modulus and tensile-strength (e.g. talc or short-fibre filled thermoplastic). The electrical properties of polymers are also adjustable, for example with carbon black (to avoid a static charge of floorings) or carbon nanotubes.

Talc was first used as a filler for PP in the 1960s. Talc filled PP was used for fan shrouds and blades in the automotive industry (Balow, 2003). The main advantage of filling with talc is the increase in the stiffness, although it also has a positive influence on the heat distortion temperature, the impact resistance and the scratch resistance (Wypych, 1999). The addition of 20 w% of talc as filler can increase the tensile modulus of PP from around 1350 MPa to around 2750 MPa (Balow, 2003). When used for application in composites, talc is white and powdered with a particle size of 1.4 to 19 µm. It demonstrates a platy particle shape with an aspect ratio of 5 – 20. Its density is between 2.7 and 2.85 g/cm3 (Wypych, 1999).

The big advantage of glass spheres is their spherical form. This form causes a better stress distribution in the vicinity of the filler particles. The relatively uniform

stress distribution is essential for the mechanical properties and can reduce the sensitivity concerning micro-cracks compared to other filler shapes. Glass spheres can improve the material properties like the hardness and the stiffness. They are also useful for decreasing the viscosity of the melt (Wypych, 1999).

2.2 Composites

Osswald and Menges (2003) divided fillers into two groups: The group of fillers that reinforce the polymer and improve the mechanical properties, and the group of fillers that are used to save the amount of polymer used by filling space (also called “extenders”). Polymers that contain fillers to improve the mechanical properties are called composites.

In composites, the different mechanical properties of the filler and the matrix (polymer) are combined. Examples of composites are talc filled polymers or fibre-reinforced polymers. They combine the advantages of polymeric materials (light weight, easy processing, etc) with special properties of other materials, for example the high mechanical properties of glass or carbon fibres. In particular, long-fibre reinforcements lead to materials that can compete with metals (e.g., carbon fibre-, aramid fibre- or glass fibre composites). Their mechanical properties like stiffness and tensile strength are superior, but with the added advantage of a significantly lower density.

The composites can be divided into two categories (Oswald and Menges, 2003):

- Low performance composites
- High performance composites

Low performance composites consist of a matrix and strengthening filler. The matrix is a polymeric material, and the filler consists of small particles (a few µm in size) of a material that is different from the matrix (e.g. glass spheres, talc, short glass fibres). These filled materials can be processed like unfilled materials, which is the big advantage of low performance composites compared to high performance composites.

If someone talks about composites, the long-fibre-reinforced polymers are usually being referred to; the so-called “high performance composites”. These composites consist of a matrix (mostly thermosets) which surrounds the load-carrying

continuous (“endless”), orientated fibres of, e.g., carbon, aramid or glass. In general, the fraction of fibres, the orientation and the binding to the matrix of the fibres specify the mechanical properties of the part. This can lead to parts that show mechanical properties comparable with metal parts with the advantage of lower weight. The isotropic character of such long fibre composites can lead to parts which take into account the different mechanical requirements in the different directions of operational demands. Therefore their use in aeronautic, shipbuilding and special automotive applications is strongly increasing.

2.3 Fatigue in general

A lot of mechanical parts are exposed to continually changing loads in their lifetime. In certain circumstances this changing load can cause a failure or a building of micro fractures at stress levels that are significant lower than the tensile strength. This phenomenon is called fatigue. In general it is caused by the slow growing of cracks or the building of micro cracks. The fatigue behaviour depends on a lot of different parameters. The operating conditions have a particularly large influence on the fatigue behaviour of mechanical parts. The type of the cyclic load (maximum, minimum, frequency, load form), the geometry of the mechanical part and the application temperature are only some of the most important factors which have a great influence on the occurrence of fatigue. The application temperature and other environmental influences can further amplify the fatigue damage. Polymers in particular show a big change in their mechanical properties with a relatively low change in temperature. The fatigue can be caused by different types of load: for example torsion, axial or bending (Moet and Aglan, 2005).

Two types of fatigue are distinguished: low cycle fatigue (“LCF”, fracture after a cycle-number in the region below 10^4 or 5 x 10^4 cycles) and high cycle fatigue (“HCF”, fracture between 10^4 – 10^7 cycles and more) (Bolotin, 1999). The so-called Woehler curve, shows the stress-level (S) (maximum stress σ_{max}, stress amplitude or mean stress σ_{mean}) over the number of cycles until break (N).

In general, the result of standardised fatigue tests with standardised specimens can only compare different materials in their fatigue behaviour. The fatigue life of real mechanical parts cannot be directly derivated from such tests because the geometry plays a very important role in the fatigue of materials, and the fatigue

load in real conditions cannot be simulated with tests on specimens with a one-dimensional load (in most cases). Further, the uniform testing conditions like the good-natured sine load and the uniformness of the load concerning the maximum stress, the R-factor and the frequency are idealisations that can rarely be found in the real nature of applications.

2.4 Characterisation of fatigue-behaviour

To ensure a comparability of the results of fatigue tests, the load conditions like frequency, R (ratio of minimum load σ_{min} and maximum load σ_{max}) and form of the load should be the same for all tests. The most common load for fatigue tests is a cyclic, sinusoidal load with constant borders σ_{min} and σ_{max}. There are different types of load concerning the algebraic sign of the load with different R:

$0<R<1$: cyclic load in the region of tensile (tension-tension)

$R>1$: cyclic load in the region of compression (compression-compression)

$R\leq 0$: cyclic load that goes over tensile and compression

$R=-1$: symmetric load over positive and negative load

These three types of testing show significantly different lifetimes in certain materials and also show different types of damage (especially in composites) (compare Zahnt, 2003). For example, creep plays a large role in some materials during tests under tension-tension conditions.

2.4.1 S-N diagrams

One way to illustrate the fatigue behaviour of a material is an S-N Diagram (also called Woehler curve). It shows the relationship between the number of cycles until failure (N) and the stress level of the applied cyclic load (S) (Figure 2.1). These Woehler curves are very useful for the characterisation of the lifetime under fatigue conditions and are specially used at high cycle fatigue (HCF).

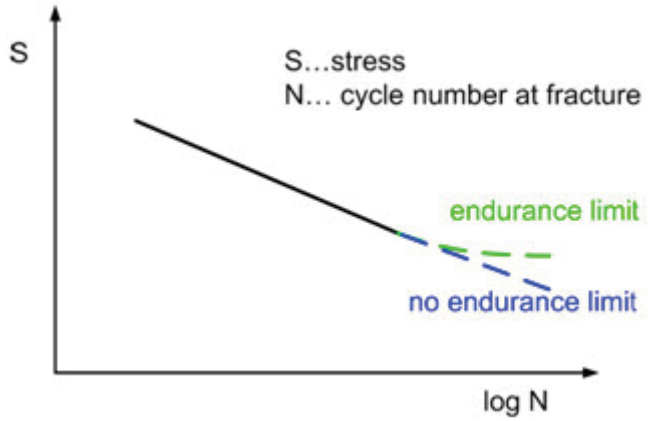

Figure 2.1: S-N curve (Wöhler curve), (Roesler, 2007)

Roesler et al. (2007) describe an endurance limit that can be characterised by a horizontal coasting of the S-N curve at high cycle numbers. This horizontal coasting is called also the fatigue limit and occurs at the S-N curves of some materials (compare Figure 2.1). Among the polymers we can find materials that show an endurance limit (e.g. polyethylene (PE), polypropylene (PP), polymethyl methacrylate (PMMA), epoxy (EP)) and others that do not (e.g. polyethylene terephthalate (PET)). No failure occurs below this endurance limit until at least 10^7 cycles (A. Moet and Aglan H., 2005).

2.4.2 Hysteresis measurement

The strain signal shows a phase shift to the signal of the applied sinusoidal stress (compare Figure 2.2), caused by the viscoelastic behaviour of polymers. This causes a hysteresis in the stress-strain diagram. While the test runs in the region of linear viscoelastic and the load has a sinusoidal form and a constant frequency, the hysteresis has an elliptical shape. This ellipse can be analysed based on the location in the stress-strain diagram, the slope and the area inside the hysteresis. This method has already been described for the case of the evaluation of the dynamic behaviour of PP/EPDM- and PP/POE-blends (Raue and Ehrenstein, 1998). If the hysteresis does not have an elliptical shape, the form of the shape can also give information about the state of the material regarding damage (Zahnt, 2003; Raue Ehrenstein, 1998).

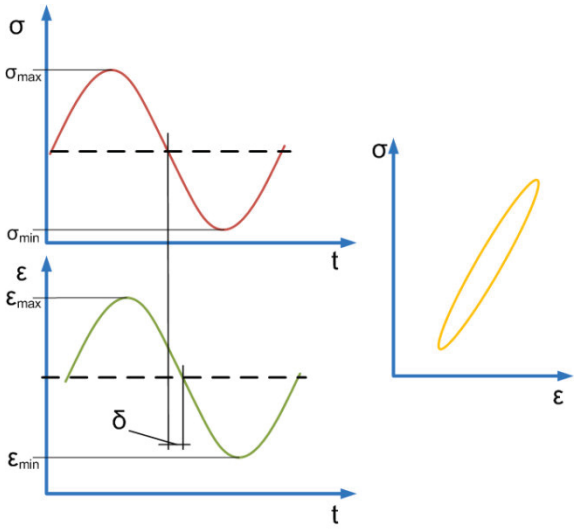

Figure 2.2: Phase shift between stress and strain at cyclic loading of polymeric materials.

2.4.2.1 Dynamic and secant modulus

Two parameters are important when obtaining information about the behaviour of the material tested during a fatigue test. These two parameters are the dynamic modulus and the secant modulus (Raue and Ehrenstein, 1998; Schulte, 1993) (see Equations 2.1 and 2.2 and Figure 2.3).

$$E_{sec} = \frac{\sigma_{max}}{\varepsilon_{max}} \tag{2.1}$$

$$E_{dyn} = \frac{\sigma_{max} - \sigma_{min}}{\varepsilon_{max} - \varepsilon_{min}} \tag{2.2}$$

where E_{sec} is the secant modulus, E_{dyn} is the dynamic modulus. For σ_{max}, σ_{min}, ε_{max}, and ε_{min} compare Figure 2.3. A decrease of E_{dyn} during the fatigue test is a sign of increasing fatigue damage of the material. On the other hand, E_{sec} also includes the creep of the material. A comparison of the change in E_{sec} and E_{dyn} can give interesting information about the appearance of damage and creep during the fatigue test (Zahnt, 2003).

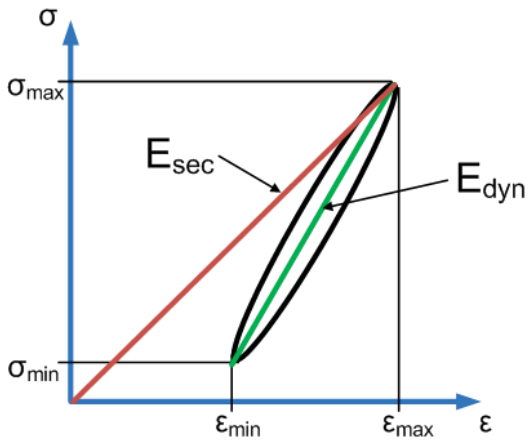

Figure 2.3: Readout of the secant modulus and the dynamic modulus from a stress-strain hysteresis under a cyclic load.

2.4.2.2 Damping

The damping is the quotient of the dissipated work (area inside the hysteresis) and the saved work (area under the hysteresis), (Figure 2.4) (Raue and Ehrenstein, 1999). It shows how much of the applied work is dissipated by inner friction. This dissipated work is transformed into heat and heats up the specimen and causes a weakening of the material. This is a big problem with polymer fatigue tests because the temperature-sensibility of the modulus and the tensile strength is very high and the heat conductivity is very low. The damping of PP is relatively high at room temperature compared to other polymers like PVC or Epoxy (Moet and Aglan, 2005). The reason for this is that the glass transition temperature (T_g) of PP is relatively close to room temperature. At around the glass transition temperature the mobility of the polymer segments is increasing but is still in a range where the movement needs enough energy to cause an appreciable amount of friction and thus a relative high energy of loss (Ehrenstein, 2001). This means the loss modulus shows a maximum.

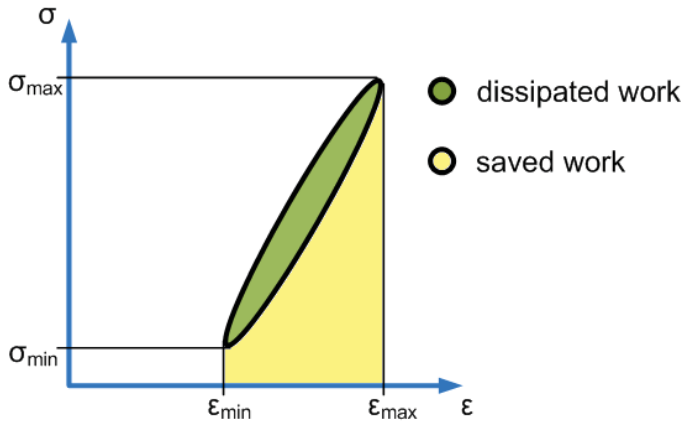

Figure 2.4: Dissipated work and saved work at cyclic load.

2.4.3 Isocyclic stress-strain diagrams

Isochronous stress-strain diagrams are a very commonly used tool for describing the creep behaviour of polymeric materials and composites. These diagrams show the development of the elongation caused by creep at different stress levels. Analogous to this, isocyclic stress-strain-diagrams (ISSDs) were proposed for the evaluation of the fatigue behaviour of composites (Zahnt, 2003; Pinter et al., 2006). These ISSDs have the potential to be the basis for a material law. In Figure 2.5 and Figure 2.6 the principle of the construction of the isocyclic stress-strain diagrams is shown (here concerning σ_{max} and ε_{max}). Therefore stress-strain pairs are collected during the runs after certain cycle numbers. This procedure is repeated for different stress levels. The stress-strain pairs of different runs (at different stress levels) are plotted into a stress-strain diagram. The connection of all the points after a certain cycle number is called an “isocyclic stress-strain curve”.

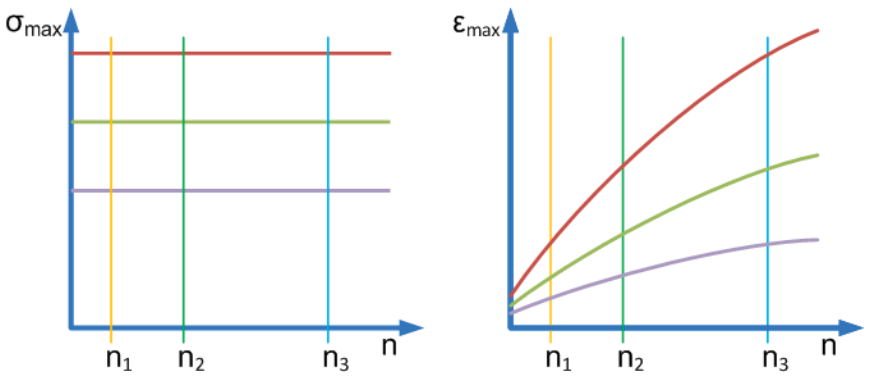

Figure 2.5: Schematic response of ε_{max} on a cyclic load with constant σ_{max} at different stress levels.

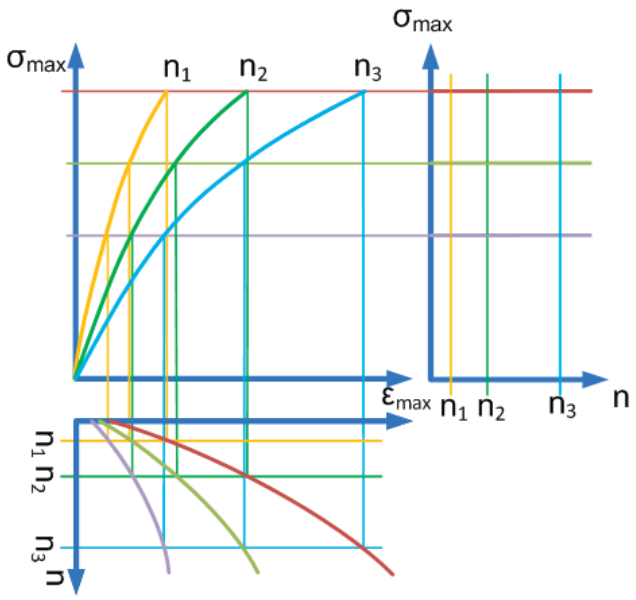

Figure 2.6: Construction of isocyclic stress-strain diagrams according to Zahnt (2003).

This ISSDs compare the strain at different stress levels at a different number of cycles (the number of cycles is according to the time in the isochronous stress-strain diagram). Compared to the SN-diagrams (SN-diagrams show only the number of cycles until break), the ISSDs give more information, especially concerning the cumulative damage and creep during the test. The mechanical fatigue caused by micro-cracks and crack growth can be evaluated, as well as the creep of the specimen during the test. Therefore there are two versions of ISSDs (Zahnt,2003, Pinter et al., 2006). One is isocyclic σ_{max}-ε_{max} diagram, and the other one is the isocyclic $\Delta\sigma$-$\Delta\varepsilon$-diagram. The isocyclic σ_{max}-ε_{max} diagram shows the development of the maximum strain with increasing stress levels after a certain number of cycles. Analogous isocyclic $\Delta\sigma$-$\Delta\varepsilon$ diagrams show the development of $\Delta\varepsilon$ at different $\Delta\sigma$. A qualitative example of an isocyclic $\Delta\sigma$-$\Delta\varepsilon$ diagram is shown in Figure 2.7. The stress-strain pairs are drawn for different numbers cycles at tests with different σ_{max} values.

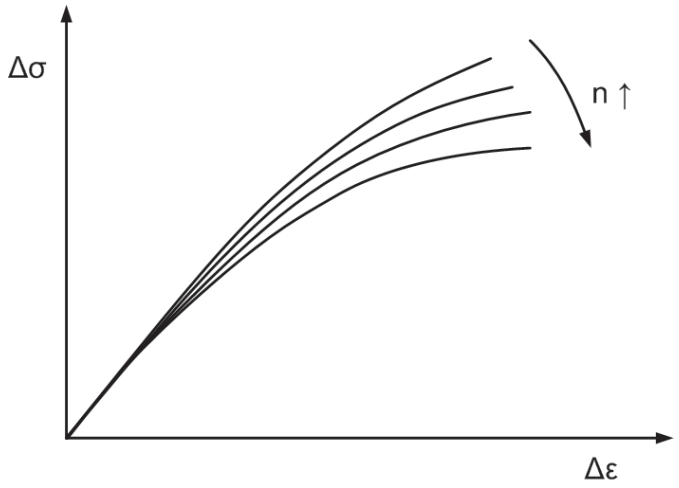

Figure 2.7: Example of an isocyclic Δσ-Δε diagram; the different curves represent the connection of the stress-strain pairs after a certain number of cycles at different stress controlled tests at different stress levels.

2.5 Fatigue testing of polymers and composites

Fatigue testing of polymeric materials and their composites needs to take into account some aspects that are not that critical in metallic materials. Due to the viscoelastic behaviour and the high influence of the temperature on the mechanical properties, it is important to differentiate between tests at a constant temperature and tests with an increased material temperature due to hysteretic heating (Kultural and Eryurek, 2005). The problem of heating up due to the dissipation of the applied mechanical work appears chiefly at high frequencies and with polymers and composites with a low modulus and a high damping at the test temperature.

2.5.1 Heat generation and damping

The problem of hysteretic heating plays an important role in fatigue tests with some polymers. This relatively high influence as compared to other materials like metals is caused by the bad heat conductivity of polymers and the relatively high damping. The high damping causes a high percentage of energy dissipation. Thus a part of the applied work (defined by stress multiplied by strain) results in heat energy. This heat energy causes the specimen to heat up. The fact that the strain also plays a role concerning the amount of heat produced leads to an influence of the modulus on the heat generation in fatigue test under load control. A low modulus causes a big elongation to reach a certain stress level. This causes a big

input of energy that is partly transformed into heat. The increasing temperature has a large negative influence on the mechanical properties of polymers. The modulus, for example, is strongly influenced by the temperature. Especially around the glass transition temperature (T_G), an increasing temperature causes an enormous decrease in the shear modulus G as well as the Young's modulus E. Because the T_G of PP lies around -10 °C to 0 °C, which is near to the room temperature, the results can be significantly influenced by a small increase in the temperature by hysteretic heating for testing at room temperature. This can be avoided by testing at low frequencies, causing less heat-generation per time, or by a cooling of the specimen. Zhou and Mallick (2005) found a strong influence of hysteretic heating for fatigue tests with talc filled PP (40 w% talc) in a frequency range between 0.5 and 20 Hz at frequencies of 5 Hz and above at a peak stress of σ_{max} = 80 % of σ_y (tensile strength). For a lower frequency they found an increase in the lifetime (in cycles until fracture) with increasing frequency.

2.5.2 Thermal fatigue

According to Osswald and Menges (2003), the rise in temperature caused by hysteretic heating is one of the main factors in the fatigue testing of thermoplastics. An increase in temperature leads (in general) to a decrease of the modulus and the tensile-strength in polymers (thermosets and thermoplastics). This decrease in the mechanical properties has also a great influence on the fatigue behaviour of polymers (Roesler et al. 2007) due to hysteretic heating during fatigue tests. It causes a higher sensitivity on the fatigue load (decrease of mechanical properties). If the temperature reaches an equilibrium at a certain temperature ("Thermal Stability"), the material will show a fracture caused by mechanical fatigue, but at a higher temperature (Moet and Aglan, 2005; Mai, 1981). This value of equilibrium can increase with advancing (mechanical) fatigue damage of the specimen because the energy dissipation increases with increasing damage. This higher temperature causes a lower fatigue lifetime by decreasing the mechanical properties. If the temperature does not reach an equilibrium, the heating up leads to a softening of the material and this leads again to an increase of the damping and the energy of loss which causes a further increase in the temperature (Figure 2.8). The temperature rises until the mechanical properties become too low for the applied load and the specimen breaks. In this case we speak of "thermal

instability" and "thermal fatigue" (Moet and Aglan, 2005). To avoid thermal fatigue, which can decrease the cycle numbers at break significantly, the frequency can be adjusted to lower values. With this decrease in the frequency, the heat production is less, and there is more time to transport away the heat energy. Another possibility for reducing the hysteretic heating is to increase the R-factor.

Kultural and Eryurek (2005) have seen a significant increase in the temperature of a specimen of calcium carbonate filled polypropylene at frequencies of 23 Hz and 50 Hz. The increase was, depending on the load, up to 40 K and more during testing at room temperature (mean stress σ_{mean} = 10 MPa, stress amplitude $\sigma_{amplitude}$ = 0.6-0.8 MPa) for pure PP as well as for PP filled with 20 w% and 40 w% of talc.

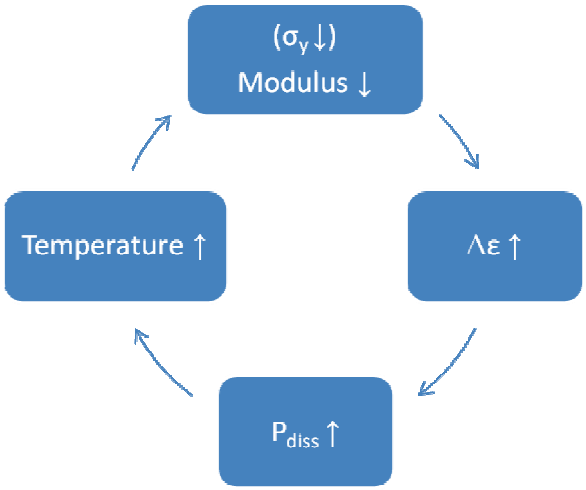

Figure 2.8: The circle of heating up at thermal fatigue, where P_{diss} is the dissipated heat (energy of loss).

According to Roesler et al. (2007), the main reason for failure of thermoplastic polymers under thermal fatigue is a decrease of the yield stress with increasing temperature. The strain amplitude increases in the stress-controlled test due to the decrease of the modulus. In Figure 2.9, the influence of thermal fatigue on the S-N-Diagram is shown in principle. In the case of thermal fatigue an apparent endurance limit occurs indicating the end of the region of thermal fatigue which fades to the line of real mechanical fatigue.

The dependence of the thermal softening limit stress to avoid thermal failure was evaluated for pure PP by Mai (1981):

$$S_0 = 17.1 - 5.32 \log f \qquad (2.3)$$

$f \ldots frequency$
$S_0 \ldots fatigue\ endurance\ strength$

This equation was evaluated at frequencies between 10^2 Hz and 10^4 Hz (Mai, 1981). For a frequency of 5 Hz this would mean a S_0 of 13.4 MPa (if the formula can be extrapolated to 5 Hz). That would mean that PP (unfilled) at 5 Hz does not show thermal fatigue at a maximum load of less than 13.4 MPa. However, Mai does not talk about the R-value that is necessary to fulfil this formula.

Zhou and Mallick (2005) have tested a talc-filled PP-Type on the influence of the frequency on the results of the fatigue tests. They have found an influence of thermal fatigue from frequencies of 5 Hz and above. At 2 Hz and below they could not determine a thermal influence and interpreted the behaviour as pure mechanical fatigue.

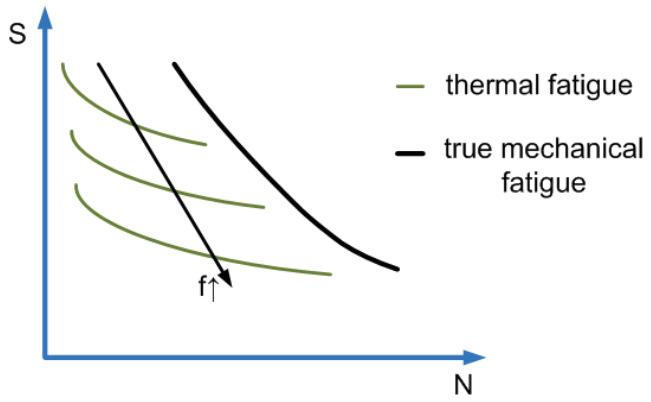

Figure 2.9: Relation of thermal fatigue and true mechanical fatigue of thermoplastic materials in the S-N-diagram (Roesler et al., 2007).

3 EXPERIMENTAL

3.1 Tested materials

The tested materials are shown bellow. The TestPP was an unspecified material. This material had to be specified roughly and was used for the first runs on the servo-hydraulic testing machinery.

- TestPP
    - Unspecified filled PP
        - Rough specification
        - Method development and implementation

After finding the best test parameters and testing conditions, comparative tests were run with different PP composites.

- Borealis Materials (provided by Borealis Polyolefine GmbH Linz, Austria)
    - Different filled PP
        - Evaluation of the fatigue behaviour
        - Tests with changing parameters

The tensile strength of the TestPP is 40 MPa (ISO 527-4). A thermo-gravimetric analysis (TGA) combined with a differential scanning calorimeter (DSC) showed a filler content of approximately 30 w% and confirmed the assumption that the matrix material is PP. Under the microscope, the filler could be identified as glass spheres (see Figure 3.1) with a diameter from approximately 3 to 50 µm.

The specimens are moulded unnotched, standardized specimens (ISO 3167, 1A, injection-moulded). The tests with this material were started to develop the best method for the fatigue testing of different filled PP-types concerning the stress range, number of tests and the data acquisition (necessary amount of data for the data-evaluation with Matlab (MathWorks, USA)) as well as getting a certain routine in testing and to avoid errors and the waste of specimens. Furthermore there was an evaluation of whether hysteretic heating at 5 Hz had a significant influence on the number of cycles at fracture.

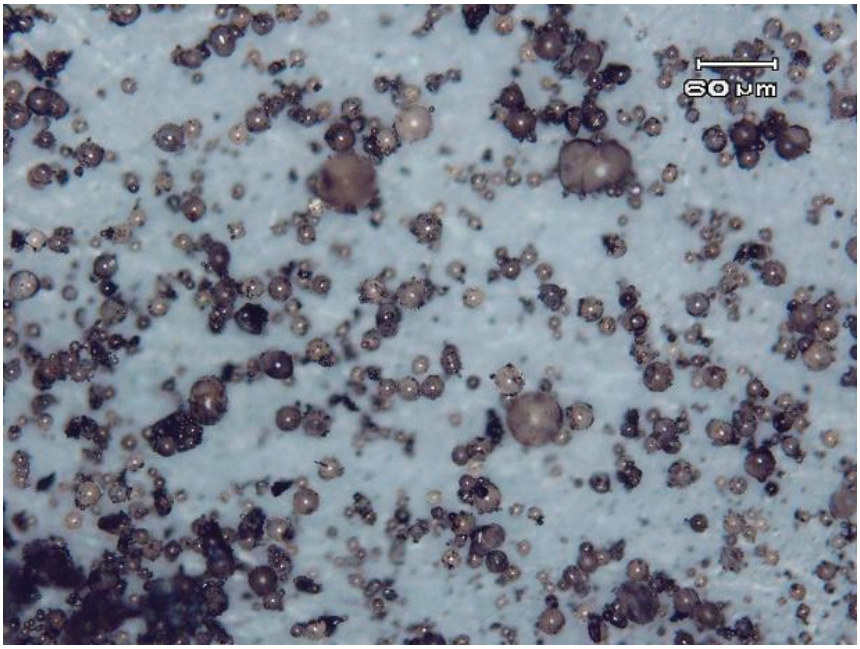

Figure 3.1: Rest (probably glass-spheres) of TestPP after a TGA up to 650 °C.

The compositions of the Borealis materials are visible in Table 3.1. The fatigue behaviour of these materials was to be compared. Therefore the common S-N-diagrams and the hysteresis measurement were to be used and the relatively new method of isocyclic stress-strain diagrams was to be adjusted. The general aim was to compare the different fillers concerning the influence on the fatigue behaviour.

Table 3.1: Tested materials from Borealis. Tested by Michael Jerabek, Borealis. (*ER2: At a tensile rate of 0.01 mm/sec.).

Notation	**Matrix**	**Filler**	**σ_y [MPa]**	**E [MPa]**
			both at a tensile rate of 0.1 mm/sec	
M1	HH450FB (PP)	no filler	31.2	1857
M2	HH450FB (PP)	10 w% talc, 1-2 µm	31.8	2574
M3	HH450FB (PP)	20 w% talc, 1-2 µm	32.0	3574
G1	HH450FB (PP)	9 w% glass spheres d=3.8-8µm	36.7	2142
G2	HH450FB (PP)	18 w% glass spheres d=3.8-8µm	32.0	2350
ER2	HH450FB (PP)	7 w% polyolefin elastomer	20.0*	1182*

3.2 Testing conditions

The tests were run at an ambient temperature of 20 ºC and a humidity of 50%. Some of the specimens where cooled by a vent. A fluctuation in temperature of around ± 2 K could not be avoided, and was partly caused by the fact that the lab was also used for teaching classes with up to 20 people.

3.3 Test program

The tests were run at different load levels and chosen such that the break appeared in a region between 5 x 10^4 and 10^6 cycles. Inside this region the different loads were spread in order to get a meaningful S-N-diagram and enough different load levels for the construction of isocyclic stress-strain diagrams. The appearance of thermal fatigue was to be avoided as much as possible.

During the tests at TestPP, different frequencies were tried as well as different R-values ($\sigma_{min}/\sigma_{max}$). Some of the tests were also run under forced ventilation with 2 vents. The load was sinusoidal with a certain maximum value σ_{max} and a certain minimum value σ_{min}, both in a positive region (only tensile). R was constant at 0.1. In general, the tests were operated at a frequency of 5 Hz. With material G1 (PP with 9 w% of glass spheres) tests at different frequencies were run to get an idea about the influence of the frequency on the fatigue life.

3.4 Test equipment

The fatigue tests were run on an MTS (810 Material Test System, MTS Systems Corporation, USA) at different load levels. The strain was measured with an MTS Extensometer, gauge length 25 mm. The development of the surface temperature was measured with an infrared camera (Fluke Ti30, Fluke GmbH, Germany).

4 RESULTS

4.1 Method development and implementation

Tests with the TestPP were run to get an idea of the right testing parameters and the best testing conditions as well as the best method of data acquisition. First, some tests were run at the planned conditions of 5 Hz and an R-value of $\sigma_{min}/\sigma_{max}$ = 0.1. These parameters where chosen to limit the time consumption (frequency of 5 Hz) and the influence of creep on the fatigue results (R = 0.1). The S-N curve of these tests is plotted in Figure 4.1. The cycle number at fracture seems to be a negative logarithmic function of the stress level σ_{max} in the range between a fracture cycle number of 10^4 and 10^6. The same behaviour was found by Zhou and Mallick (2005) for talc filled PP. Four runs at a stress level of σ_{max} = 34 MPa showed a fracture between 5,000 and 8,000 cycles, while a run at a stress level of σ_{max} = 28 MPa ended with the fracture of the specimen after more than 10^6 cycles. This means that the whole range of stress levels (for fractures between 10^4 and 10^6) is within a range of 6 MPa concerning σ_{max}. At these stress levels, σ_{max} corresponds to 70 to 85 % of the tensile strength.

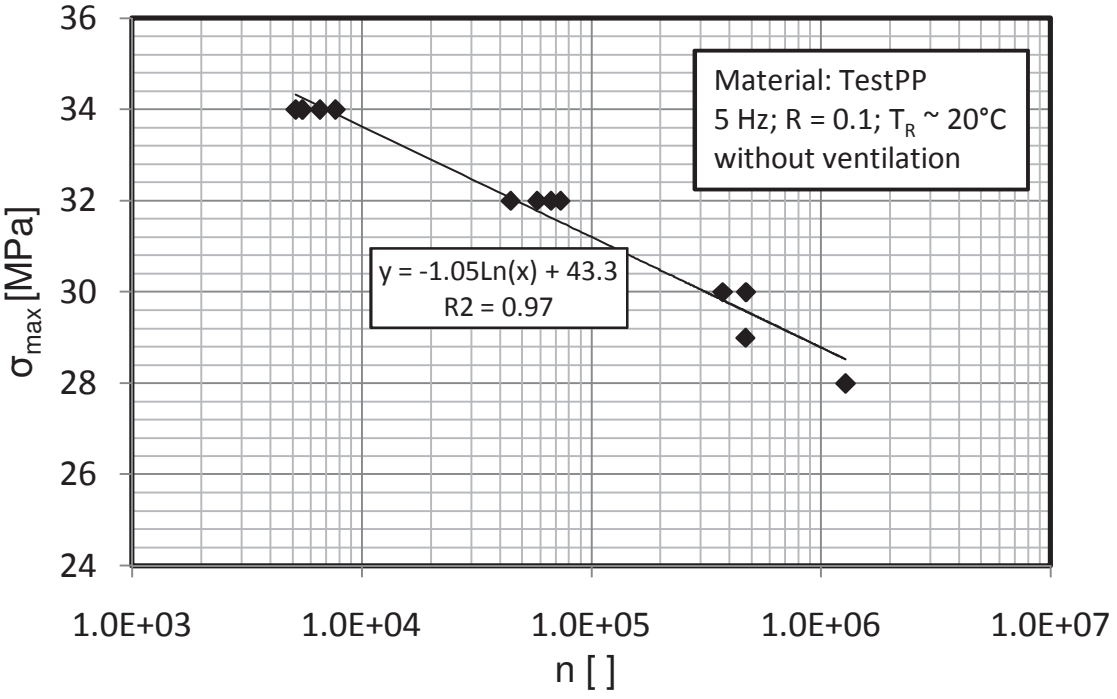

Figure 4.1: S-N curve of material TestPP without ventilation.

4.1.1 Hysteretic heating and thermal fatigue

A significant increase in the temperature was observed during these tests at a frequency of 5 Hz and an R-value of 0.1. This increase was found to depend on the load level. At higher load levels a higher increase in temperature was measured. This change in the temperature during the fatigue test caused a significant change to the results, caused by the fact that polymeric materials show a big influence of the temperature on the mechanical properties (e.g., modulus or tensile strength). The increase in temperature is caused by hysteretic heating, so the test frequency also plays an important role (compare Kultural and Eryurek, (2005) and Zhou and Mallick, (2005)). The influence of the R-value on the heat production will also be discussed in the following chapters.

The increase in the surface temperature was found to be a function of the number of cycles and the maximum load. In Figure 4.2, an infrared photograph of the specimen surface of material TestPP during a fatigue run at a frequency of 5 Hz is shown. Near the shoulders of the specimen the surface temperature is significantly lower than at the centre of the specimen. This is caused by the better heat transfer near to the shoulders of the specimen and by the metallic grips.

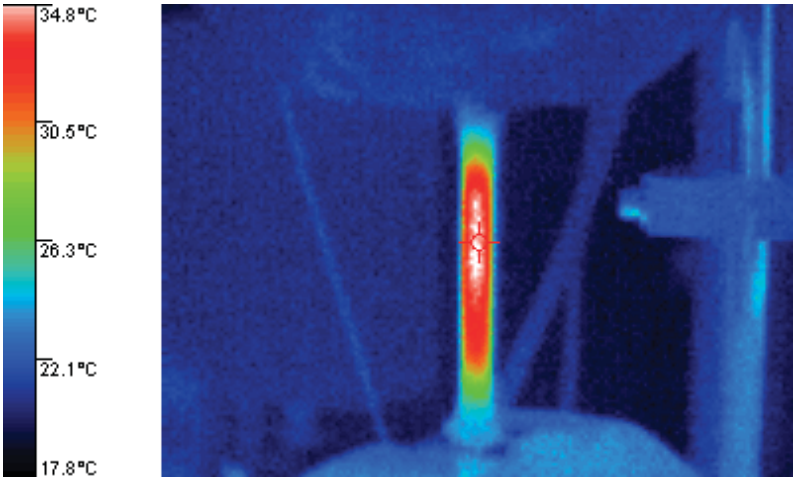

Figure 4.2: Infrared photograph of the specimen at σmax = 32MPa, R = 0.1 and 5 Hz at material TestPP (T_R ~ 20 °C, without ventilation).

At a σ_{max} of 32 MPa, a steady increase of the maximum surface temperature of the specimen was measured (Figure 4.3). The temperature reached 35 °C (ambient temperature ~20 °C) after 10,000 cycles and 42 °C a short time before fracture (after 65,800 cycles; fracture after 66,660 cycles). At a stress level of σ_{max} = 34

MPa, the temperature increased from the ambient temperature of ~ 20 °C to a temperature of ~ 55 °C before fracture (Figure 4.3). The development of the dynamic modulus during the fatigue test is plotted in Figure 4.4. The decrease of the dynamic modulus with the increasing cycle number is caused by the increase of the temperature and the increase in material damage. The damping shows an increase with the number of cycles at these parameters (Figure 4.5). In the case of the test at σ_{max} = 34 MPa, the damping increases from ~ 0.1 after 200 cycles to a value of ~ 0.18 just before fracture. This is an increase of 80 %. However, the more meaningful parameter for getting an idea about the development of the heat generation is the energy of loss. This is an absolute value, whereas the damping is the relation between the energy of loss and the saved energy that also varies during the test. The energy of loss shows a higher increase during the test from ~ 0.1 J/(mm^{3}s) after 200 cycles to ~ 0.55 J/(mm^{3}s) short time before fracture (Figure 4.6). This is an increase of around 450 %. This is partly caused by the increase of the damping, but the rest is caused by the decrease of the modulus and the increase of $\Delta\varepsilon$ during the test.

At the run at σ_{max} = 32 MPa, the damping is lower compared to the test at σ_{max} = 34 MPa. The damping increases from ~ 0.85 at 200 cycles to ~ 0.12 a short time before fracture. In Figure 4.7 the behaviour seen in Figure 4.3 to Figure 4.6 is outlined again. The development of the temperature and the mechanical parameters is shown for a run at 34 MPa at 5 Hz and an R-factor of 0.1. The temperature of the specimen increases during the test until the specimen breaks at a maximum surface temperature of approximately 55° C. At the same time, the energy of loss increases and the dynamic modulus decreases. These three parameters affect each other (Figure 4.8). An increasing temperature decreases the modulus. This increases $\Delta\varepsilon$ at the stress controlled run and causes an increase in the heat dissipation. If equilibrium is not reached between the generated heat and the heat transfer to the environment, the temperature increases until the mechanical properties are too weak for the applied load, and the specimen breaks. This case is called thermal fatigue (Moet and Aglan, 2005).

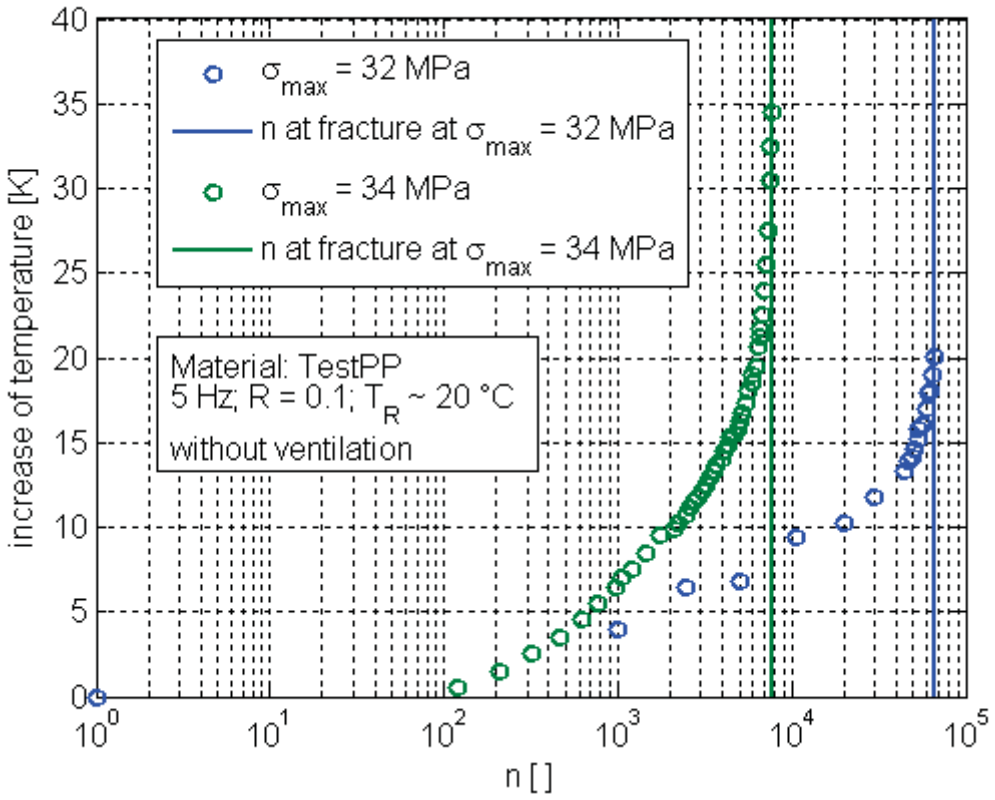

Figure 4.3: Increase of the maximum surface temperature during a fatigue test.

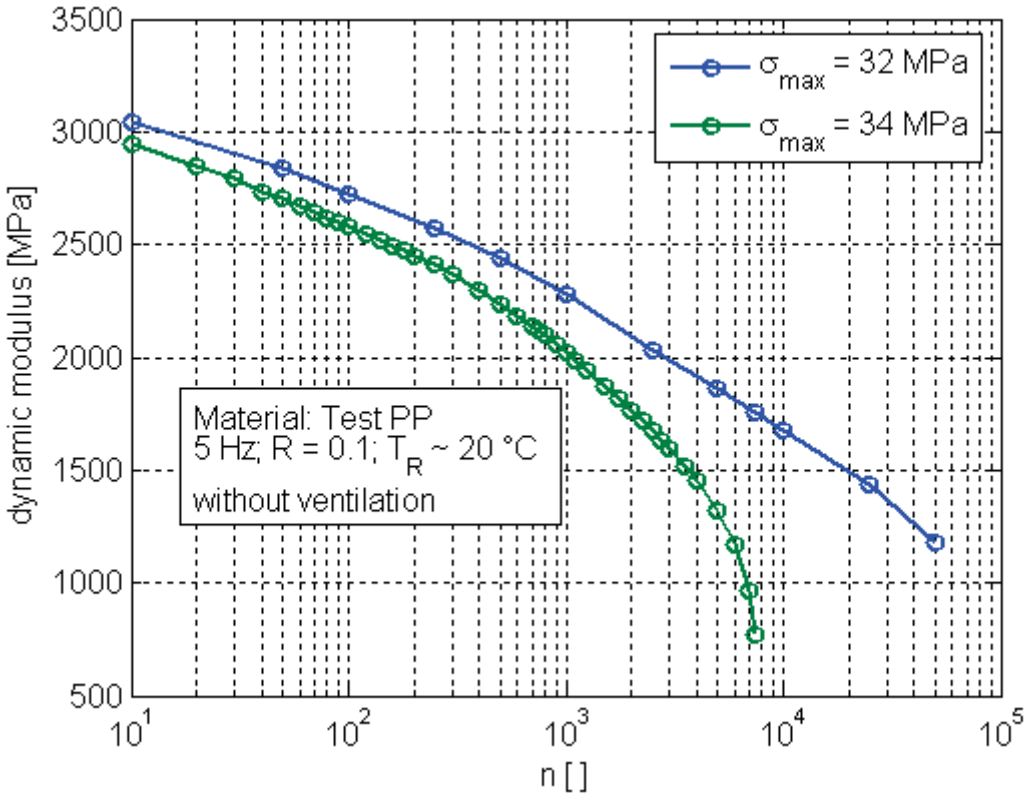

Figure 4.4: Development of the dynamic modulus during the fatigue test.

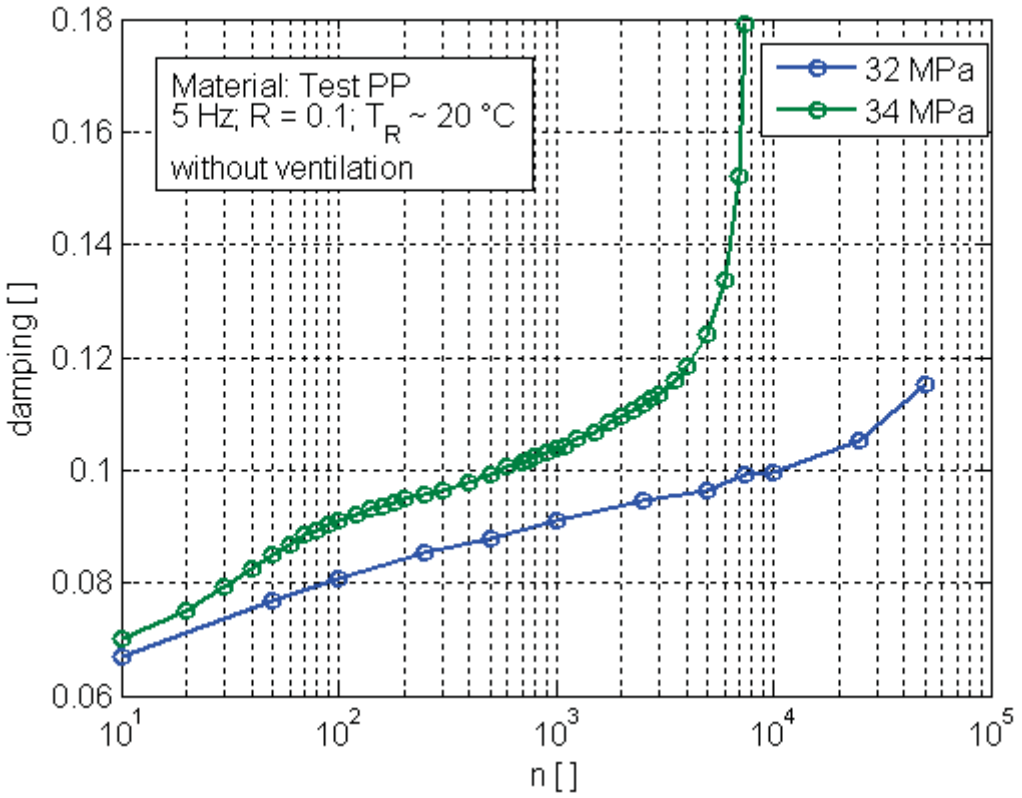

Figure 4.5: Development of the damping during a fatigue test.

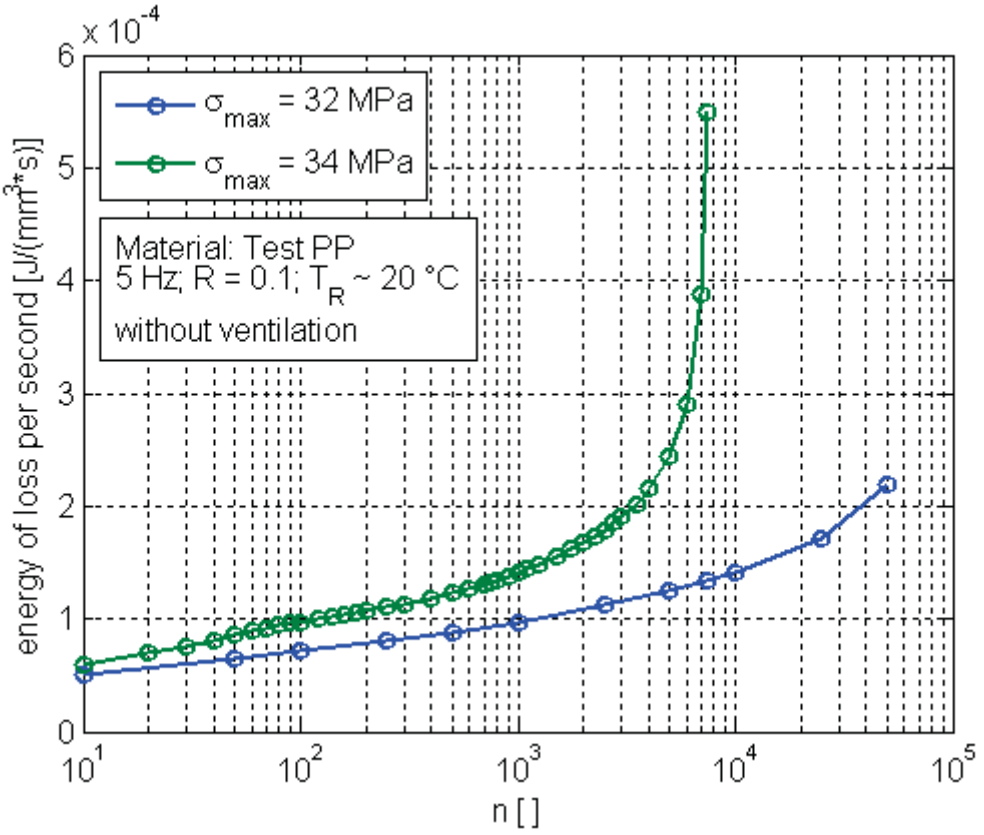

Figure 4.6: Development of the energy of loss per second (heat generation) during a fatigue test.

The influence of the temperature on the damping is dependent on the temperature at which the tests are performed. Near the T_G of the material, the change of the damping is very temperature-dependent (Naranjo et al., 2008). The direct influence of Δε on the damping could not be proved, but there are some hints that can be seen as an indication of this direct influence. One of these hints is the increase of the damping with increasing strain caused by an increase of the load (Figure 4.5). Another hint can be found in section 4.1.2 in the comparison of the generated heat and the dynamic modulus.

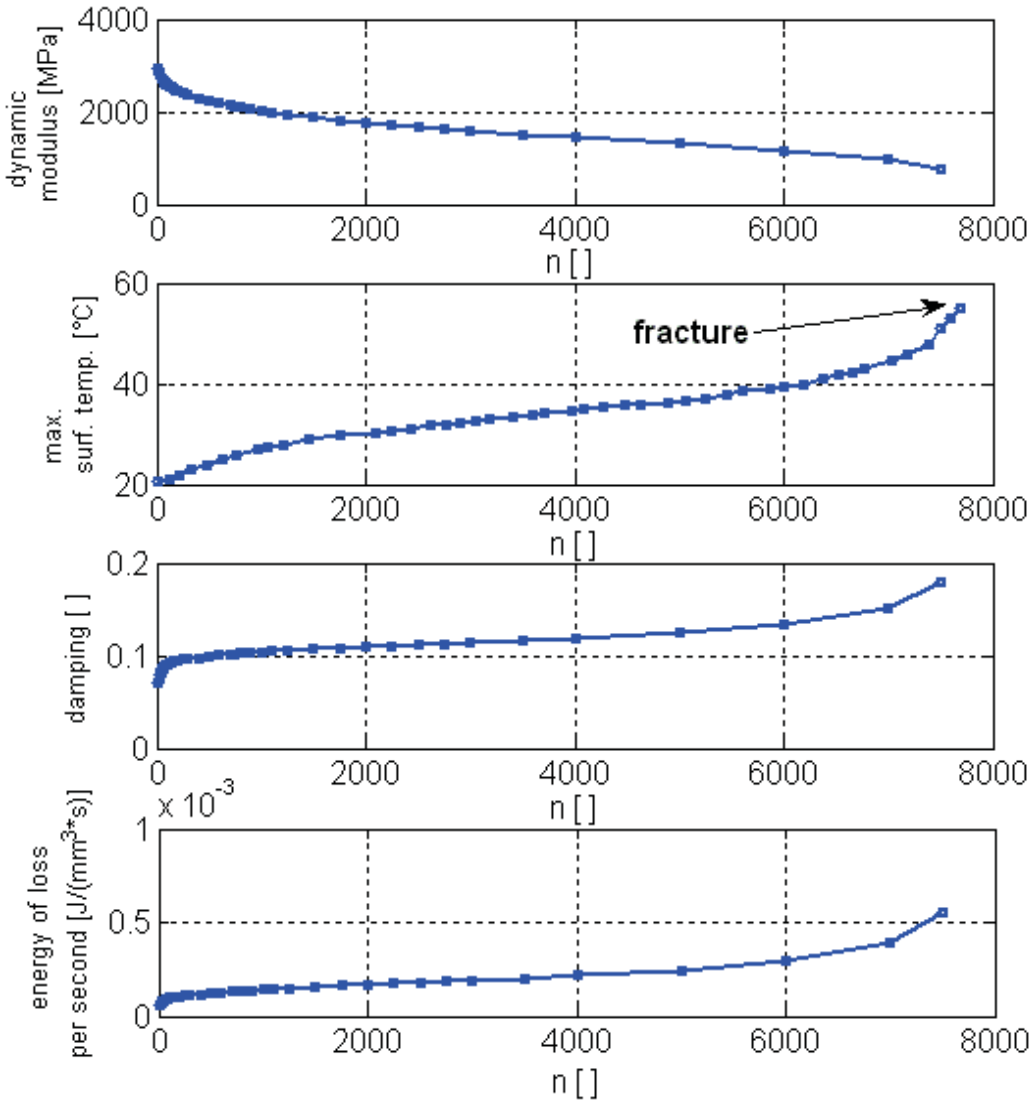

Figure 4.7: Data of a run of TestPP at σmax = 34 MPa, R = 0.1, f = 0.5 and without ventilation. From top: modulus, maximum surface-temperature, damping and energy of loss over cycle number.

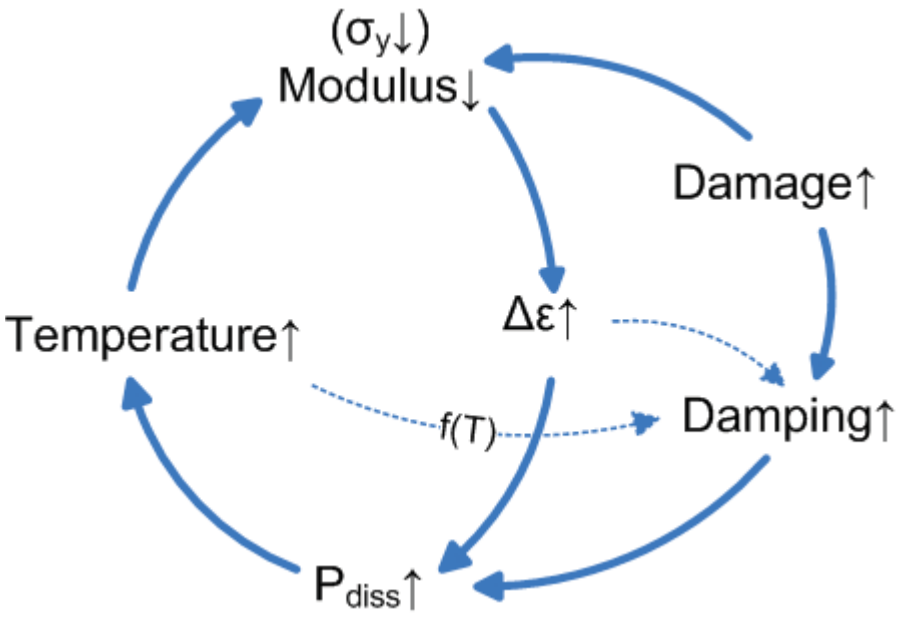

Figure 4.8: Interrelation of modulus, damage, temperature, dissipated power (P_{diss}), damping, strain ε, and yield-stress-σ_y.

In general, the increasing temperature influences the result of the fatigue test. Whether the rise of the temperature is high enough to cause a significant change of the test results or not, depends on the test parameters. This means that at lower stress levels the influence is negligible, whereas at high stress levels the increased temperature causes a fracture long time before the fracture caused by real mechanical fatigue. The test frequency is also an important factor that influences the degree of heat generation. Thus some different ways to avoid or lower the heating up of the specimen and especially the occurrence of thermal fatigue were studied. First tests showed that there are several ways to decrease the rise of the temperature during testing. A decrease in the frequency is very efficient but means an increase in testing time. An increase in the R-ratio also shows a very positive effect on the hysteretic heating, but increases the mean stress $\sigma_{mean,}$ which leads to an increase in creep and influences the results of the fatigue testing. An increase in R also causes a decrease in the strain rate at a fixed frequency and a decrease of Δε (ε_{max}-ε_{min}), which is another important value influencing the fatigue lifetime. Another possibility to decrease the temperature of the specimen is cooling by ventilation. These different possibilities will be discussed bellow.

4.1.1.1 Cooling

Tests were run with air ventilation of the specimen in order to evaluate the possibility of avoiding thermal fatigue and lowering the increase in temperature during testing by increasing the heat transfer to the environment. A forced convection was applied by ventilation with two vents. This ventilation caused an increased heat transport by convection and thus a lower increase in the specimen temperature. To get an idea about the influence of this action, the development of the maximum surface temperature and the lifetime of the runs under ventilated conditions where compared with runs without ventilation. The ventilation caused a significantly lower increase of the maximum surface temperature during the tests. As can be seen in Figure 4.9, the increase in the temperature during the test was significantly lower compared to the tests without ventilation, although the stress level was higher. Under ventilated conditions, the temperature during a test at σ_{max} = 35.5 MPa reached only 24.1 °C up to 40,000 cycles (fracture at 66,000 cycles). This shows the efficiency of the heat transfer by forced convection. Unfortunately a conclusion can not be made about the development of the temperature inside the materials and the influence of the ventilation on the core temperature of the specimen.

The cycle number at fracture with ventilated conditions and a σ_{max} of 35.5 MPa reached the cycle number at fracture at conditions without ventilation and a σ_{max} of 32 MPa. The increase of σ_{max} at the ventilated test causes an increase in the heat generation. This increase can be seen in the parallel shift of ~ 0.06 J/(mm^{3}s) in the curve of the heat generated (Figure 4.10). The heat generated during the run without ventilation at a σ_{max} of 34 MPa shows a totally different development. While the development is linear, with increasing number of cycles during the run with ventilation (at a σ_{max} of 35.5 MPa) and at the run at a σ_{max} of 32 MPa, here the energy of loss increases exponentially with increasing the cycle number (see Figure 4.11). So the additional produced heat, caused by the increase of the stress level from σ_{max} = 32 MPa to σ_{max} = 35.5 MPa, seems to be compensated by the forced convection. In particular, the sudden exponential increase of the energy of loss - seen in the presentation with a linear x-axis in Figure 4.11 - seems not to appear as it did with the run without ventilation and σ_{max} = 34 MPa. This might be a

hint for avoiding thermal fatigue. The linear increase of generated heat seems to be caused by true mechanical fatigue.

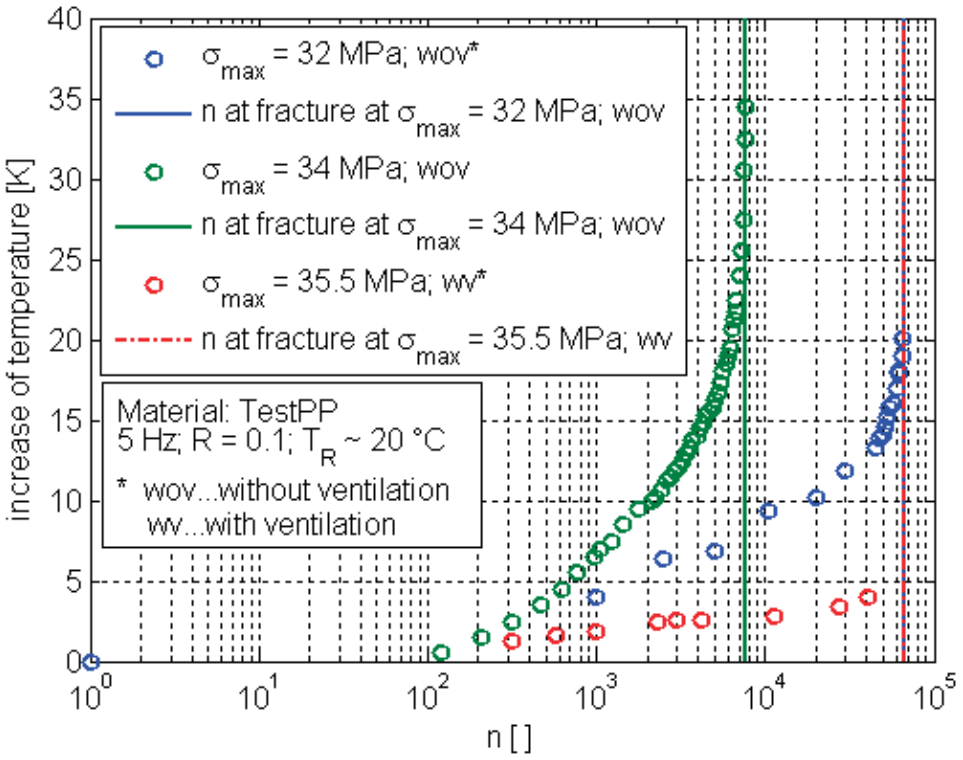

Figure 4.9: Influence of ventilation on the increase of the maximum surface temperature.

In Figure 4.12, the development of the relative dynamic modulus during the fatigue test is shown. The specimen that was run under ventilation at a σ_{max} of 35.5 MPa shows a similar curve to the specimen without ventilation at σ_{max} = 32 MPa. The run without ventilation at σ_{max} = 34 MPa shows a significantly faster decrease of the modulus. The comparison of the curve of the ventilated specimen (σ_{max} = 35.5 MPa) and the run without ventilation at σ_{max} = 34 MPa also shows the obvious positive influence of the ventilation.

An examination of the S-N diagram (Figure 4.13) shows a significant increase in the lifetime under ventilated conditions. The lower temperature leads to better mechanical properties (higher modulus and lower yield stress) and a lower damage to the material.

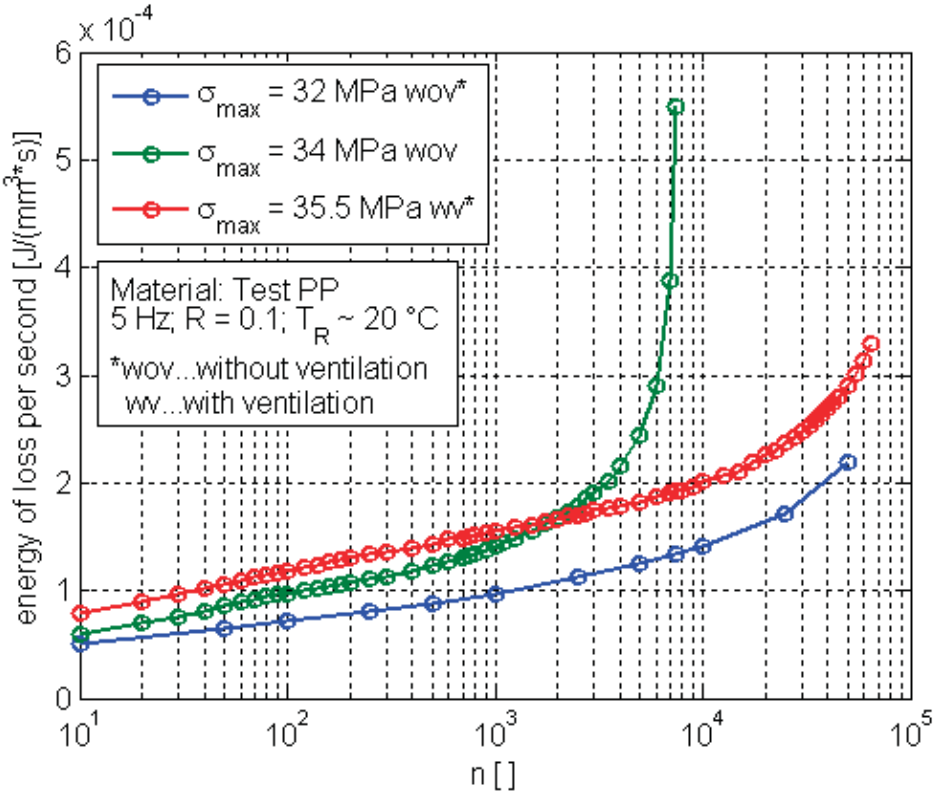

Figure 4.10: Influence of ventilation on the development of the energy of loss.

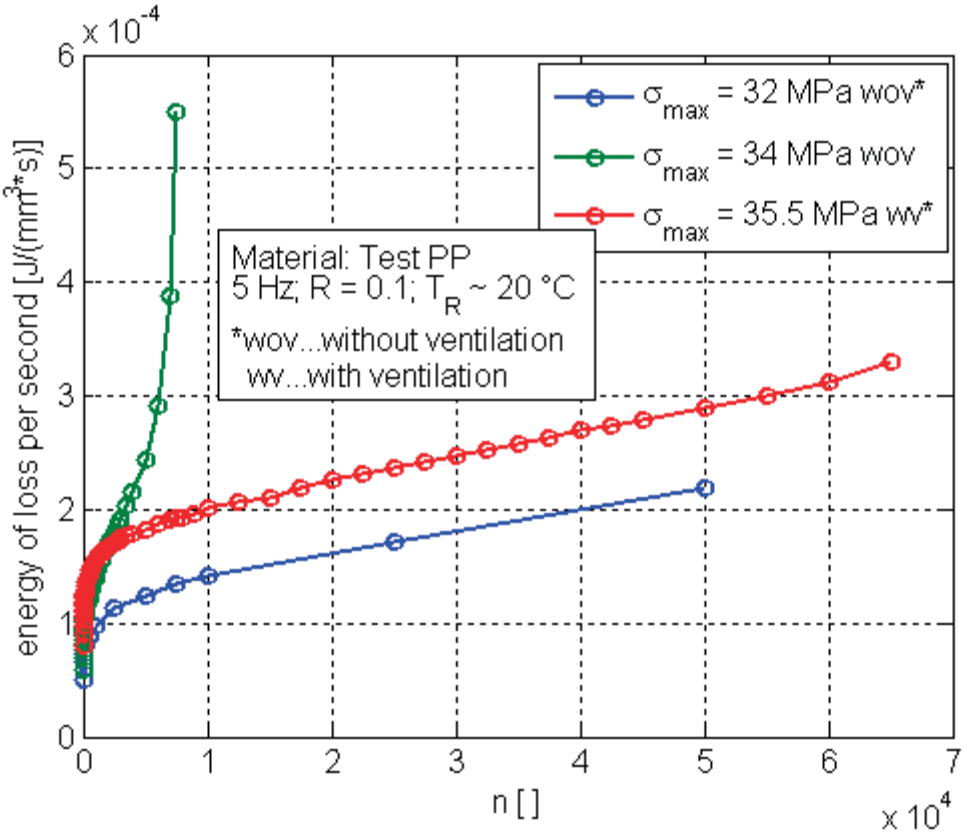

Figure 4.11: Influence of ventilation on the development of the energy of loss (linear x-axis).

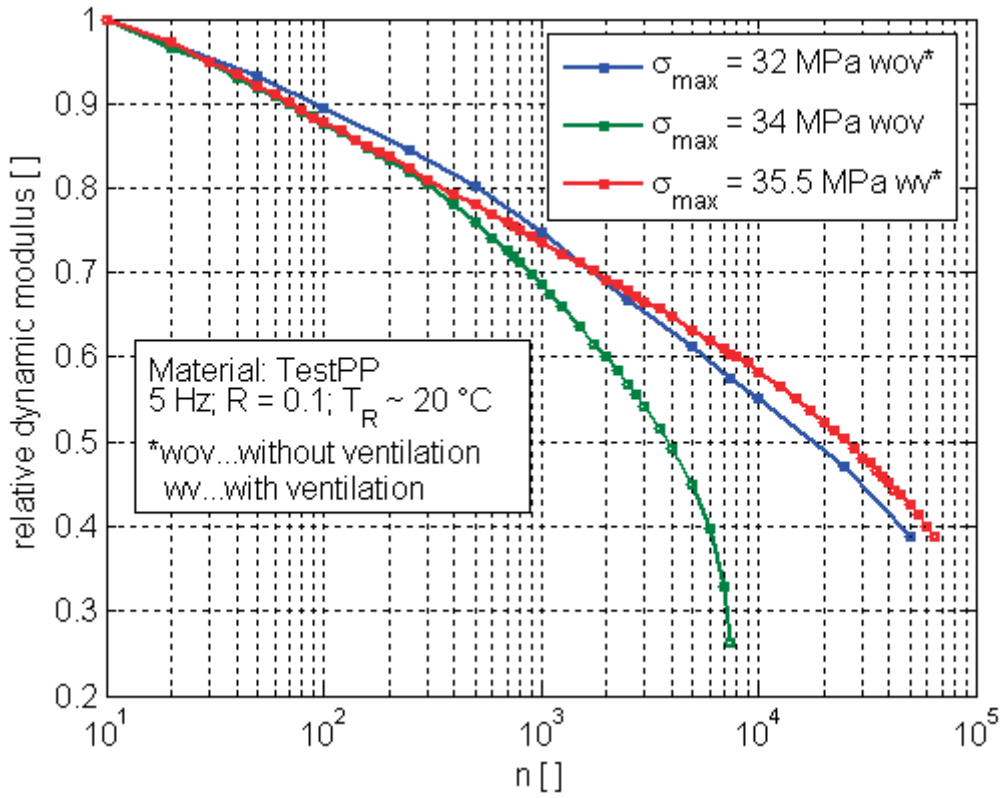

Figure 4.12: Development of the dynamic modulus relative to the dynamic modulus after 10 cycles.

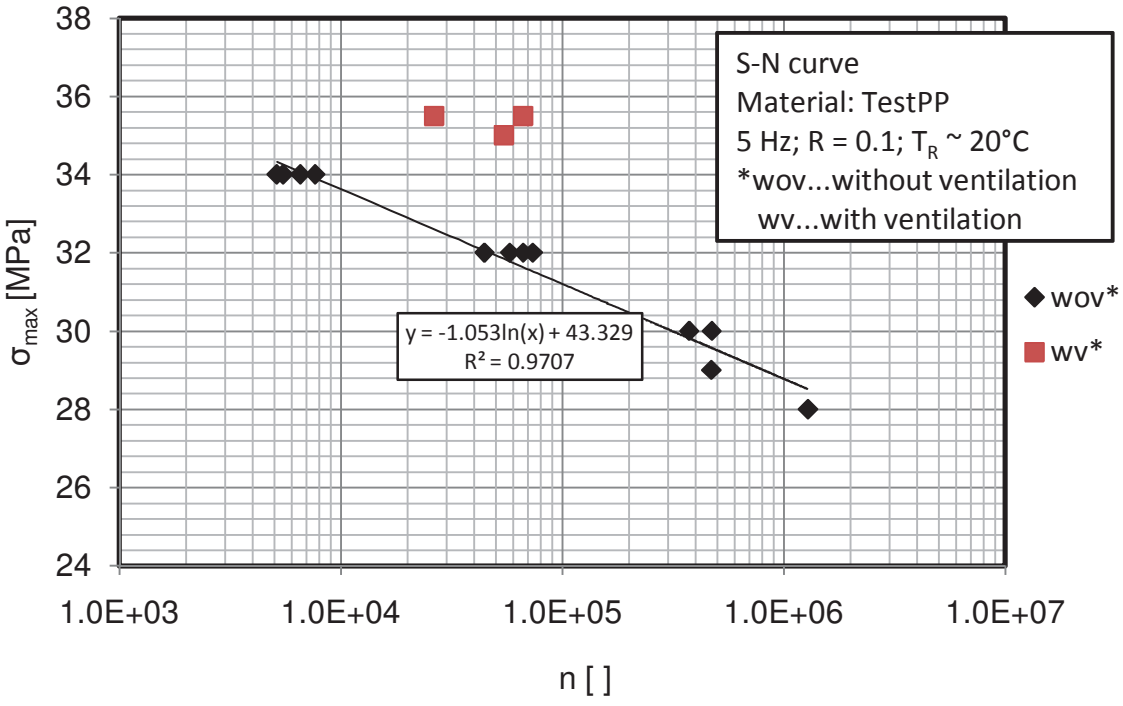

Figure 4.13: Influence of ventilation on the S-N diagram.

4.1.1.2 Frequency

The frequency is a very important factor concerning hysteretic heating and thermal fatigue. The produced heat is more or less directly proportional to the frequency of the load. A formula to describe the influence of different parameters on the thermal fatigue can be found in Moet and Aglan (2005):

$$\dot{U}_g \sim f J'' \sigma_{max}^2 \qquad (4.1)$$

$\dot{U}_g \ldots heat\ generated\ by\ hysteretic\ heating$

$f \ldots test\ frequency$

$J'' \ldots loss\ compliance$

A first test with a frequency decreased to 3 Hz showed a decrease of the maximum surface temperature during the run, compared to the test at 5 Hz, of 3-5 degrees. Four tests at 5 Hz, all at a maximum stress of 32 MPa, brought cycle-numbers at break of 73,500, 58,000, 45,500 and 66,600 cycles. The test at 3 Hz and the same stress level caused a fracture after 123,500 cycles. This could also be an outlier, but it seems to be an indication that the lower increase of the temperature due to the lower heat generation plays a role. A different frequency also means different tensile rates, which can also lead to different results. Lowered tensile rates can cause a lower modulus and a higher strain at a certain stress level. This can lead to changed results compared to tests at higher frequencies. To avoid thermal fatigue in general, it would be possible to run the tests at lower frequencies. The frequency that was found by Zhou and Mallick (2005) to avoid the influence of thermal fatigue at talc-filled PP lies around 2 Hz. The biggest problem is that the time to reach cycle numbers of up to 10^6 gets too high with these small frequencies.

4.1.1.3 R-value

Tests were also run with different R-factors at a stress level of σ_{max} = 34 MPa and a frequency of 5 Hz. A higher R-value means smaller $\Delta\sigma$, a smaller $\Delta\varepsilon$ and a lower energy of loss per cycle. This can also decrease the hysteretic heating significantly. The influence of lowering the R-value on the lifetime can be seen in Figure 4.14. An increase of R increases the lifetime significantly. This might be a combination of two effects: first, the decrease of heat generation (see Figure 4.15) and second, the decrease of $\Delta\varepsilon$. The decrease of $\Delta\varepsilon$ leads to less movement and less fatigue, whereas the part of the mean stress increases. The fact that the increase of R also increases the mean stress $(\sigma_{max}-\sigma_{min})/2$ causes an increase in the creep.

Figure 4.15 (logarithmic n-axis) and Figure 4.16 (linear n-axis) show the influence of the R-value on the development of the energy of loss during the fatigue test. At R = 0.1 and R = 0.2, the energy of loss shows an exponential increase, whereas at higher R-values (0.3, 0.4, 0.5) the energy of loss increases more or less linear during the lifetime (Figure 4.16). The development of the maximum surface temperature at different R-values (R = 0.1, 0.3 and 0.5) is compared in Figure 4.17. While at the run at R = 0.1 the maximum surface temperature increases up to 55 °C, the temperature stays in the range between 20 and 25 °C at the test at R = 0.5. The temperature development at R = 0.3 shows a development that lies between the curves of R = 0.1 and R = 0.3. This seems to be an indication that at this stress level (σ_{max} = 34 MPa) level and at this frequency (f = 5 Hz) the thermal fatigue occurs at the R-values of 0.1 and 0.2.

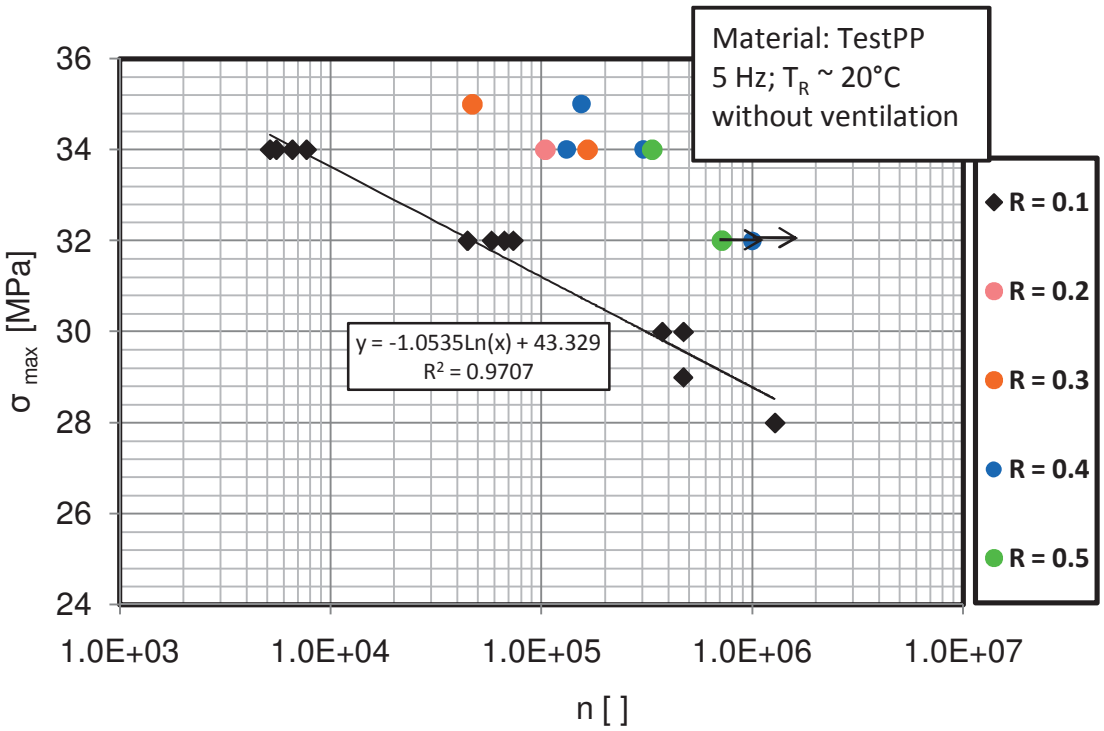

Figure 4.14: Influence of the R-value $\sigma_{min}/\sigma_{max}$ on the S-N diagram of TestPP.

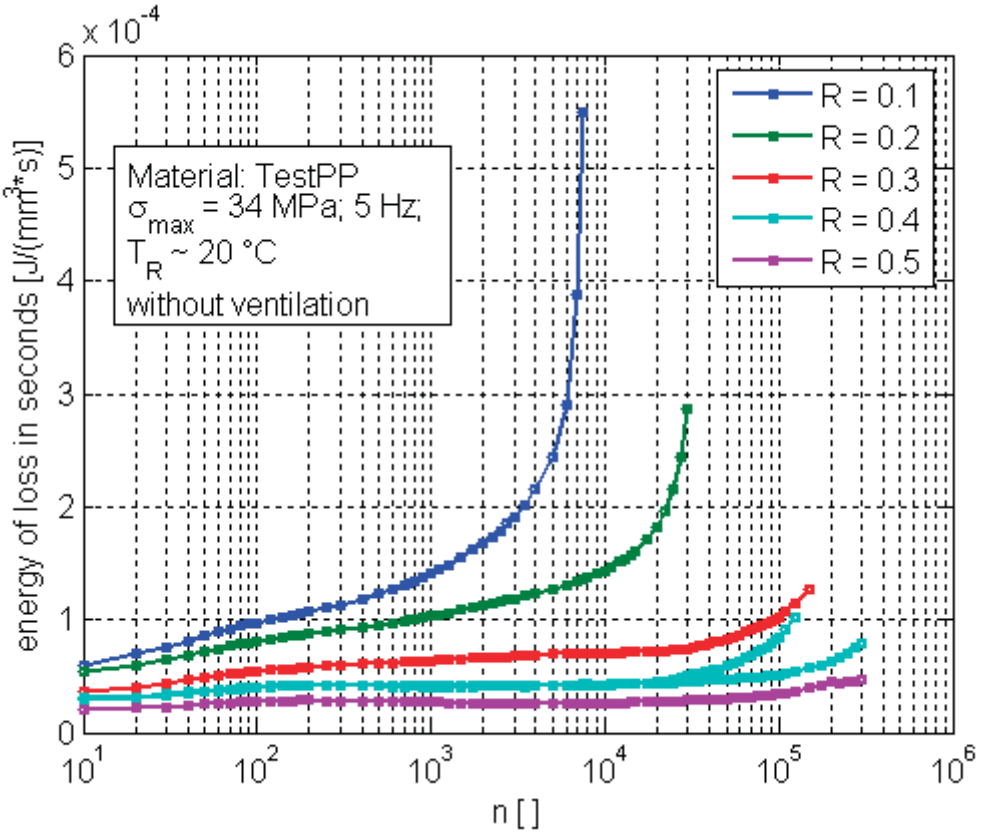

Figure 4.15: Influence of R-value on the development of the energy of loss.

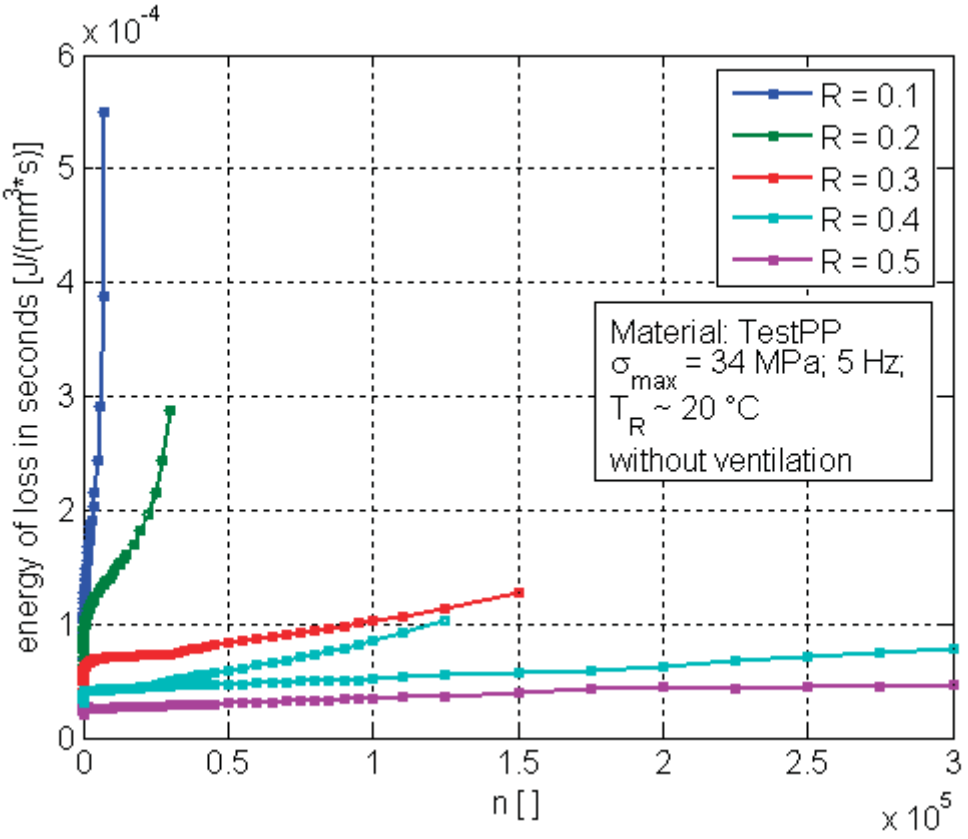

Figure 4.16: Influence of R-value on the development of the energy of loss (linear n-axis).

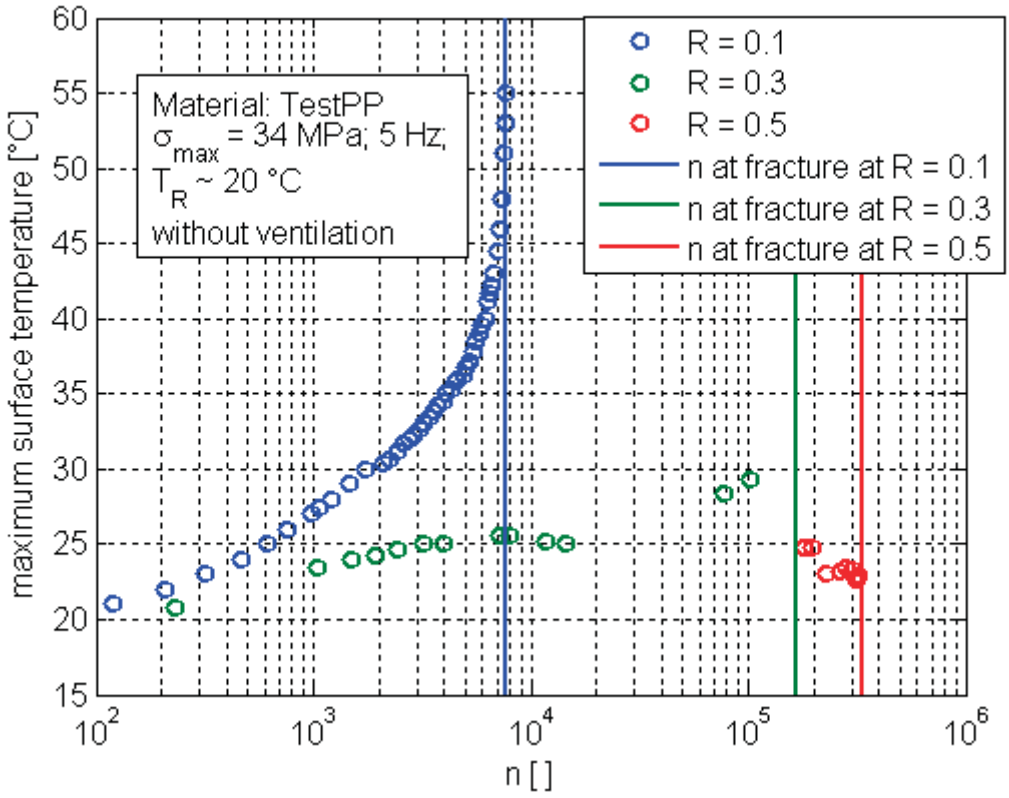

Figure 4.17: Influence of the R-value on the development of the maximum surface temperature.

The dynamic modulus also develops in dependence to the R-value. A lower R-value causes a faster decrease of the dynamic modulus during the fatigue test (Figure 4.18). This might be caused by the lower specimen temperature due to the lower energy of loss, and by a decrease of Δε.

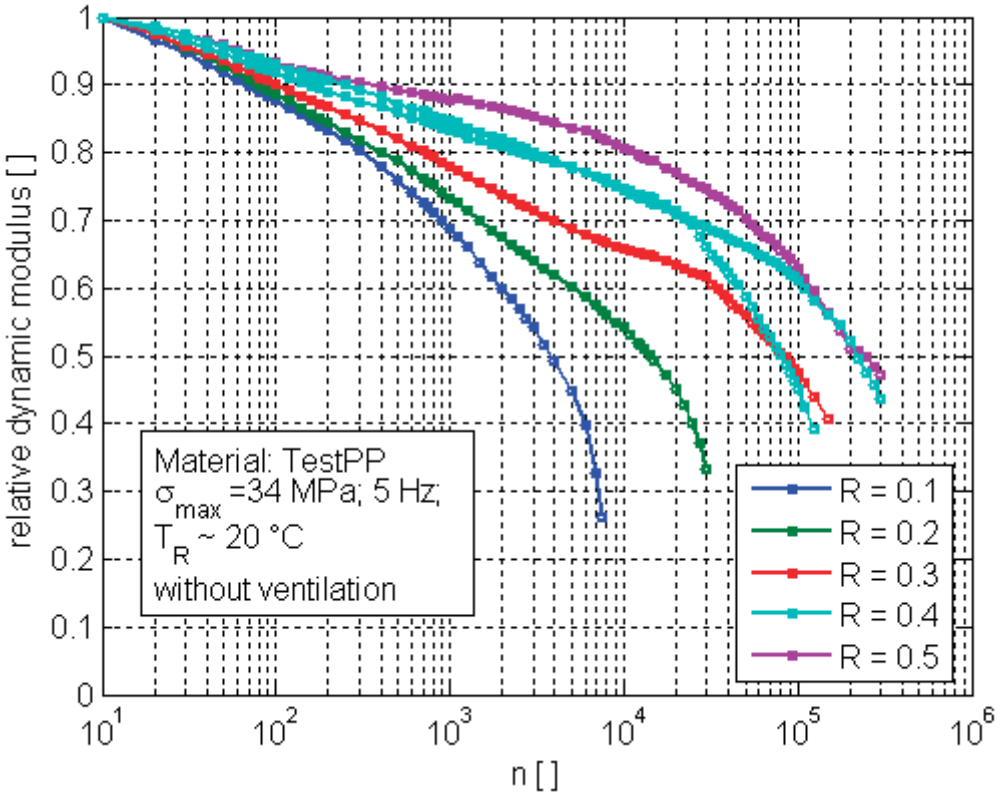

Figure 4.18: Development of the relative dynamic modulus at different R-values.

The decrease of Δε is also has an influence on the mechanical fatigue. Δε is a driving parameter that is needed to arrive at mechanical fatigue. To decrease the R-value, and with this Δσ and Δε, means to decrease the mechanical fatigue and to increase the creep that is depending on the mean stress. So an increase of R has the disadvantage that the influence of creep increases.

4.1.2 Influence of hysteretic heating on the maximum surface temperature and the modulus

To evaluate the effect of hysteretic heating on the development of the maximum surface temperature and on the dynamic modulus, a simple test was run under unventilated conditions. First, a heating of the specimen (TestPP) was caused by a test at 5 Hz, an R-factor of 0.1 and a stress level of σ_{max} = 34 MPa. After 3,000 cycles a maximum surface temperature of 37° C was reached (see Figure 4.19).

Immediately after, the testing parameters where changed to a σ_{max} of 32 MPa and a frequency of 1 Hz (R = 0.1). Due to this change the surface temperature started to decease. An evaluation of the development of the heat generated and the dynamic modulus shows that the dynamic modulus changes during the cooling down of the specimen. The change lies in the region of around 200 MPa. This decrease might also be caused partly by other viscoelastic effects due to changing of the frequency and the load level.

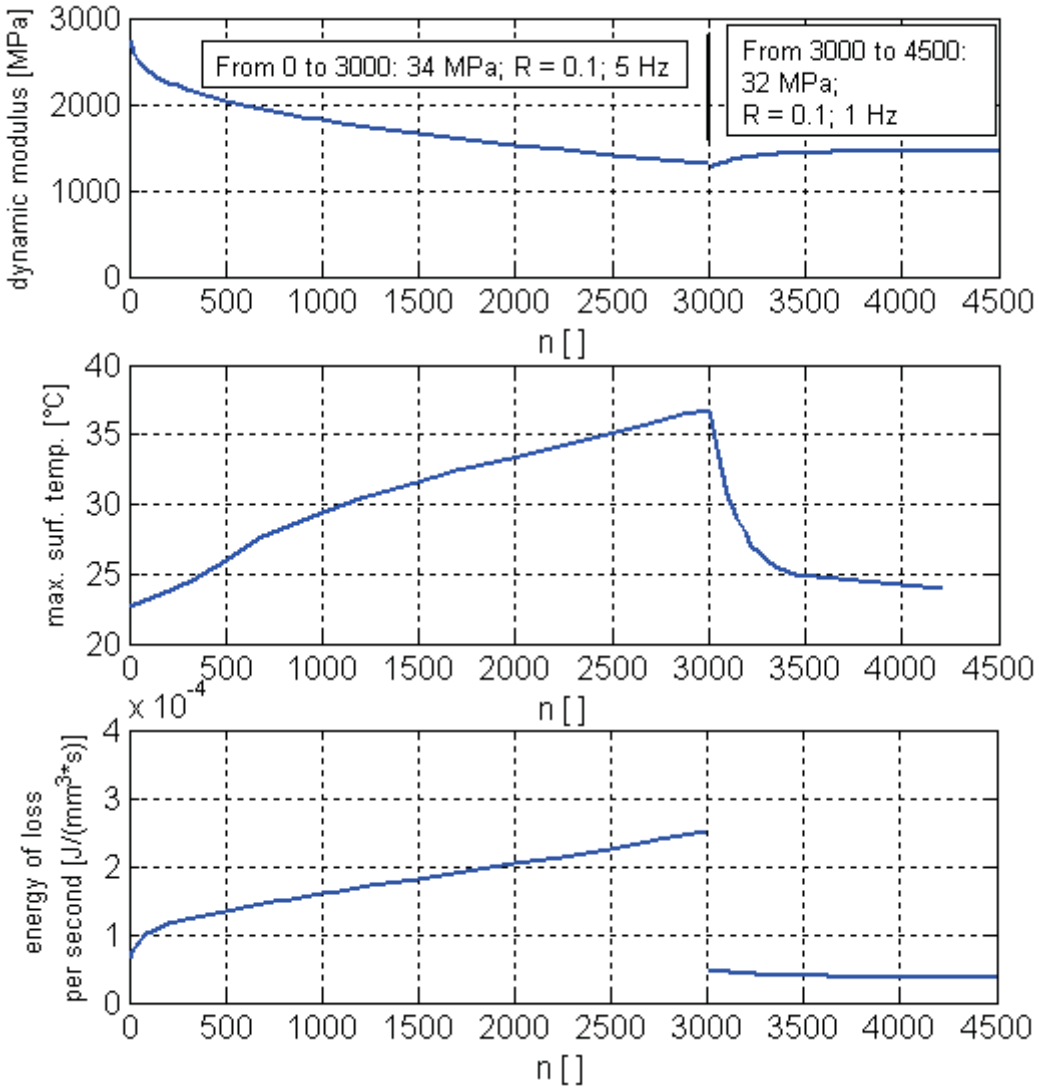

Figure 4.19: Development of the dynamic modulus (top), the maximum surface temperature (middle) and the energy of loss per second (bottom) during a run with two different loads but without a break between the different load levels.

Thus the main part of the change in the modulus that can be found during the fatigue testing can be assigned to the fatigue of the material. The heat generated increases during the first 3,000 cycles from ~ 1 * 10^{-4} J/(mm^3*s) to ~ 2.5 * 10^{-4}

J/(mm^3*s), nearly linearly. At the lower frequency and the lower load, the loss energy stays more or less constant. How much of the increase during the first 3,000 cycles is caused by the increase of inner friction due to an increase of the fatigue damage, and how much is caused by the higher strain due to a lower modulus at the increased temperatures can be estimated from the development of the energy of loss with the decrease of the temperature (Figure 4.19 and Figure 4.20). A zoom into the diagram of the loss energy in the region between 3,000 and 4,500 cycles (Figure 4.20) shows that the energy of loss per second decreases with the decreasing temperature of the specimen, as seen in Figure 4.19. This decrease is, in this case, around 20 %. So 20 % of the total energy of loss seems to be caused by the heating up of the specimen. The rest might be caused by the material damage. This 20 % absolute, or ~ 35 % of the increase of generated heat causes the phenomenon of thermal fatigue. The increase in temperature during the test increases the heat generation, and the increase of heat generation again further increases the temperature.

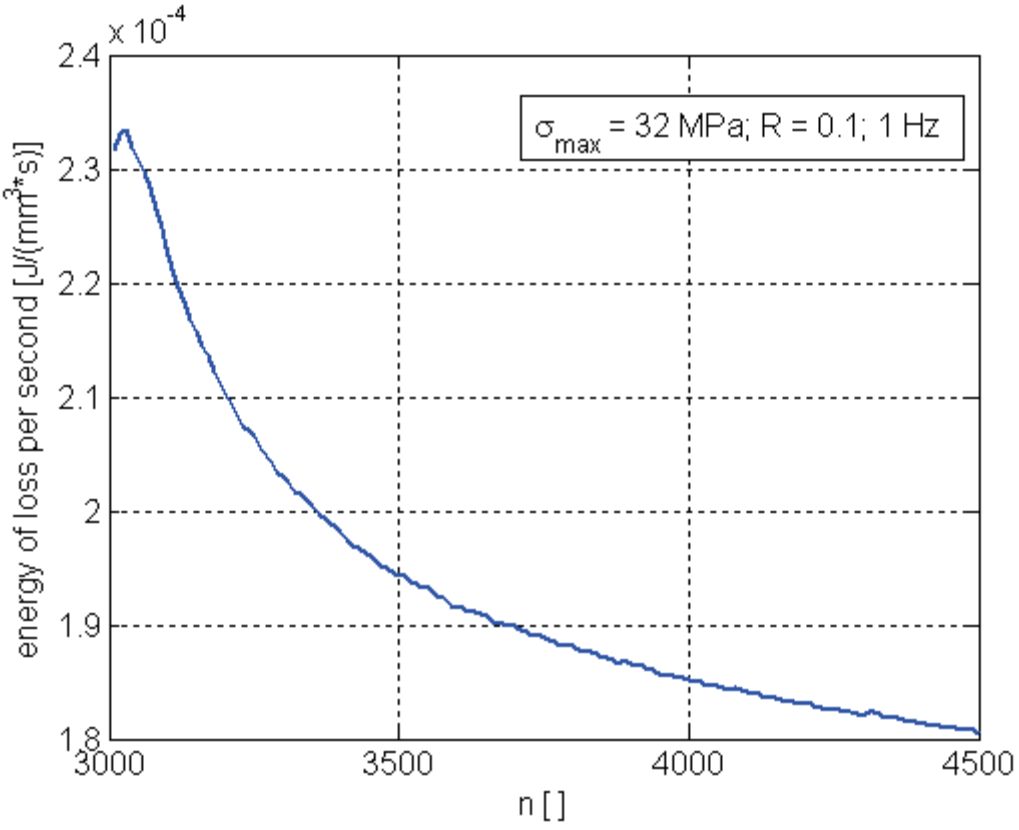

Figure 4.20: Zoom into the energy of loss diagram of Figure 4.19.

After a certain time the increased temperature causes a fracture of the very temperature sensitive material. These conclusions seem to agree with the observations made in section 4.1.1. For a generalisation, further tests would be advisable.

The decrease of Δε due to the increase of the modulus from 1275 MPa to 1465 MPa during the cooling down of the material (from 3000 to 4500 cycles) seems to be responsible only for a part of the decrease of the energy of loss. The decrease in the damping during the same time (Figure 4.21) also causes a decrease of the energy of loss.

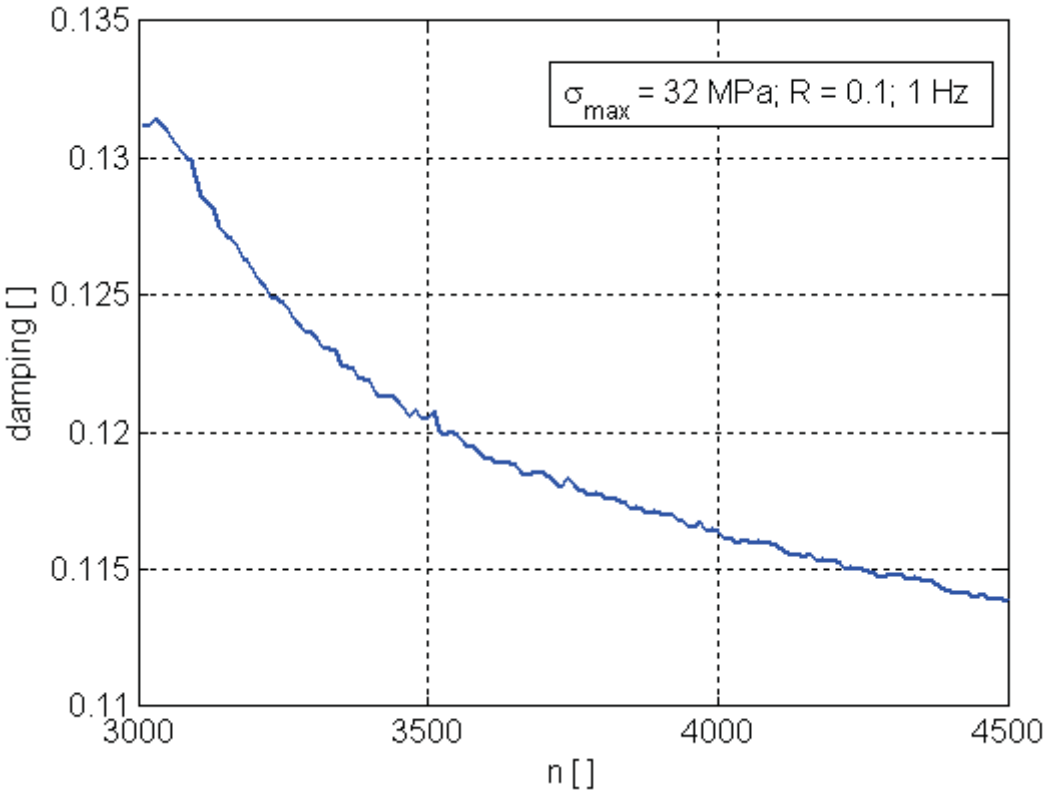

Figure 4.21: Development of the damping in the same range of cycle numbers like in Figure 4.20.

4.1.3 Isocyclic stress-strain diagrams

Figure 4.22 shows the isocyclic σ_{max}-ε_{max} diagram at a frequency of 5 Hz and an R-value of 0.1. A significant change of the strain in dependence on the number of cycles starts already at relatively low stress-levels. This change is caused by creep and material damage.

Figure 4.23 shows the isocyclic $\Delta\sigma$-$\Delta\varepsilon$ diagram of the same tests. It shows the development of $\Delta\varepsilon$ at different $\Delta\sigma$. The increase of $\Delta\varepsilon$ with increasing $\Delta\sigma$ is mainly caused by failure but might also be influenced by the increase in the temperature during the test. In this diagram the damage corresponds with the splitting up of the isocycles. With increasing stress level, the splitting up of the isocyclic curves increases. At low stress levels, the splitting up is much lower compared to the isocyclic σ_{max}-ε_{max} diagram. This means that at low stress levels the creep is dominant, whereas the damage starts to get more important at higher stress levels.

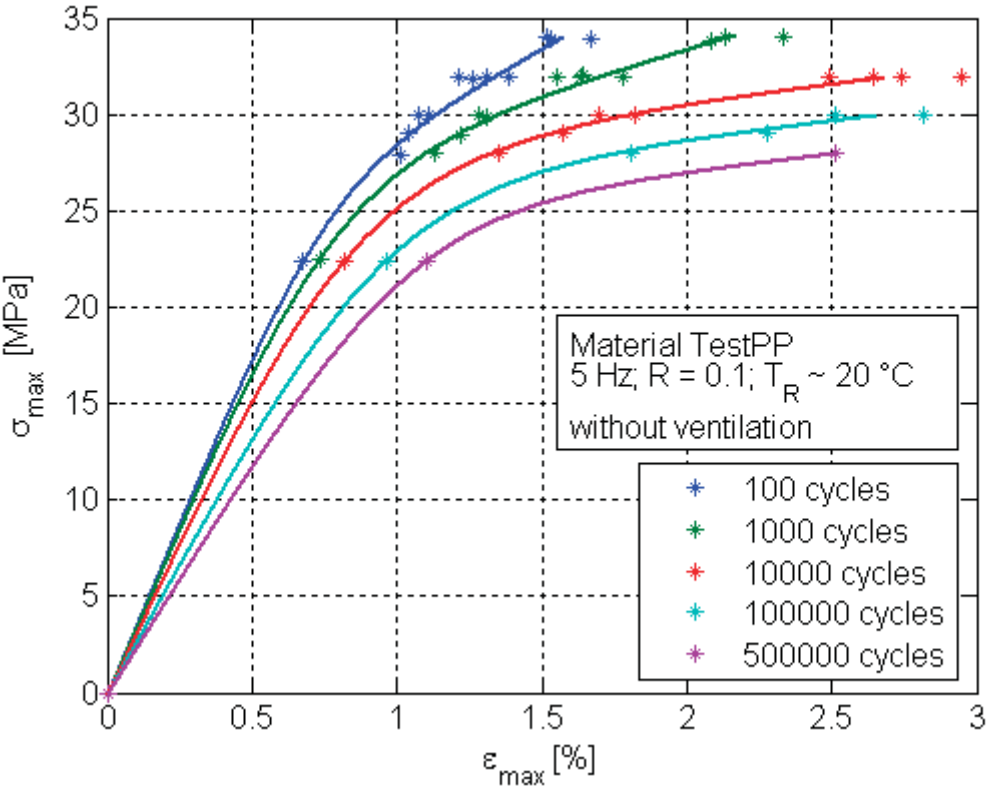

Figure 4.22: Isocyclic σ_{max}-ε_{max} diagram of TestPP.

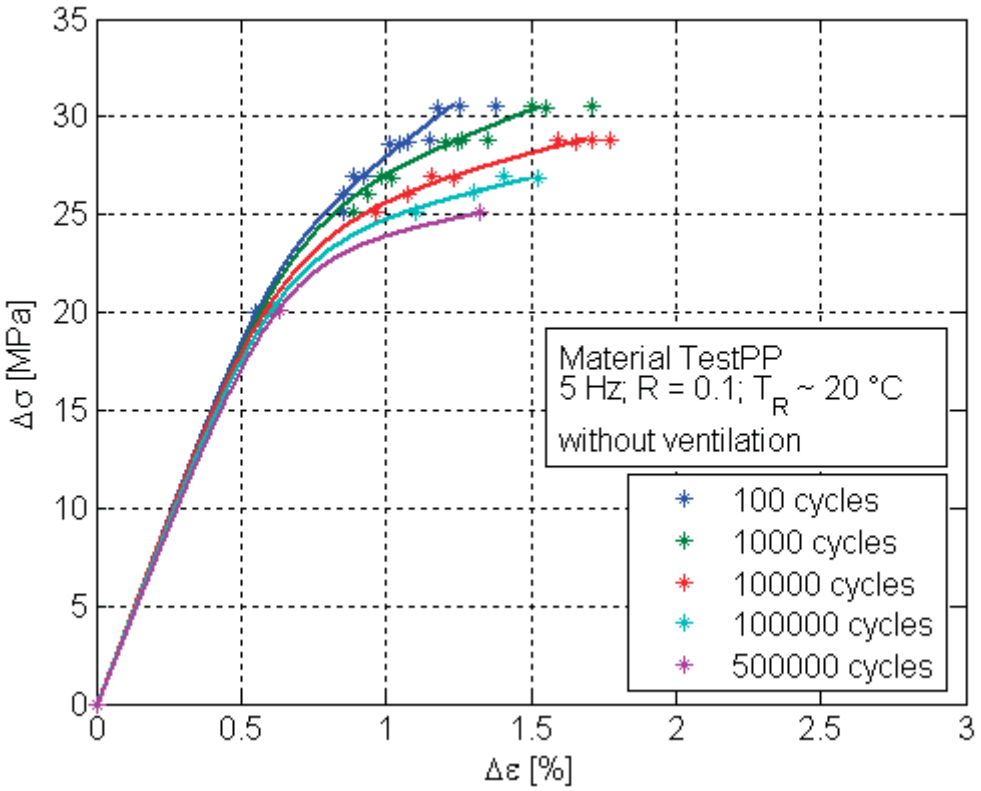

Figure 4.23: Isocyclic Δσ-Δε diagram of TestPP.

4.1.4 Stiffness decrease

As already seen, the change of the dynamic modulus can be a value that shows the progress of the fatigue during a cyclic load. In Figure 4.24 the change of the dynamic modulus with the numbers of cycles (shows the change of the damage of the material) relative to the dynamic modulus at the beginning of the test of material TestPP is shown. A continuous decrease of the dynamic modulus until break is visible. This is an indicator for a continuous increase of damage in the material. Tests at higher load levels show a faster decrease of the relative dynamic modulus. At runs with a σ_{max} of 34 MPa a decrease of around 60 % was detectable up to a cycle number of 5,000. A test at a σ_{max} of 28 MPa showed a decrease of the dynamic modulus of ~ 45 % after 900,000 cycles while a test at a σ_{max} of 22.5 MPa only looses ~ 20 % of his stiffness. So the decrease of the modulus is strongly dependent on the stress level. At higher stress levels, the modulus decreases faster during a cyclic load. The dynamic modulus at fracture also seems to be dependent on the stress level. Lower stress levels cause a fracture at higher cycle numbers and higher dynamic modulus before fracture.

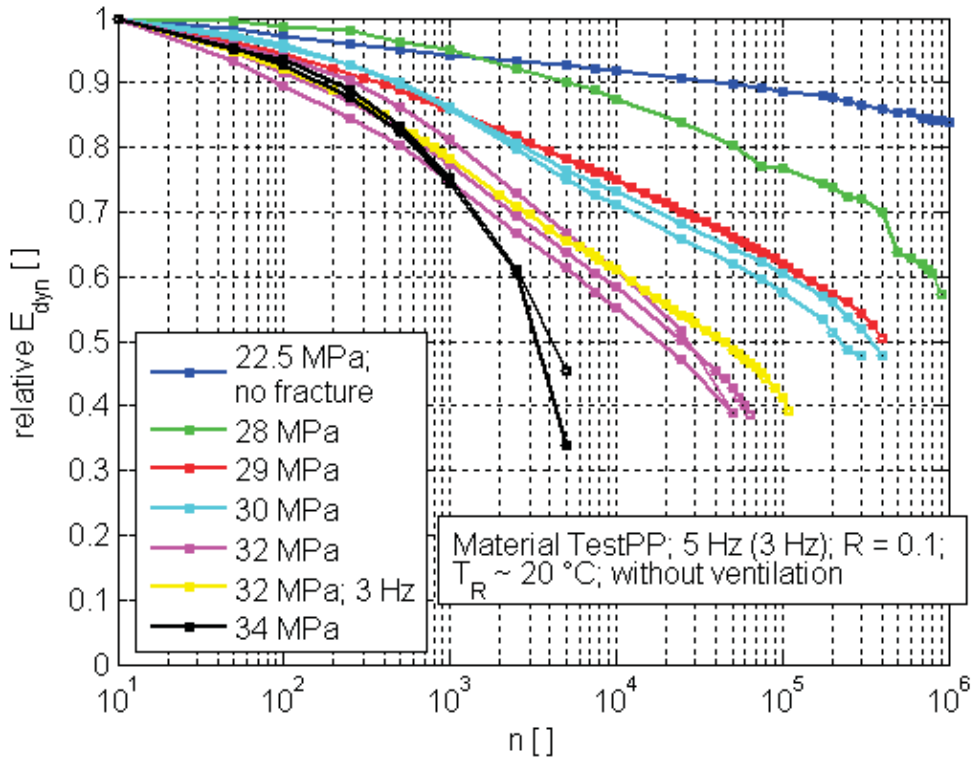

Figure 4.24: Change of the dynamic modulus over the number of cycles at different σ_{max}.

Figure 4.25 shows the change of the relative secant modulus (damage and creep). Here a similar picture can be seen. With increasing load level the decrease of the secant modulus is more pronounced. In Figure 4.26 a comparison of the development of the relative secant modulus and the relative dynamic modulus is shown at two load levels. At the test at σ_{max} = 22.5 MPa, the decrease of the secant modulus is more than double the decrease of the secant modulus. This is a sign of the dominance of the creep at this test. At the test at σ_{max} = 34 MPa, the difference between the two moduli is much lower and barely increases during the test. This shows that the fatigue damage is the dominant phenomenon at this stress level.

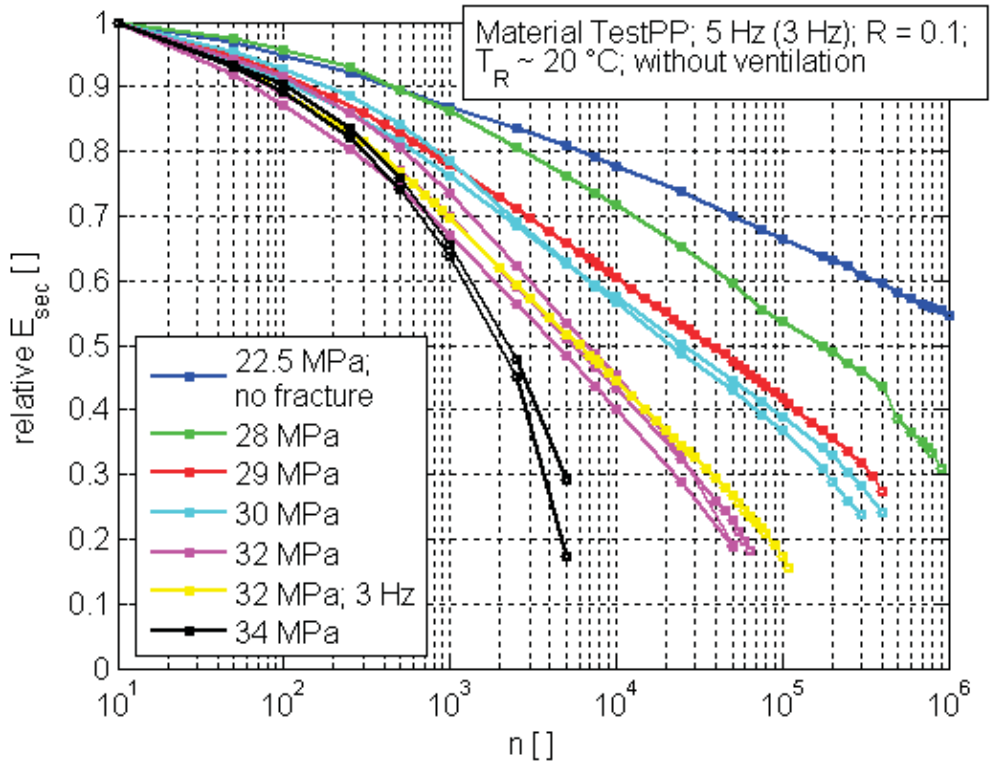

Figure 4.25: Change of the relative secant modulus over the number of cycles at different σ_{max}.

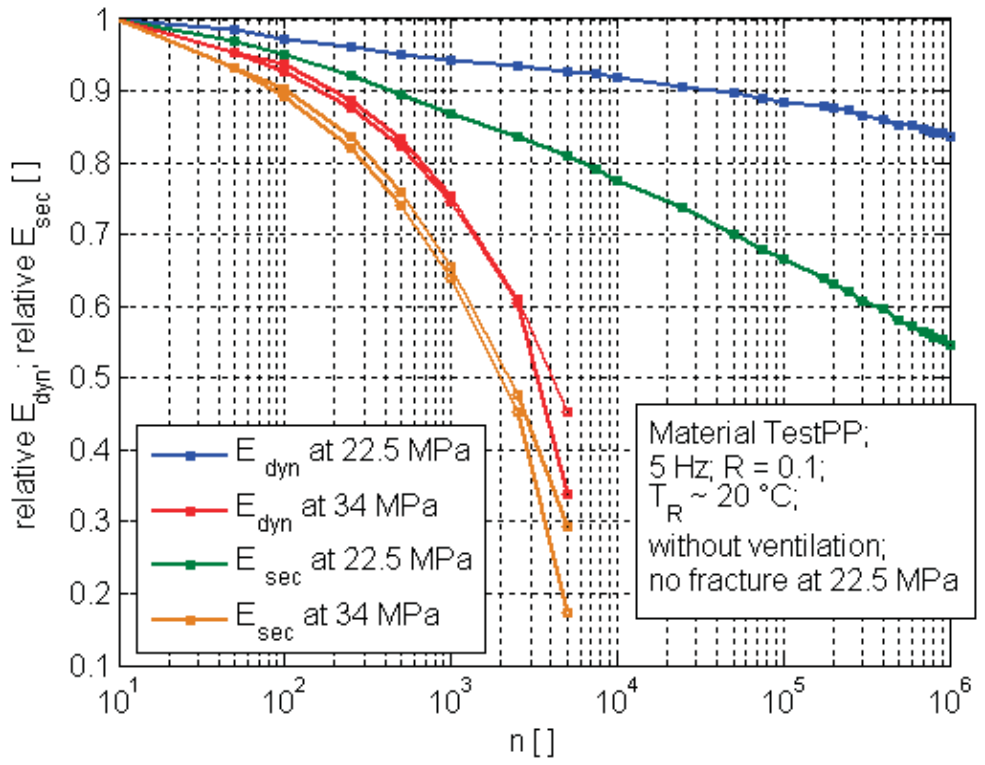

Figure 4.26: Change of the relative secant modulus compared to the change of the relative dynamic modulus.

4.1.5 Chosen test parameters for further tests

After these investigations with tests with different test parameters a certain understanding of the influences of the different parameters on the problem of hysteretic heating and thermal fatigue was acquired. The R-value seems to be a possibility as well as the frequency to vary the hysteretic heating. The problem of a decrease in the frequency is the increase of time needed for a fatigue test with a certain number of cycles. A decrease in the frequency from 5 to 2 Hz that would be sufficient to avoid a thermal fatigue also at high stress levels (Zhou and Mallick, 2005) would cause an increase of the test time for the same cycle numbers by a factor of 2.5. The increase of the R-value also has a big disadvantage: the increase of the influence of creep on the fatigue test. So the best way to avoid a thermal fatigue and long testing times in this case seems to be cooling by ventilation.

4.2 Effect of fillers and filler-contents on the fatigue behaviour

Bellow we see a comparison of different filled PP-composites from Borealis. These tests were run under cooling by ventilation (air-temp.: ~ 20 °C). The increase in the surface temperature was measured during testing. In general, the maximum temperature at the surface of the specimen was around 23 ±2 °C during the fatigue test.

4.2.1 Influence of filler type

Two different types of fracture occurred during the runs with the different composites and the pure PP. While the pure PP (material M1) and the PP filled with 7 w% polyolefin elastomer (material ER2) showed a ductile failure with necking, the materials filled with reinforcing particles (G1 and G2, filled with 9 and 18 w% of glass spheres, and M2 and M3, filled with 10 and 20 w% of talc) showed a brittle fracture. In figure two, the two types of fracture are shown for material ER2 (ductile fracture) and material G2 (brittle fracture). These two types of fracture are different in their phenomenology and cannot be compared.

Figure 4.27: Ductile fracture with necking at ER2 (PP filled with 7 w% of polyolefin elastomer) at σ_{max} = 24.5 MPa (top) and brittle fracture at material G2 (PP filled with 19 w% of glass spheres) at σ_{max} = 26.75 MPa (bottom). Test conditions: R = 0.1, 5 Hz, with ventilation, T_R ~ 20 °C.

4.2.1.1 Comparison of reinforcing particles glass and talc

In the S-N diagram it is clear that with material M3 some specimen broke at a lower cycle number than expected (Figure 4.28)

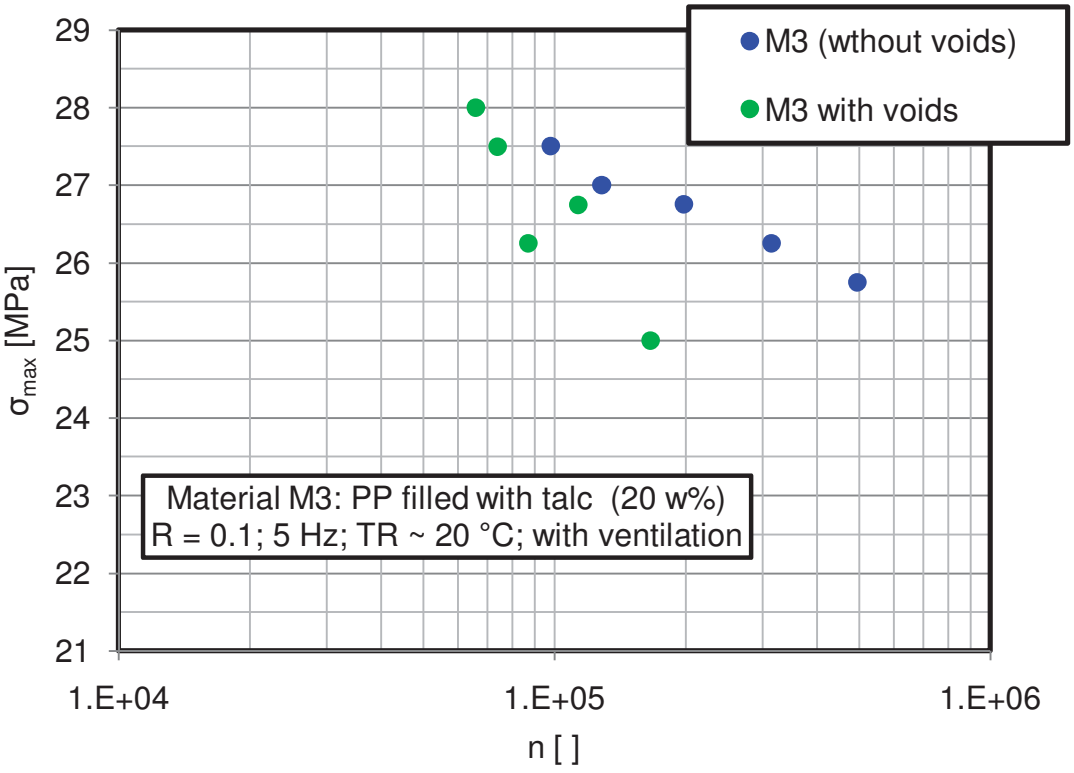

Figure 4.28: S-N diagram of material M3 (7 v% talc).

A further investigation of the fracture surfaces by/with an SEM showed small voids at the specimen that broke after a relatively short lifetime (green points in Figure 4.28). These voids could not be found in the other specimen (blue points in Figure 4.28). These voids seem to be cavities or bubbles and might be the result of the processing at conditions that are not optimised. In Figure 4.29 a SEM micrograph shows the fracture surface of a specimen that showed an unexpectedly early fracture (σ_{max} = 26.25 MPa), The influence of the voids seems to be significant especially at low stress levels.

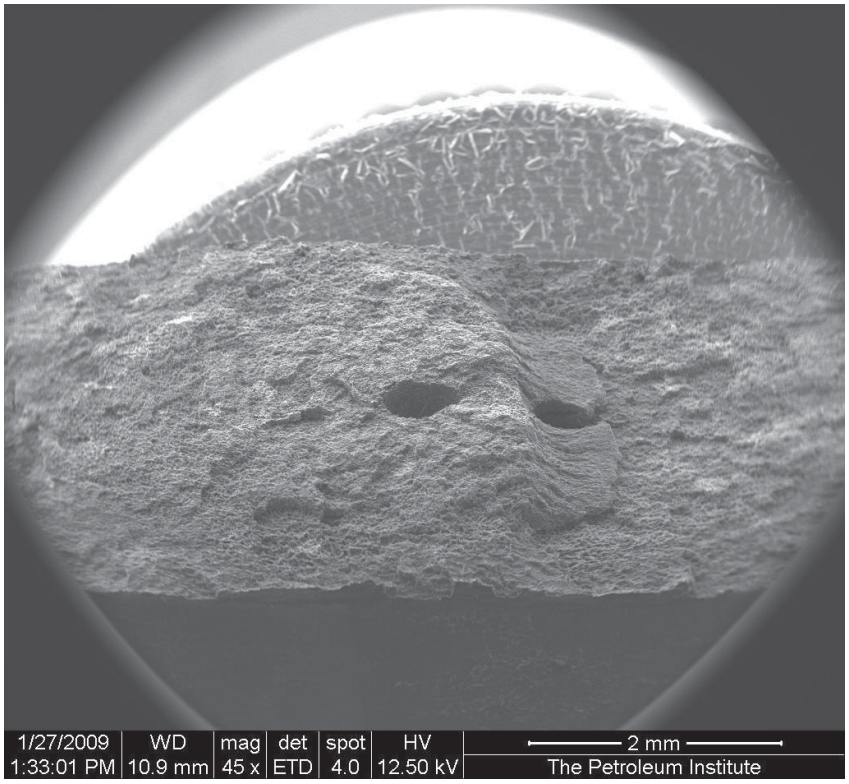

Figure 4.29: Fracture surface of material M3 at σ_{max} = 26.25 MPa with voids in the centre of the fracture surface (two cavities).

In Figure 4.30 the materials G2 (18 w% of glass spheres) and M3 (20 w% of talc) are compared concerning their lifetime. No significant differences could be found in the S-N diagram. Thus the influence of the type of filler seems to be negligible concerning the fatigue lifetime for these two fillers at the used testing range and used the testing conditions used.

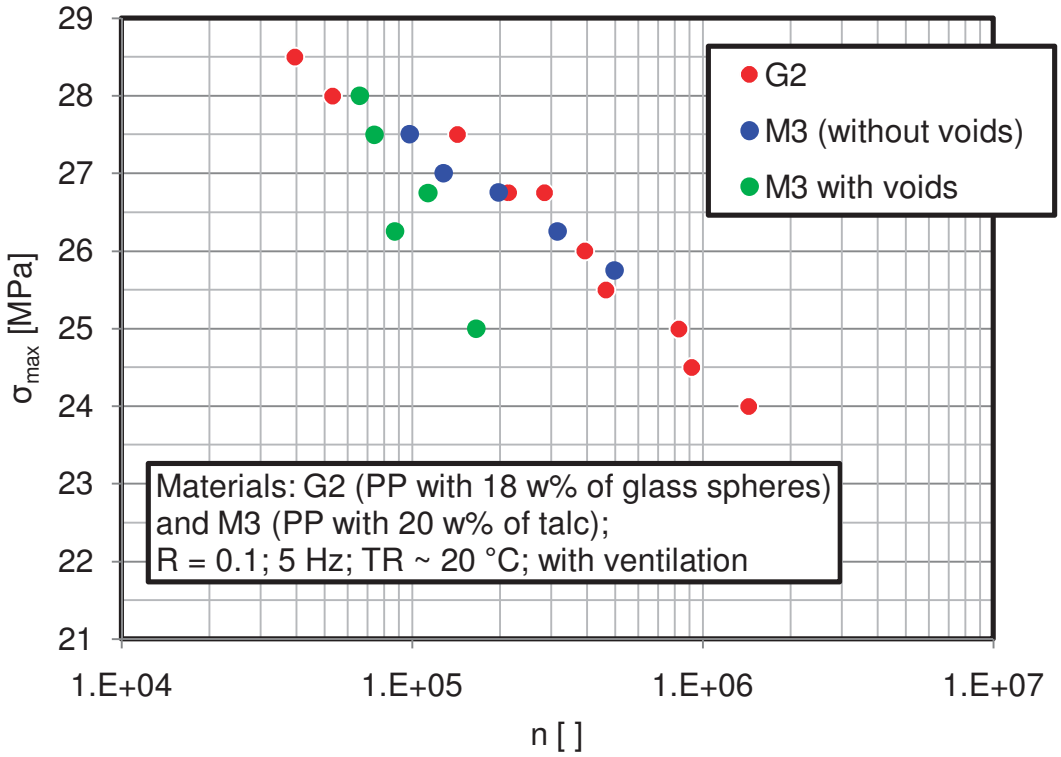

Figure 4.30: S-N diagram of different filled PP.

The development of the dynamic modulus during the fatigue test at a stress level of σ_{max} = 26.75 MPa is shown in Figure 4.31. The dynamic modulus decreases steadily during the entire test for both materials. This is an indication of a steady increase of damage in the material during the fatigue test. A comparison of the relative dynamic modulus shows a faster decrease of the dynamic modulus for material G2 (Figure 4.32). Figure 4.33 shows the development of the secant modulus for the same tests. The development of the relative secant modulus also shows a stronger decrease for material G2 (Figure 4.34). A comparison of Figure 4.32 and Figure 4.34 shows that both, damage and creep appear in a significant value at these stress levels. While the decrease of the dynamic modulus is around 40 % (mainly caused by fatigue damage) during the fatigue tests, the secant modulus decreases by about 80 % (caused by fatigue damage and creep).

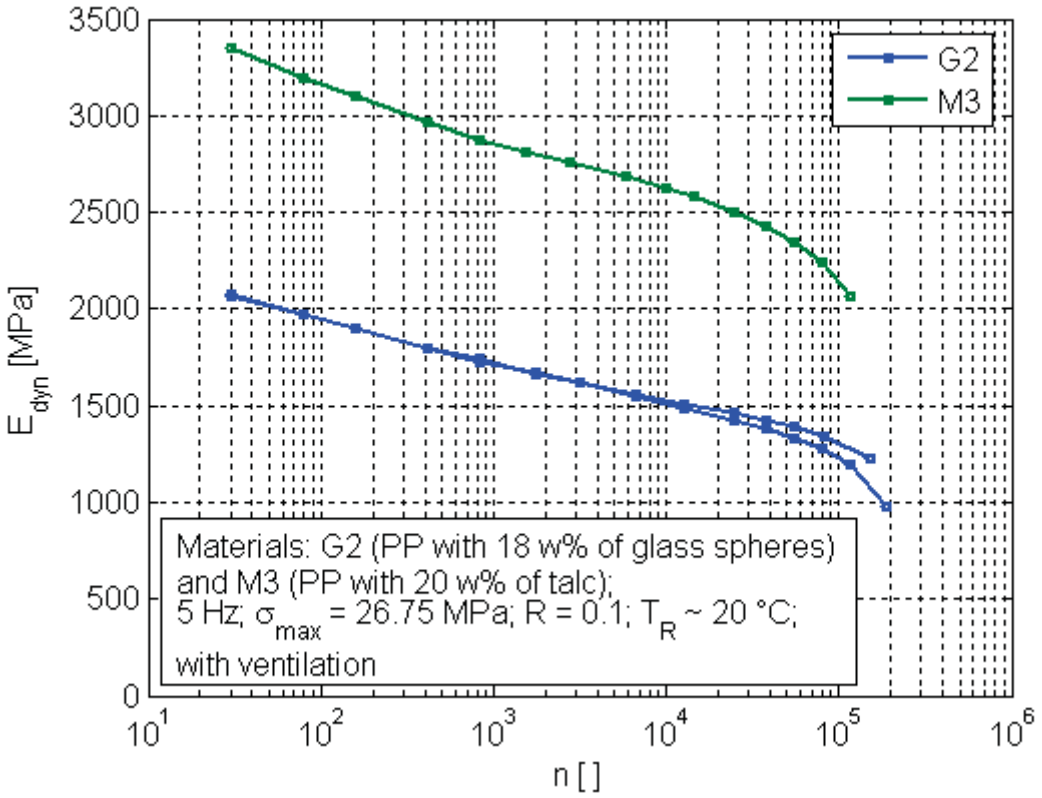

Figure 4.31: Development of the dynamic modulus for materials G2 and M3.

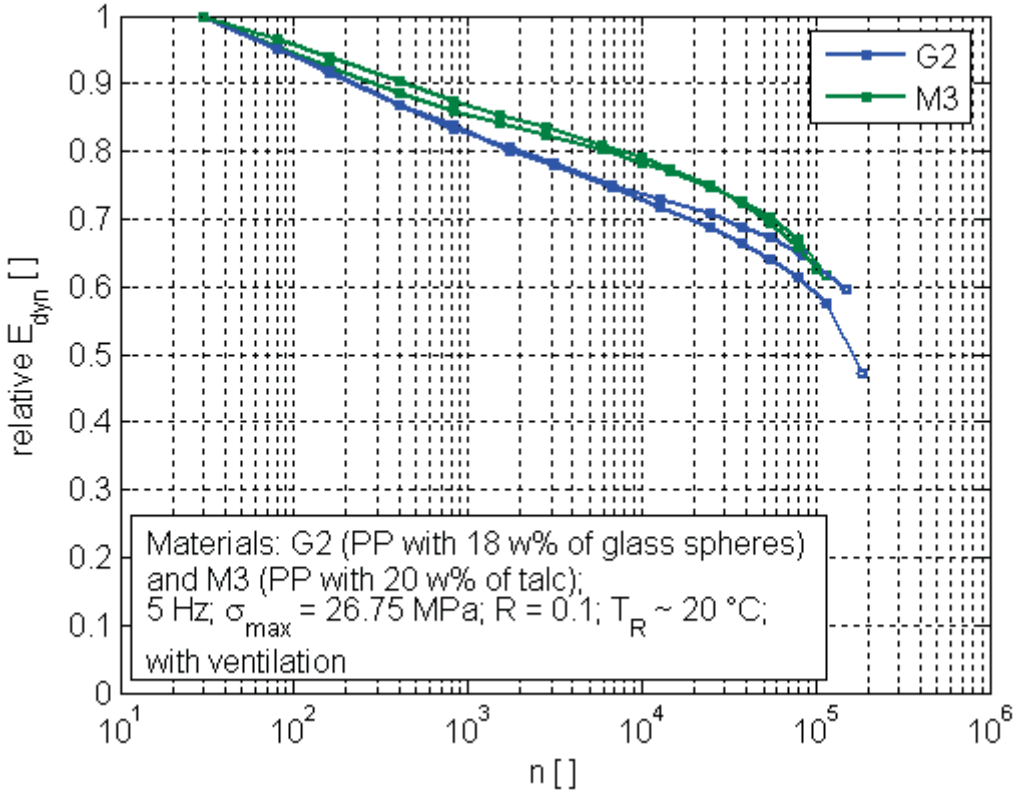

Figure 4.32: Development of the relative dynamic modulus for materials G2 and M3.

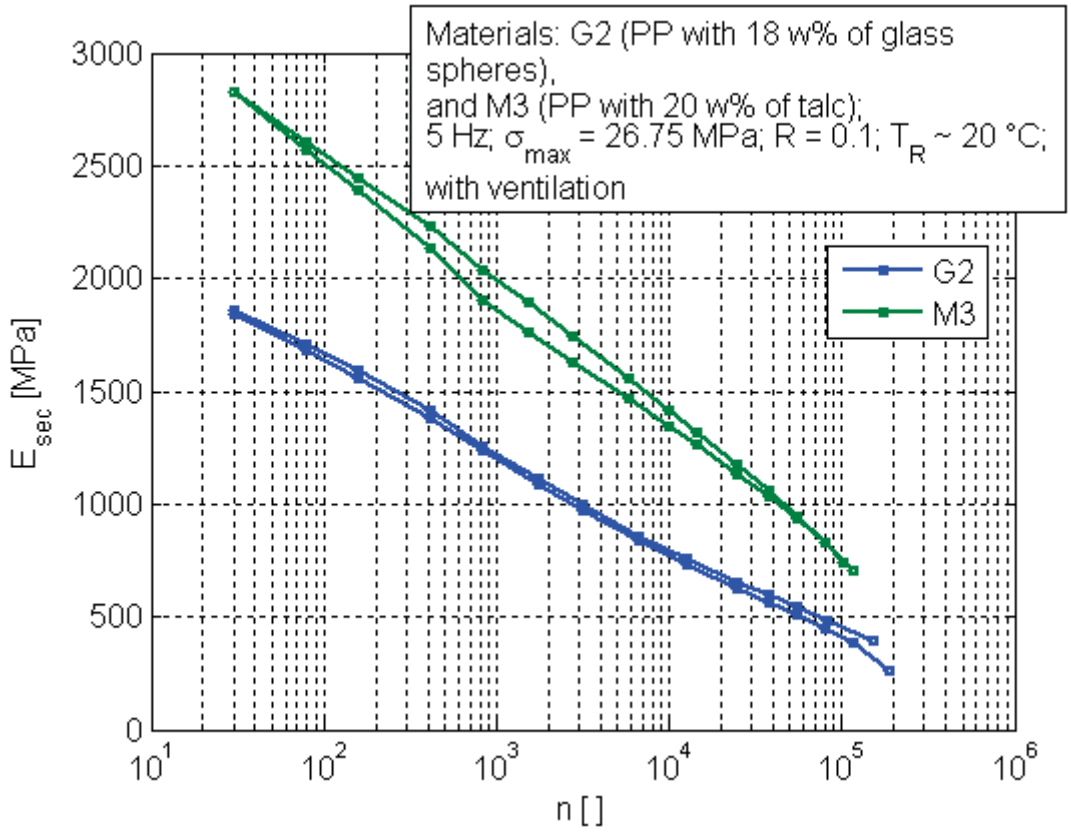

Figure 4.33: Development of the secant modulus for materials G2 and M3.

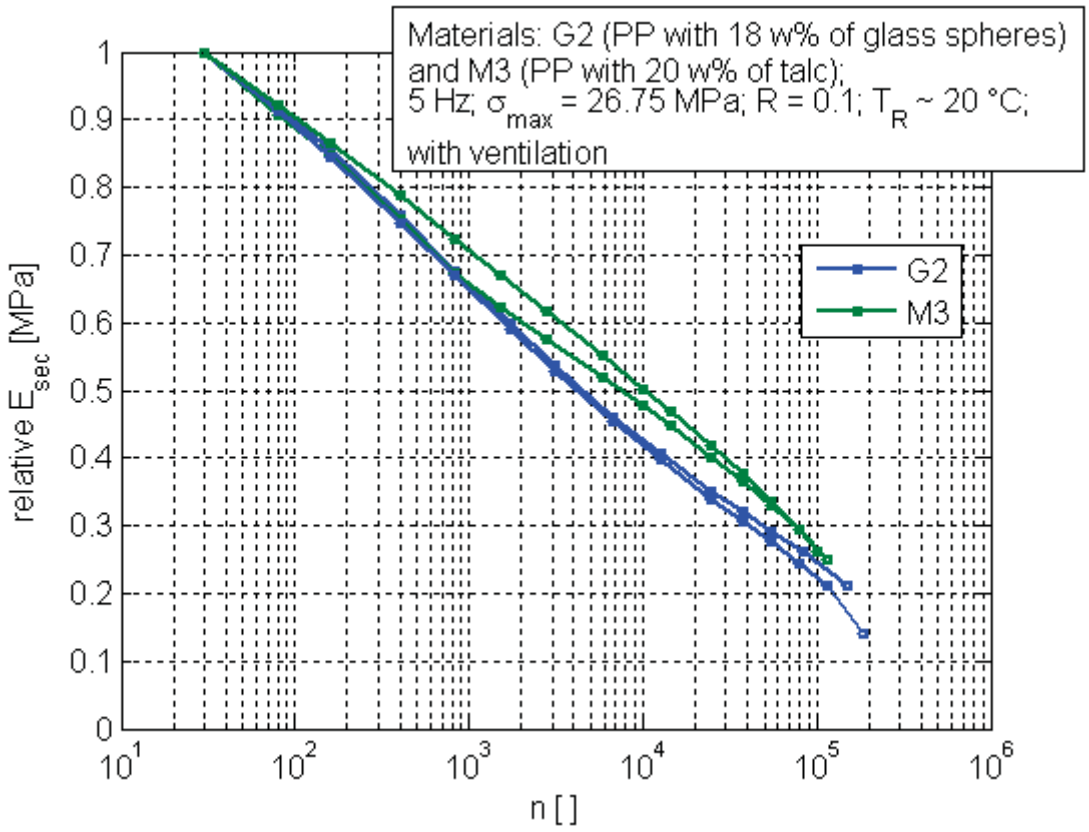

Figure 4.34: Development of the relative secant modulus for materials G2 and M3.

In the isocyclic stress strain diagrams (Figure 4.35 and Figure 4.36), the influence of the voids at M3 is negligible because the voids are a local problem and do not influence the stiffness (extensometer measures the strain over 25 mm). A difference in materials G2 and M3 is visible in the isocyclic diagrams, especially in the slope of the curves. In Figure 4.35, the influence of the filler type is significant at both plotted cycle numbers. A comparison of Figure 4.35 and Figure 4.36 shows that at low stress levels the creep seems to dominate while at higher stress levels the fatigue damage also starts to increase rapidly with the cycle number.

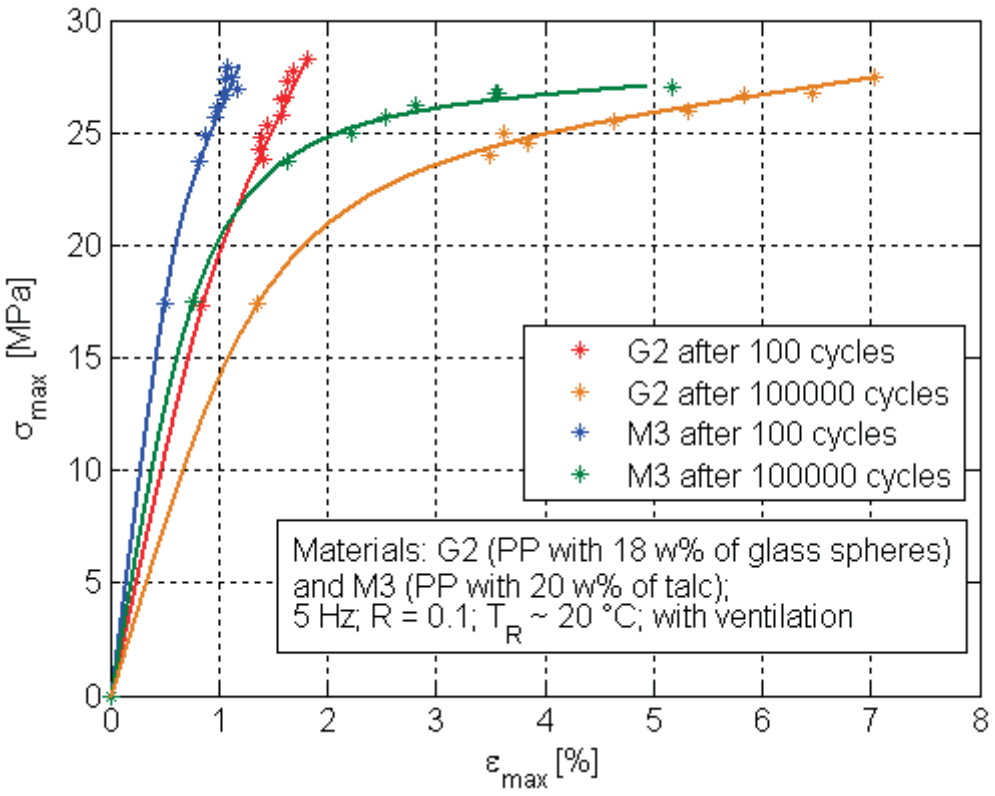

Figure 4.35: Isocyclic σ_{max} - ε_{max} diagram of materials M3 and G2.

The difference in the slope of the different materials in the Δσ-Δε diagram (Figure 4.36) shows the difference in the modulus of the materials. As expected, the material filled with talc shows a higher stiffness compared to the material filled with glass spheres. A significant splitting up of the isocyclic Δσ-Δε curves seems to start at a Δσ of above 15 MPa. That means that there does not appear a significant damage at stress levels bellow a Δσ of 15 MPa during the first 100,000 cycles.

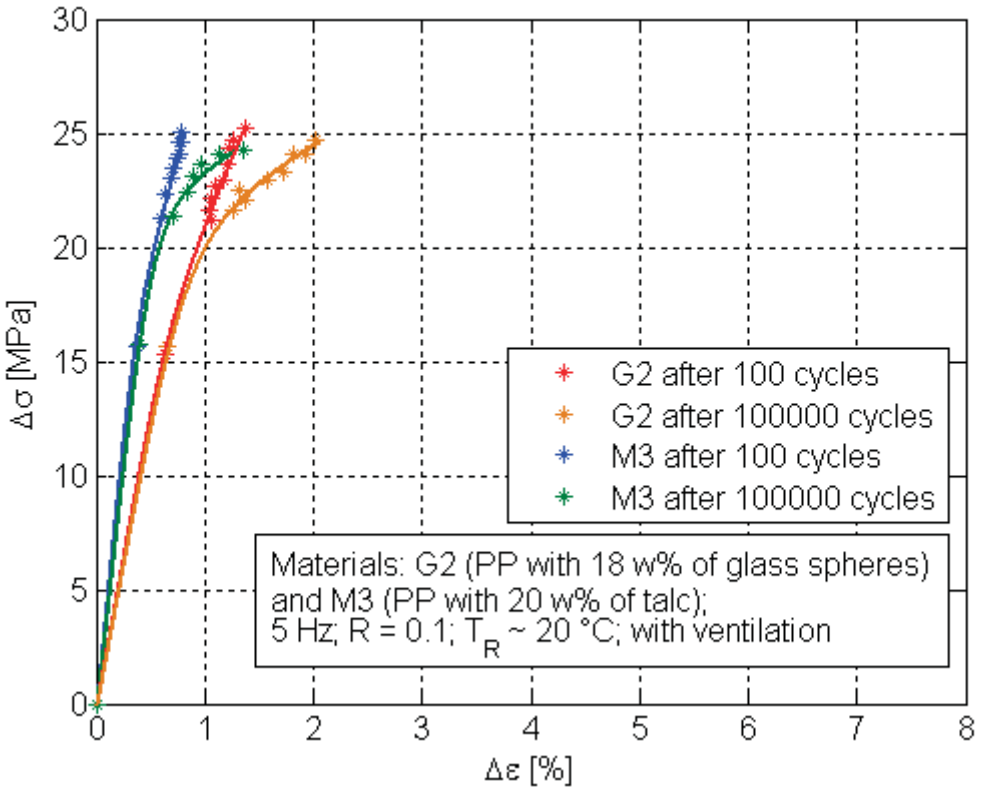

Figure 4.36: Isocyclic Δσ - Δε diagram of materials M3 and G2.

4.2.1.2 Materials M1 and ER2

Unlike the glass and talc filled PP-types, material ER2 (PP filled with 7 w% of TPO) and material M1 (pure PP) showed a ductile fracture with necking during the fatigue tests (compare Figure 4.27). This type of fracture is totally different to the brittle fracture and therefore the results cannot be compared. Because of this only a few runs were performed with these materials. The results can be seen in Figure 4.37. For material ER2 an S-N curve was found that lies distant from the others (rubber-filled). This was expected because of the total different mechanical properties compared to the other tested composites (lower modulus and lower tensile strength, compare Table 3.1). The S-N-diagram for ER2 shows also a significant lower value compared to the pure PP (M1). This correlates to the results found for the tensile tests.

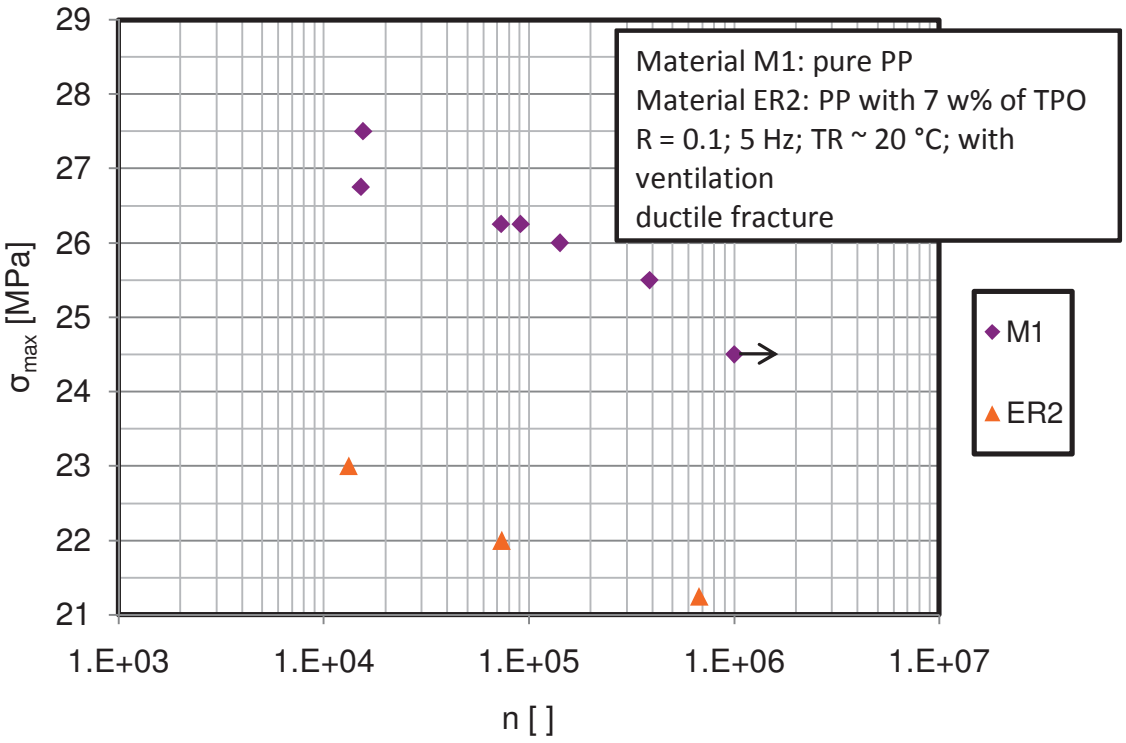

Figure 4.37: S-N diagram of materials M1 and ER2.

4.2.2 Influence of filler content

4.2.2.1 Polypropylene filled with glass spheres

The S-N diagram of the PP filled with 18 w% of glass spheres (G2), run under ventilated conditions, can be seen in Figure 4.38. The tests were run at stress levels between 24 MPa and 28.5 MPa. The points build a rather linear S-N curve. The only exceptions seem to be the runs at stress levels of 28 MPa and above. There the influence of thermal fatigue might be a problem. The S-N curve without the two measured points at 28 MPa and above (green curve) shows a significantly different slope to the S-N curve that includes these points (red curve).

A comparison of two tests - one at 27.5 MPa and one at 28.5 MPa – concerning the development of the maximum surface temperature may provide a possible explanation (Figure 4.39). While at the run at 27.5 MPa the maximum surface temperature stays around 22 to 24 °C, the temperature at the run at 28.5 MPa increases to 26.8 °C at ~ 36,000 cycles and to 32 °C before fracture.

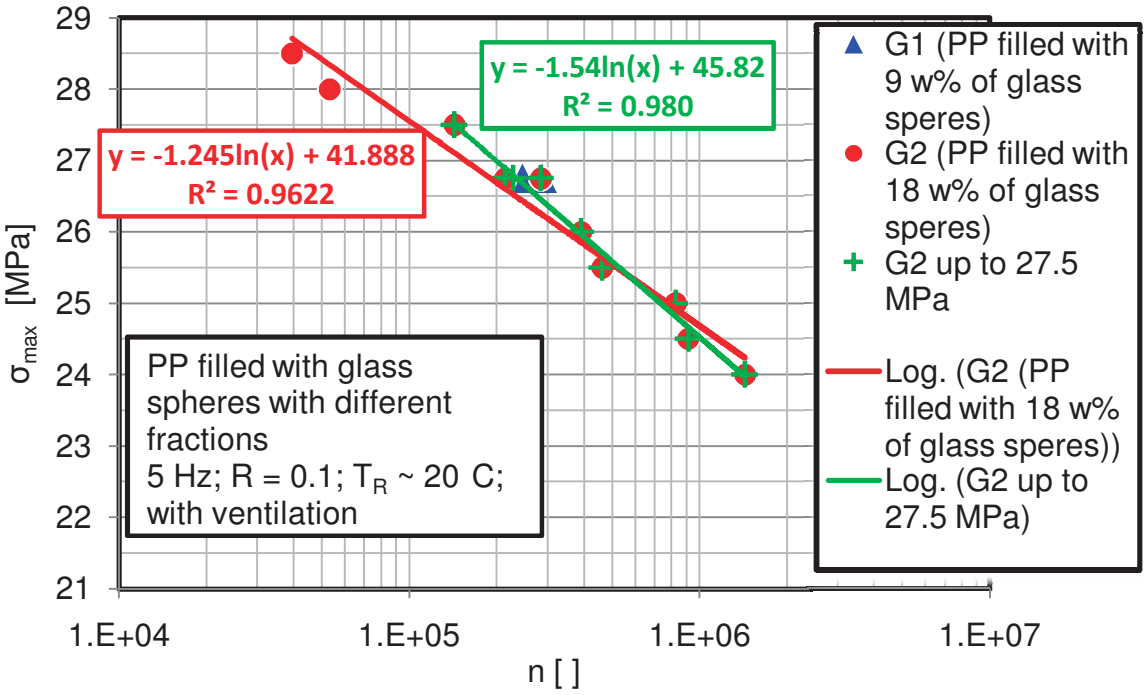

Figure 4.38: S-N curve of PP filled with glass spheres.

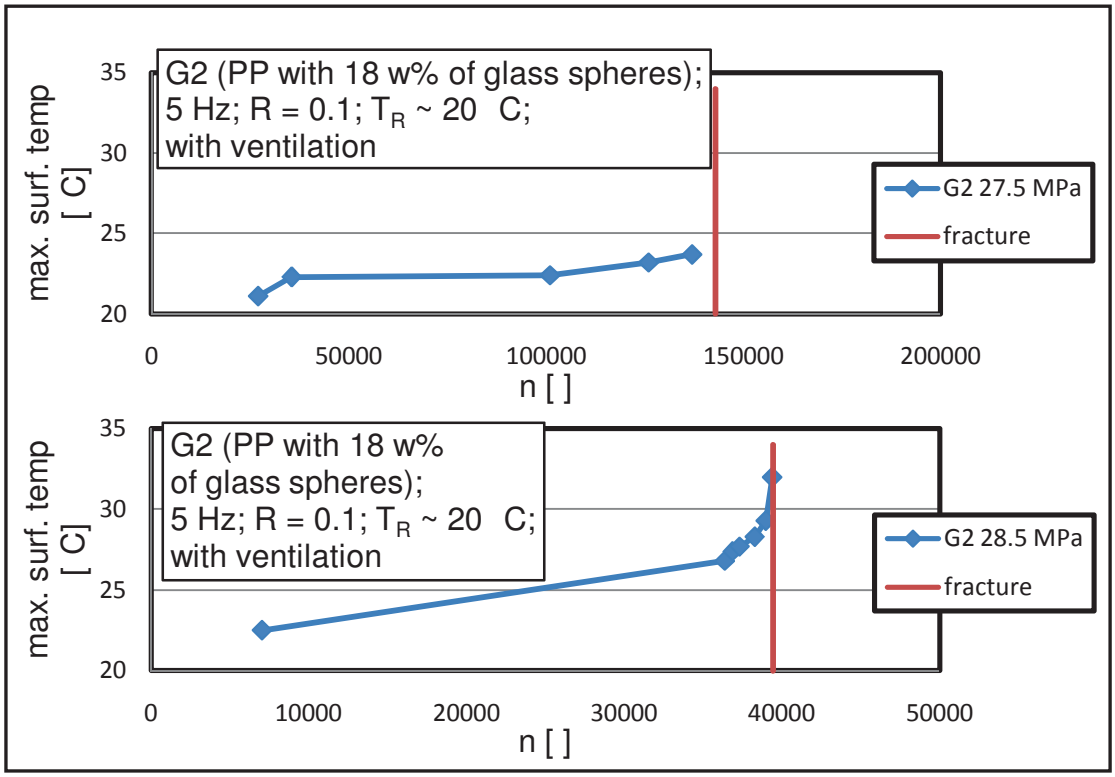

Figure 4.39: Development of the temperature at different stress levels.

Even if this increase of temperature is only observed a short time before fracture, the increase (that might start in this case maybe after 80 % of the lifetime) seems

to be a hint that thermal fatigue starts to play a role at these stress levels. At the other stress-levels thermal fatigue probably also plays a role a short time before fracture, when the energy of loss starts to get too high. But the influence of it seems to increase with an increasing stress level.

The influence of the filler amount was not expected to be significant between G1 (9 w% glass spheres) and G2 (18 w% glass spheres). Therefore only two tests were run with material G1 at a stress level of σ_{max} = 26.75 MPa. As expected, the lifetimes for G1 are in the same region as for runs with G2 at the same stress level. A comparison of the development of the dynamic modulus shows that both materials behave quite similarly (Figure 4.40). A difference in the modulus at the different filler contents of ~ 100 MPa can be detected in this diagram. Figure 4.41 shows the development of the secant modulus at G1 and G2. In this diagram hardly any difference can be detected in the behaviour of the two materials. So the materials also behave similarly concerning the creep.

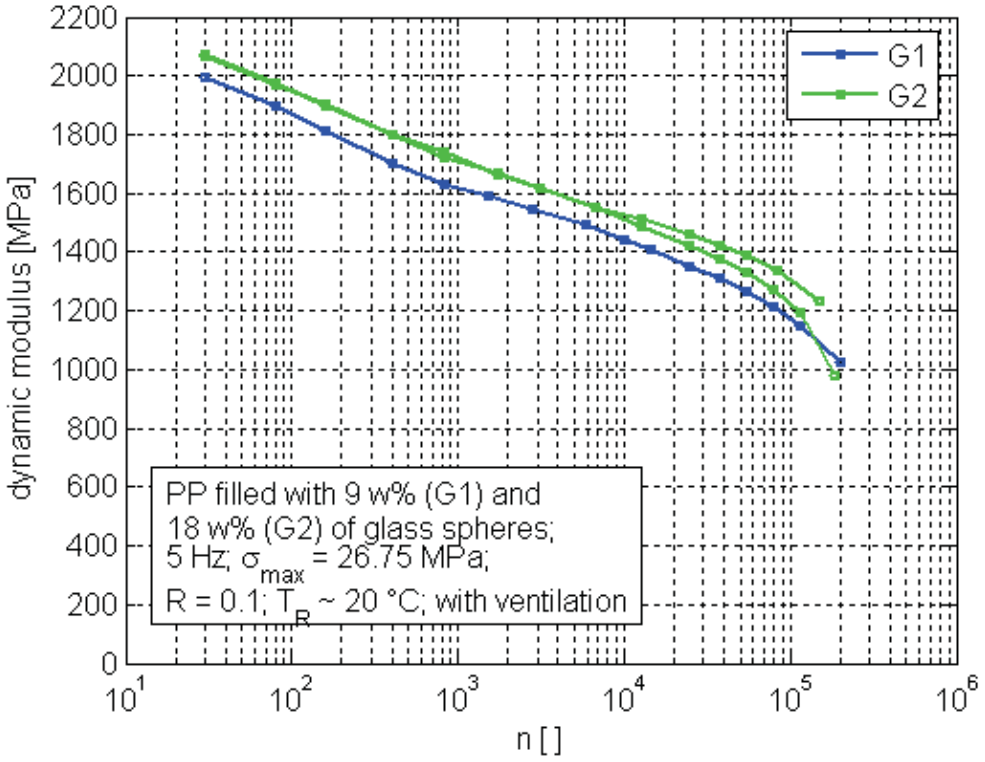

Figure 4.40: Development of the dynamic modulus at materials G1 and G2.

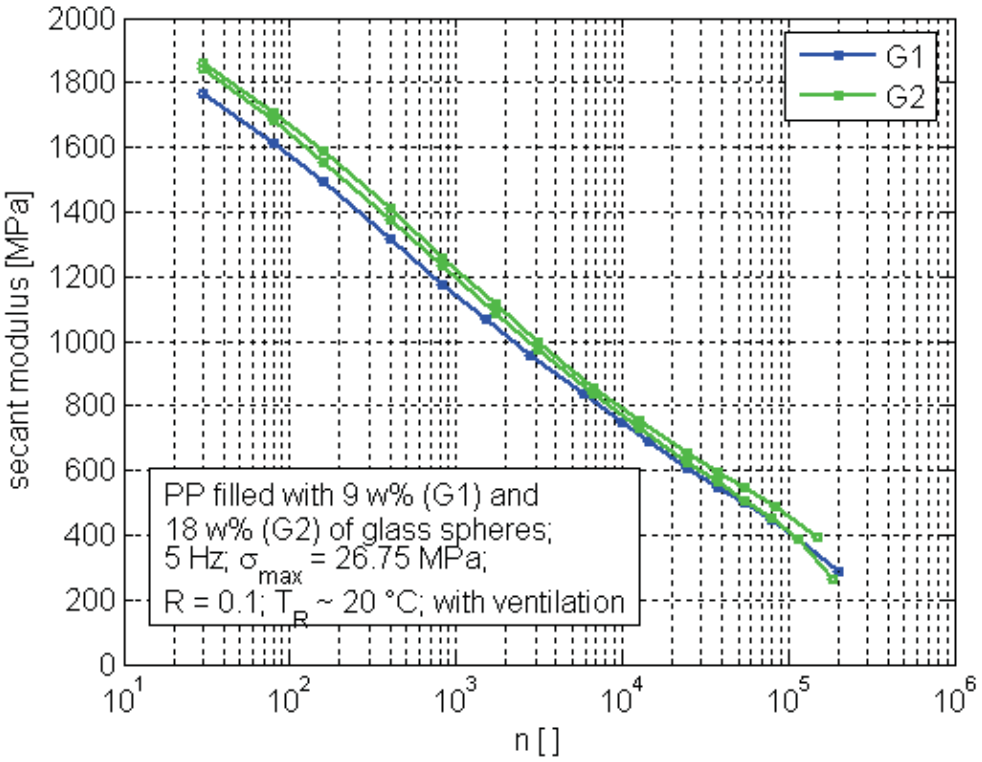

Figure 4.41: Development of the secant modulus at materials G1 and G2.

In Figure 4.42 and Figure 4.43 the similar behaviour of the two materials during the fatigue test is more obvious. The curves of G1 and G2 are more or less congruent in these diagrams. While the dynamic modulus decreases to 50 % of the modulus after 30 cycles, the secant modulus ends at 15 to 20 % of the start level. This means both, creep and fatigue damage are occurring in a high range at these materials. Figure 4.44 compares the development of the relative dynamic modulus and the relative secant modulus at different stress levels. At both stress levels (σ_{max} = 25 MPa and σ_{max} = 27 MPa) the secant modulus shows a significant higher slope than the dynamic modulus. This means that creep is occurring in a significant range at both stress levels.

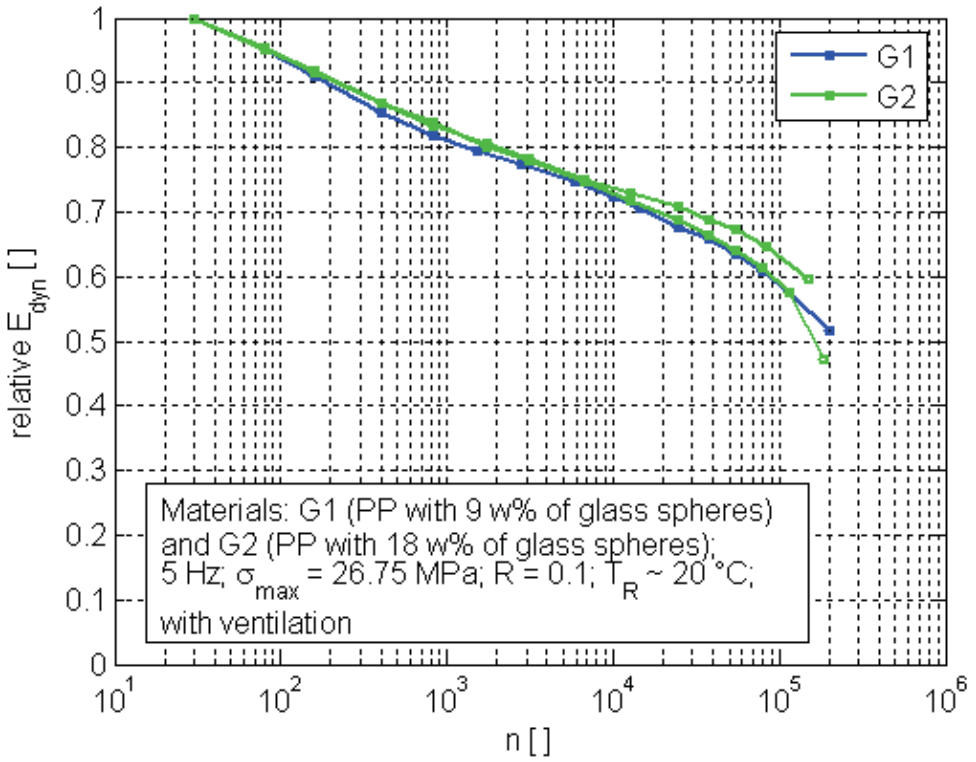

Figure 4.42: Development of the relative dynamic modulus for materials G1 and G2.

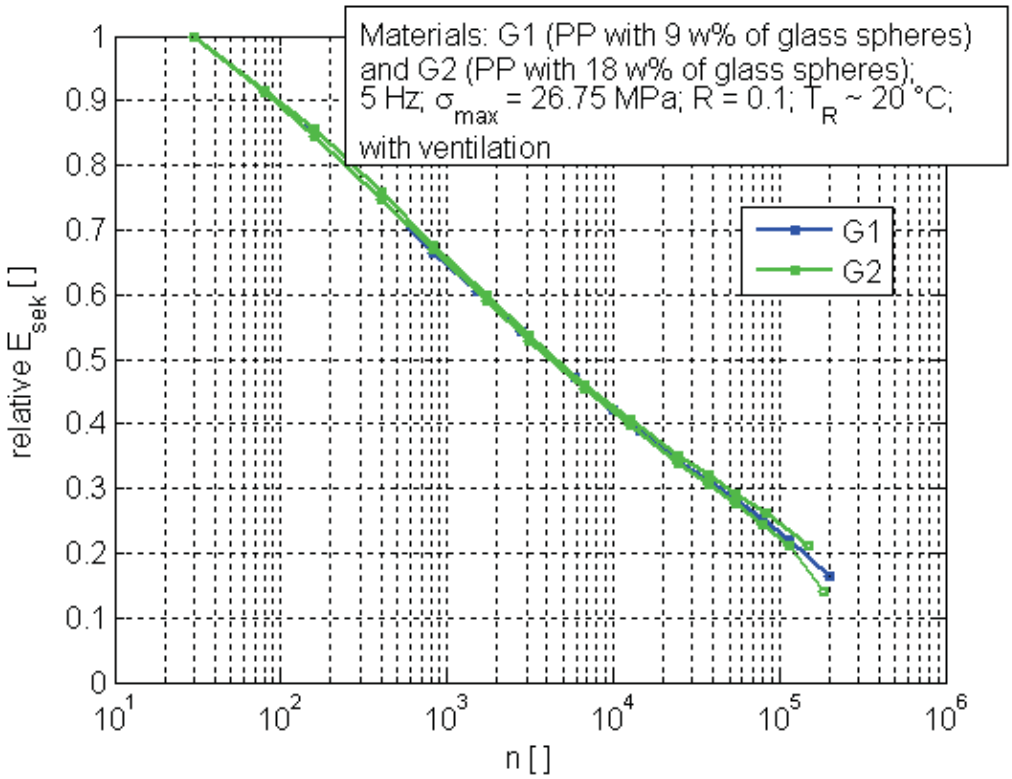

Figure 4.43: Development of the relative secant modulus for G1 and G2.

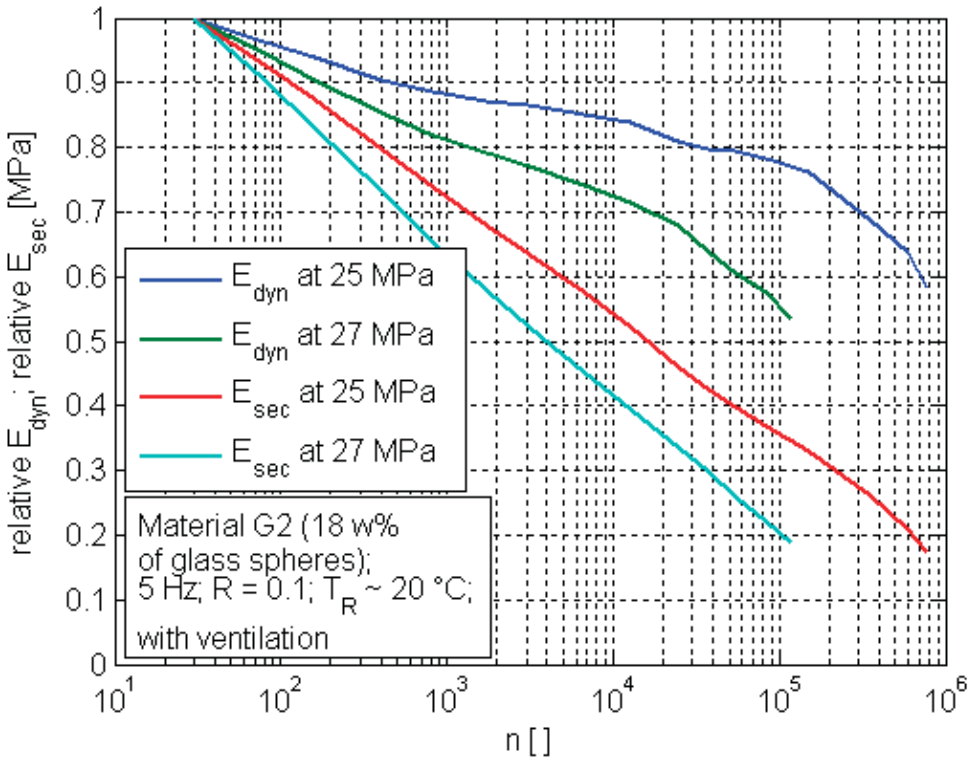

Figure 4.44: Development of the relative dynamic modulus and the relative secant modulus for material G2.

4.2.2.2 Polypropylene filled with talc

The S-N diagrams of the two talc filled polypropylene types shows a slight but obvious influence of the filler content (Figure 4.45). The composites with the lower content (M2, 10 w%) seem to show a better fatigue performance than the composite with the higher content (M3, 20 w%). The lifetime was found to be significantly higher for M2 compared to M3 at all stress ranges. M2 showed nearly the double of the lifetime of M3 at the stress level of σ_{max} = 27.5 MPa.

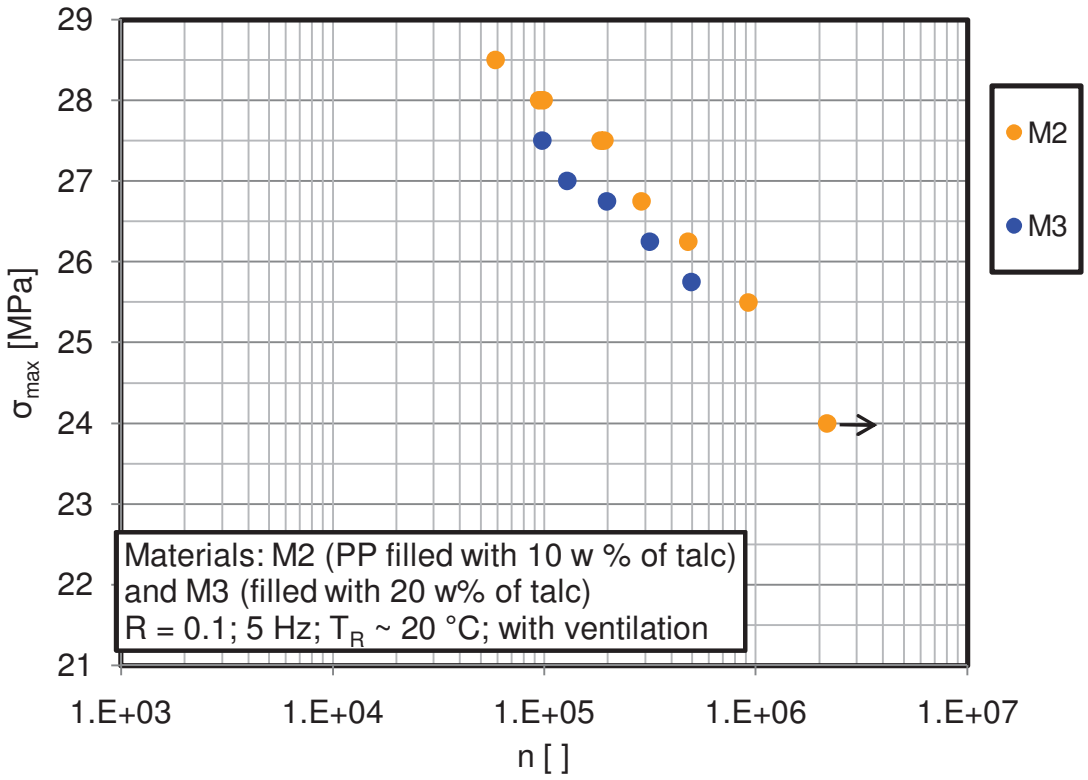

Figure 4.45: S-N curve of PP filled with different fractions of talc.

A comparison of the dynamic modulus shows a more or less parallel development of the modulus at material M2 (10 w% talc) and M3 (20 w% talc) with an increasing cycle number. M3 shows a significantly higher modulus over the whole lifetime, as expected (Figure 4.46). A comparison of the relative dynamic modulus (dynamic modulus relative to the dynamic modulus after 30 cycles) shows that the general behaviour concerning development of the dynamic modulus of the materials with the different content of glass spheres is similar (Figure 4.47). At higher cycle numbers (>10^4), the material with the higher content of filler (M3) shows a faster decrease of the modulus. This means that material M3 shows a higher sensitivity concerning fatigue. The same result was found in the S-N diagram (Figure 4.45). A comparison of the development of the secant modulus of M2 and M3 shows no significant difference. So the creep seems to be independent of the filler content between M2 and M3 (Figure 4.48). Both materials show a strong decrease of the secant modulus during the fatigue test. A short time before fracture the secant modulus is not more than 20-25 % of the secant modulus after 30 cycles.

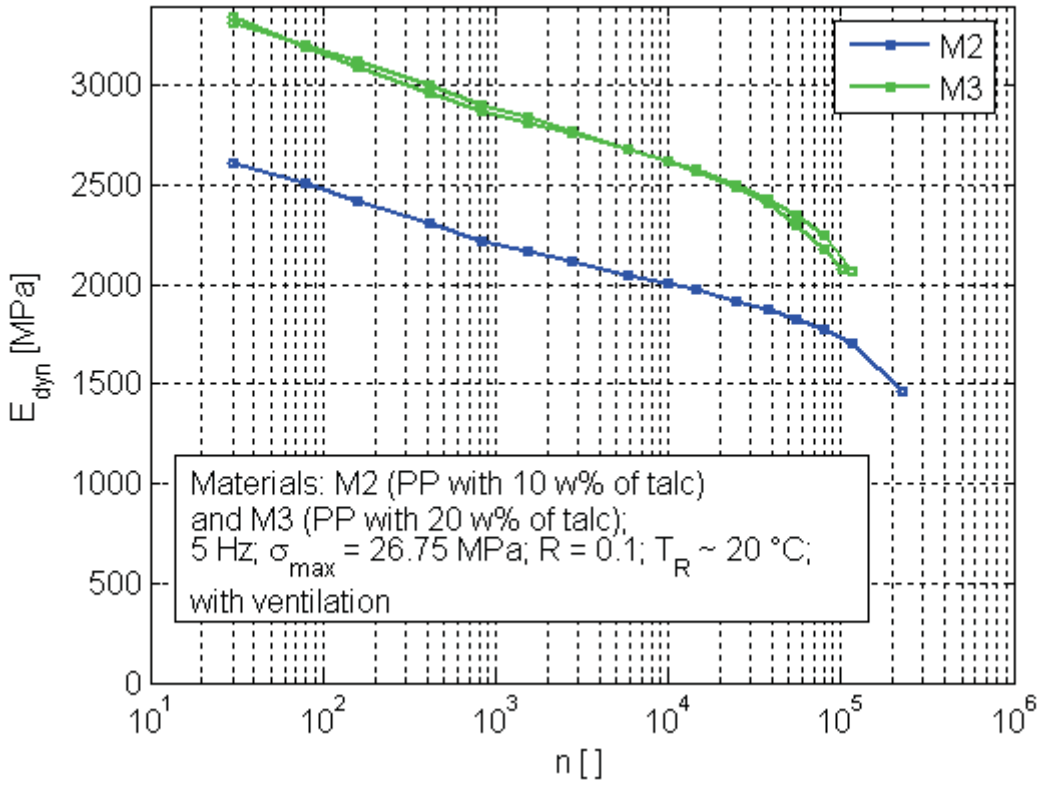

Figure 4.46: Development of the dynamic modulus at M2 and M3.

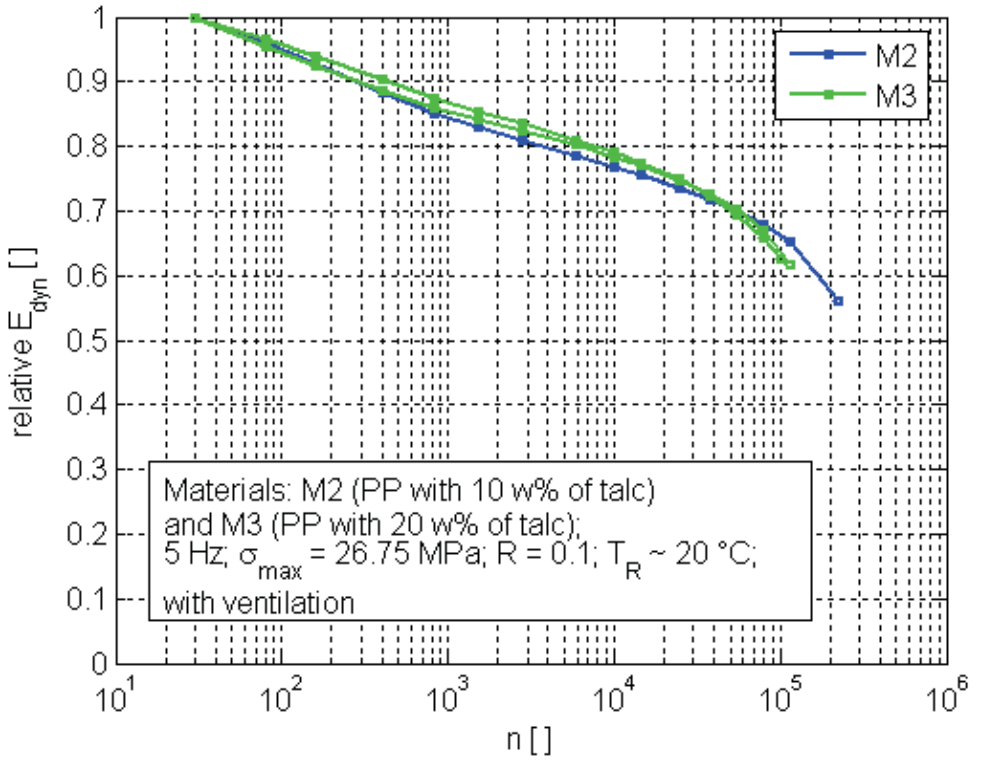

Figure 4.47: Development of the dynamic modulus relative to the dynamic modulus after 30 cycles (M2 and M3).

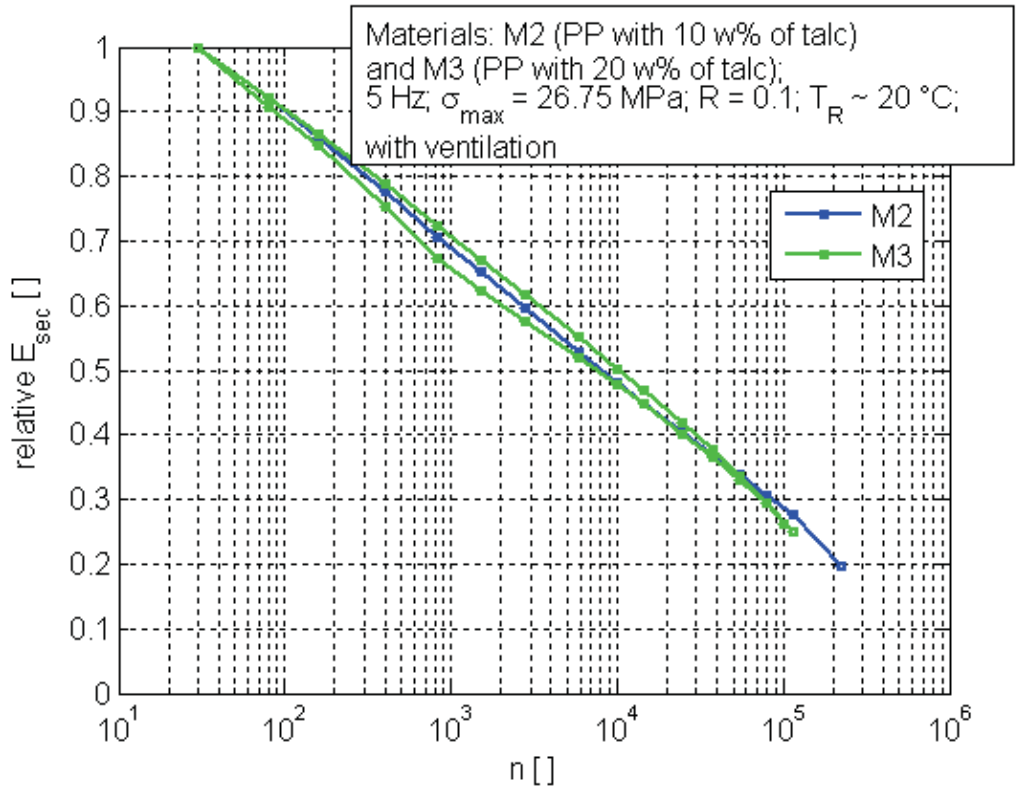

Figure 4.48: Development of the secant modulus relative to the secant modulus after 30 cycles (M2 and M3).

A comparison of two runs at different stress levels with material M2 shows that at a stress level of σ_{max} = 17.5 MPa the dominating factor is the creep. The decrease of the dynamic modulus (shows the increase of material damage) is only about 10 % during the first 500,000 cycles while the secant modulus (influenced by material damage and creep) decreases by around 50 %. In the case of σ_{max} = 28 MPa, the situation is different. At the beginning, the secant modulus shows double the decrease of the dynamic modulus, so both fatigue damage and creep are appearing at a high range. In the last region before fracture the two moduli start to develop in parallel, which means that the material damage starts to dominate. A difference in the materials M2 and M3 is visible in the isocyclic stress-strain diagrams (Figure 4.50 and Figure 4.51). The onset of the splitting up of the isocyclic $\Delta\sigma$-$\Delta\varepsilon$ curves at different cycle numbers seems to start in the same region of load level of around $\Delta\sigma$ = 15 MPa for both materials (Figure 4.51). The higher fraction of filler in material M3 causes a stiffer material behaviour (visible in the slope of the isocyclic stress-strain curves).

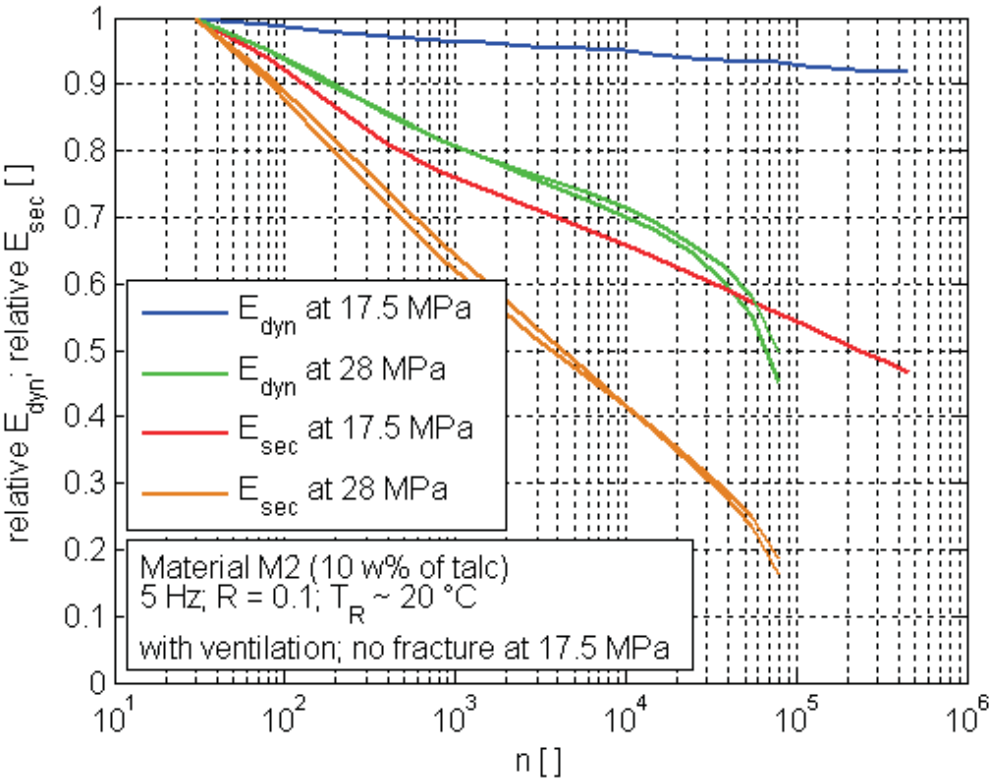

Figure 4.49: Development of the dynamic modulus and the secant modulus for two stress levels for material M2.

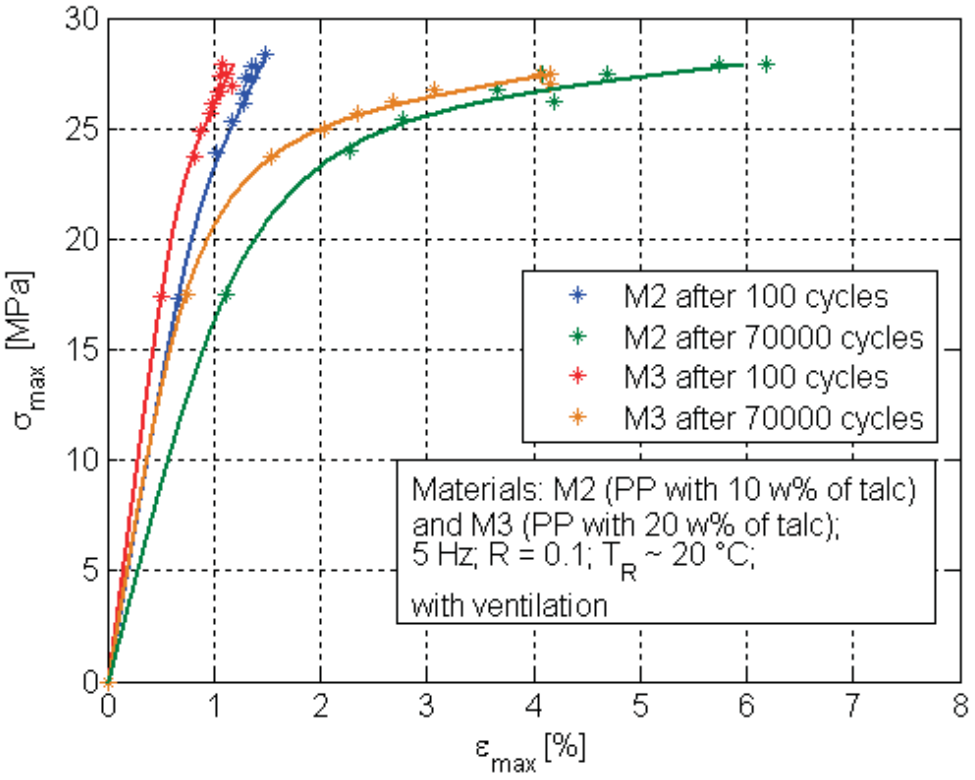

Figure 4.50: Isocyclic σ_{max}-ε_{max} diagram of talc filled PP with different talc contents.

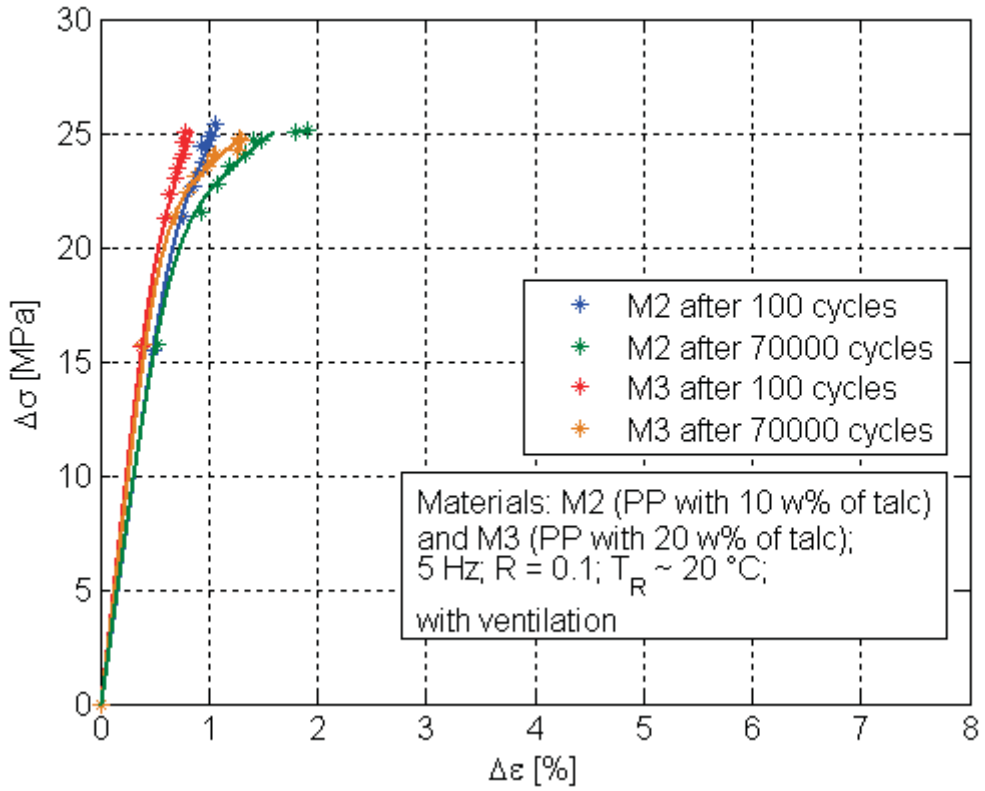

Figure 4.51: Isocyclic Δσ-Δε diagram of talc filled PP with different talc contents.

4.3 Additional investigations

4.3.1 Influence of the test frequency on the fatigue behaviour

Frequency tests were run with material G1, to evaluate the dependence of the fatigue lifetime on the frequency. The tests were run at a constant R of 0.1, a σ_{max} of 26.75 MPa and under ventilation at T_R ~ 20 °C. It was found that in the range of 0.5 to 5 Hz the lifetime (number of cycles until break) increases with the frequency (Figure 4.52). This could be due to the higher time of high load per cycle at lower frequencies. If we look at the time until break in hours (Figure 4.53), the situation is different. The higher frequency shows a negative influence on the lifetime (hours). This is caused by the fact that the load rate has a big influence on the lifetime, as well as the time of stay at high levels. An increase in the load rate increases the modulus of the material and causes a lower Δε. This decreases the material damage per cycle.

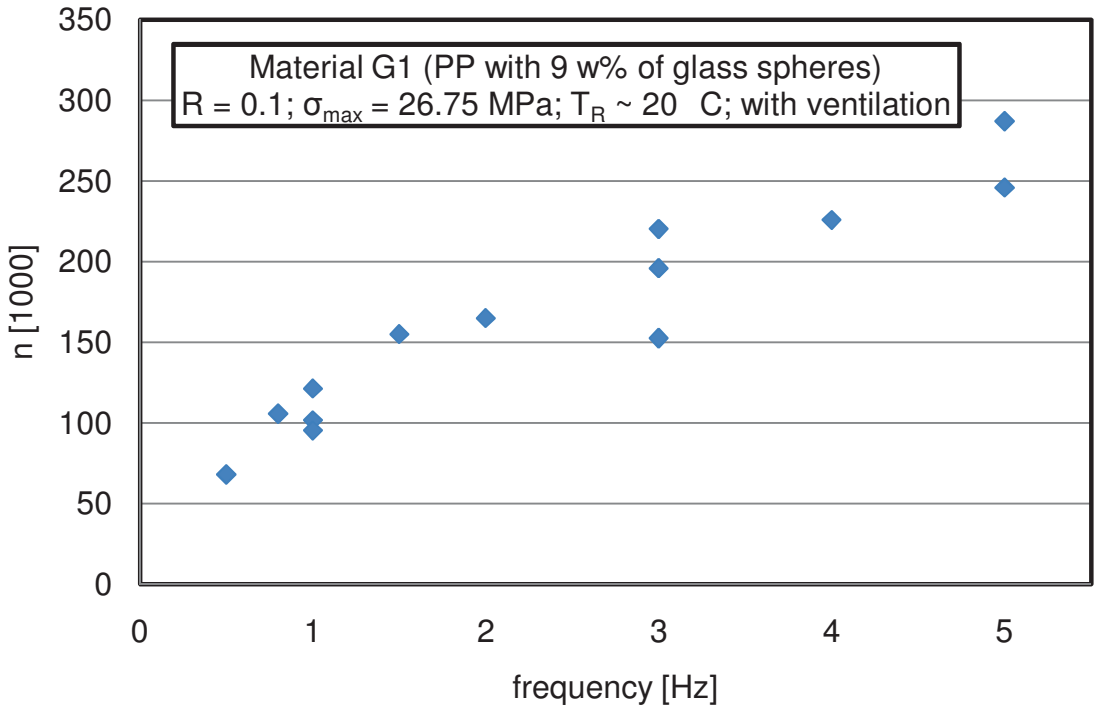

Figure 4.52: Lifetime of material G1 at different test frequencies in cycles until fracture.

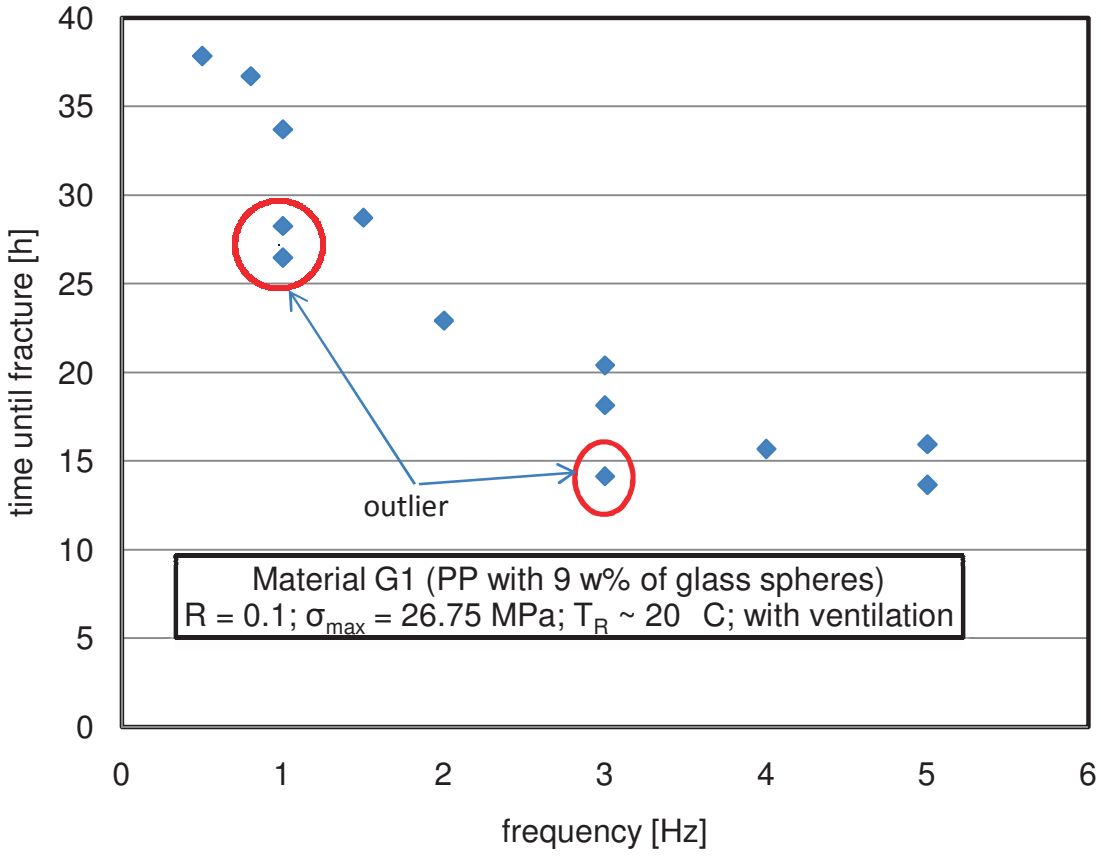

Figure 4.53: Lifetime of material G1 at different test frequencies in hours until fracture.

In Figure 4.53, three outliers are marked. These three runs broke at cycle numbers that seem to be to low compared to the other runs. An investigation of the fracture surface showed agglomerations of filler particles at the specimen with the outlying fracture cycle number at 3 Hz (Figure 4.54).

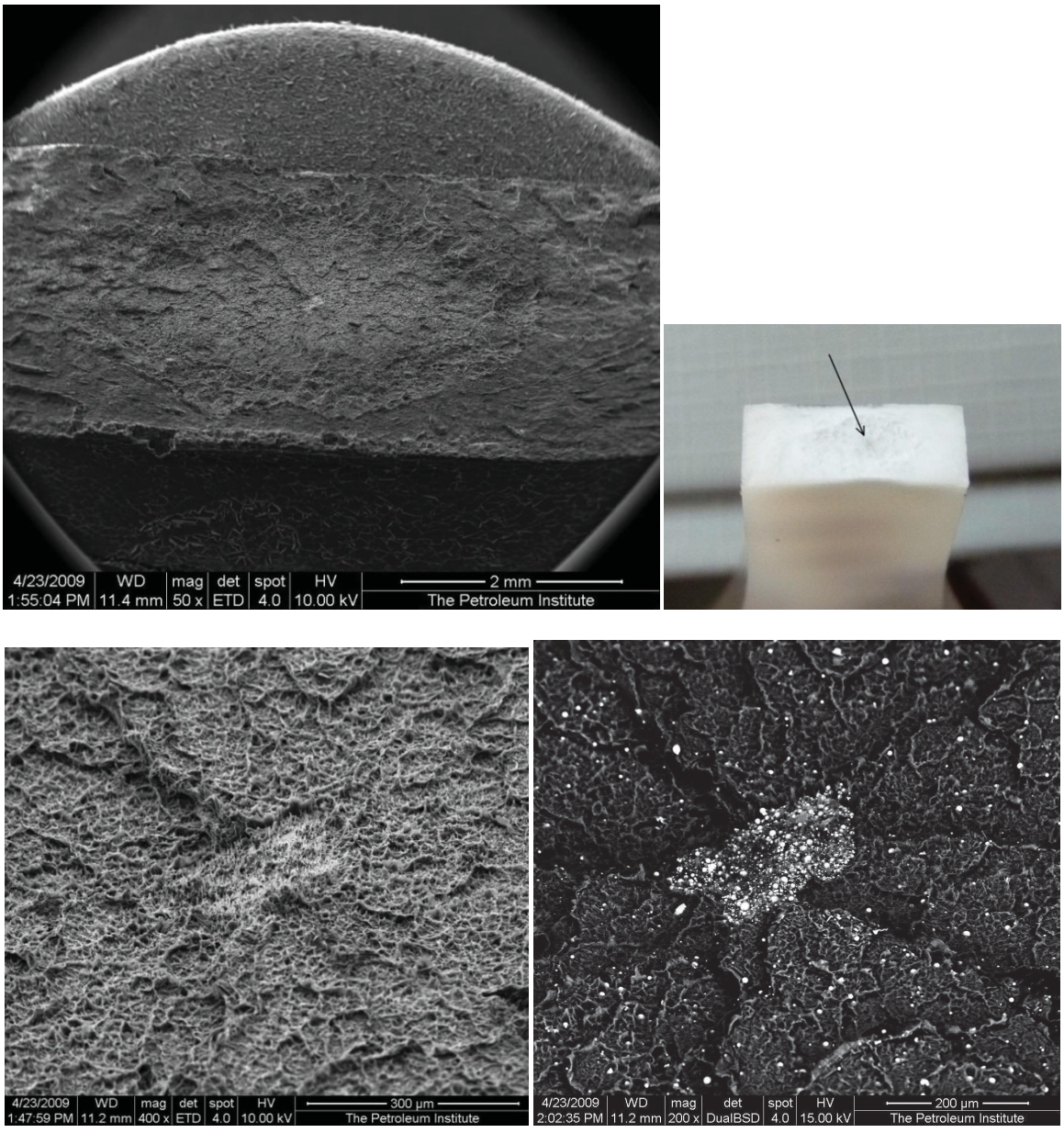

Figure 4.54: SEM (and top right photo) of break-surface of G1 at 3 Hz and outlying low lifetime; agglomeration in the centre of the fracture surface as possible reason for reduced lifetime.

These specimens with a decreased lifetime also did not show whitening (stress whitening) over the whole diameter, as the other specimen showed after fracture.

This seems to be a hint that the specimen broke at a weak point, at a little inhomogeneity, and a long time before it would break without this inhomogeneity.

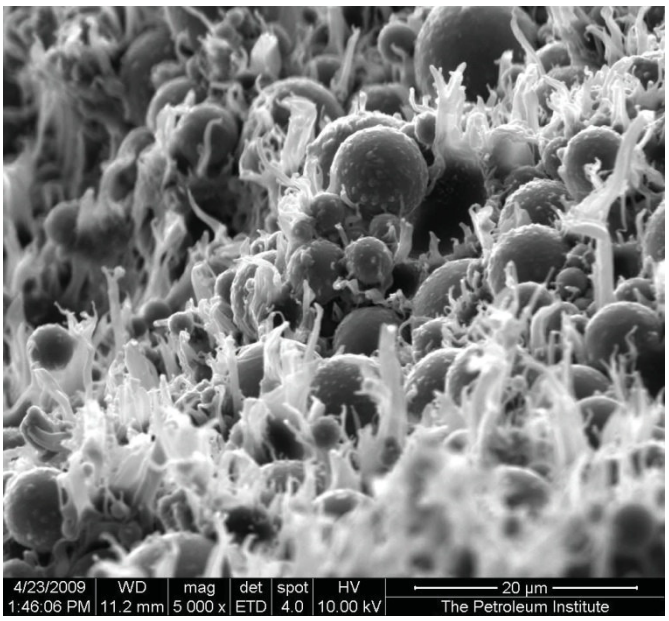

Figure 4.55: Zoom into the area of agglomeration in Figure 4.54.

4.3.2 Development of the damping and the generated heat

An increase in the damping with the load level is obvious in Figure 4.56 for material G2. This behaviour could also be found with the other materials. The fast increase of the damping until 2 * 10^2 cycles is caused by the slow attainment of the maximum stress, as seen in the development of the stress-strain hysteresis during the fatigue test (Figure 4.58). In the linear presentation, the difference in the development of the damping between the different stress levels is more obvious (Figure 4.57). The slope of the curves increases with the stress level. While the damping reaches a quasi constant level of damping between 0.07 and 0.08 at a stress level of σ_{max} = 17.5 MPa, the damping at a stress level of σ_{max} = 28.5 MPa starts at a value of around 0.14 after ~ 200 cycles and reaches a value of more than 0.21 before fracture. In the runs without ventilation, the damping increases faster. This correlates with the results that were found at the TestPP.

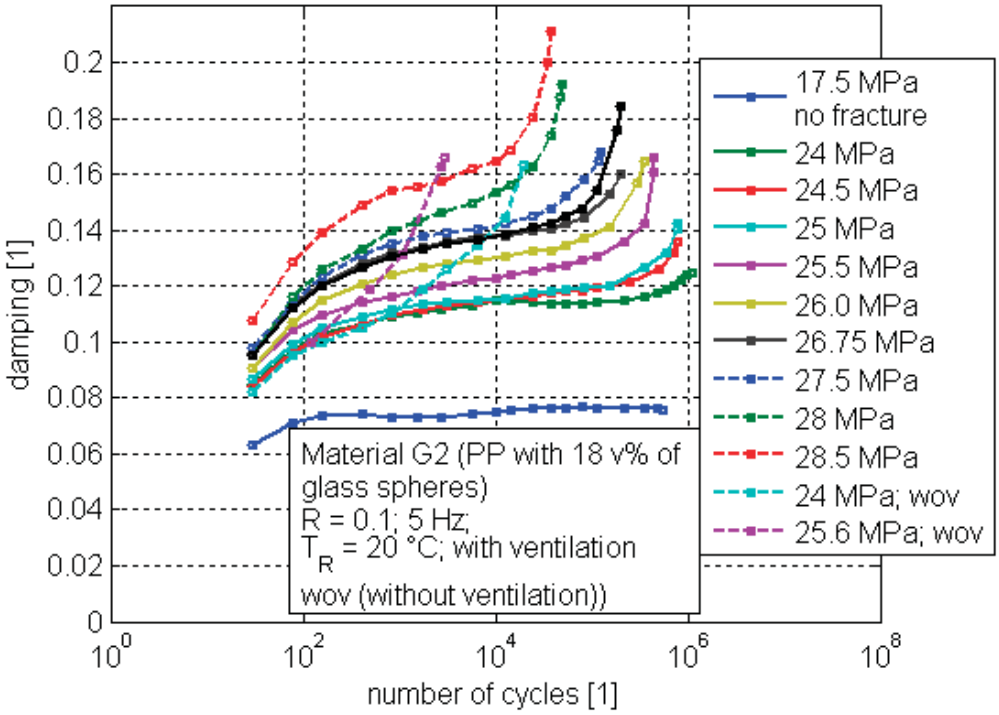

Figure 4.56: Damping over number of cycles for G2 (logarithmic exposition).

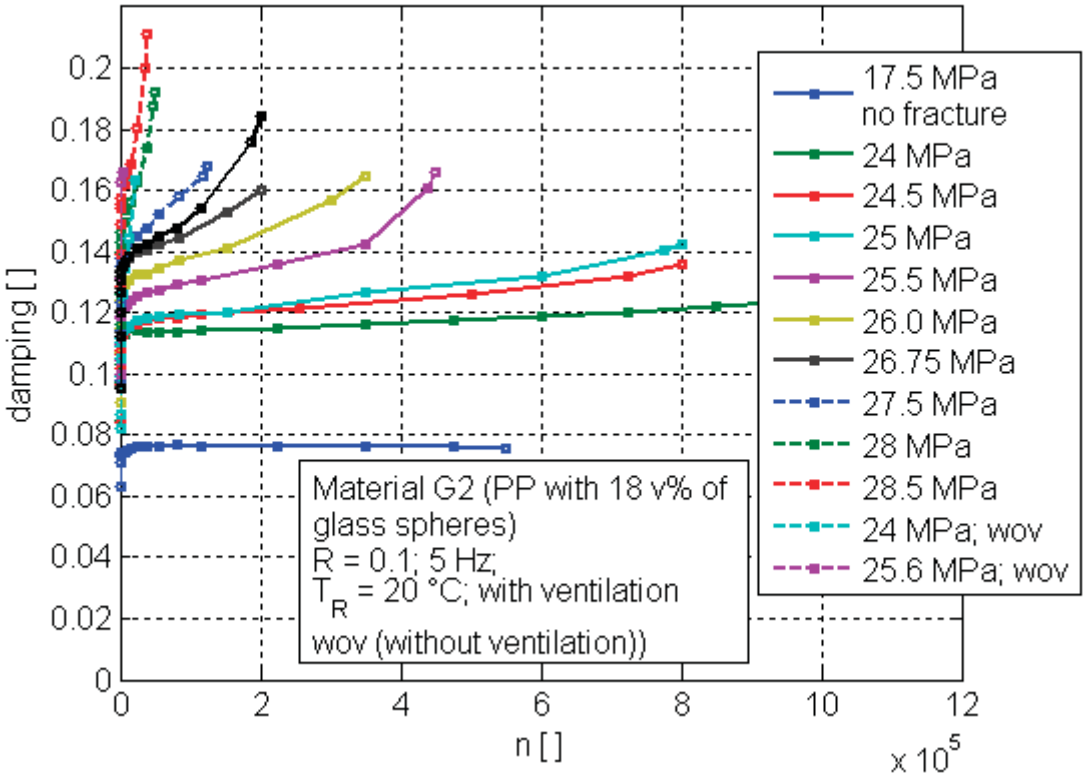

Figure 4.57: Damping over number of cycles for G2 (linear exposition).

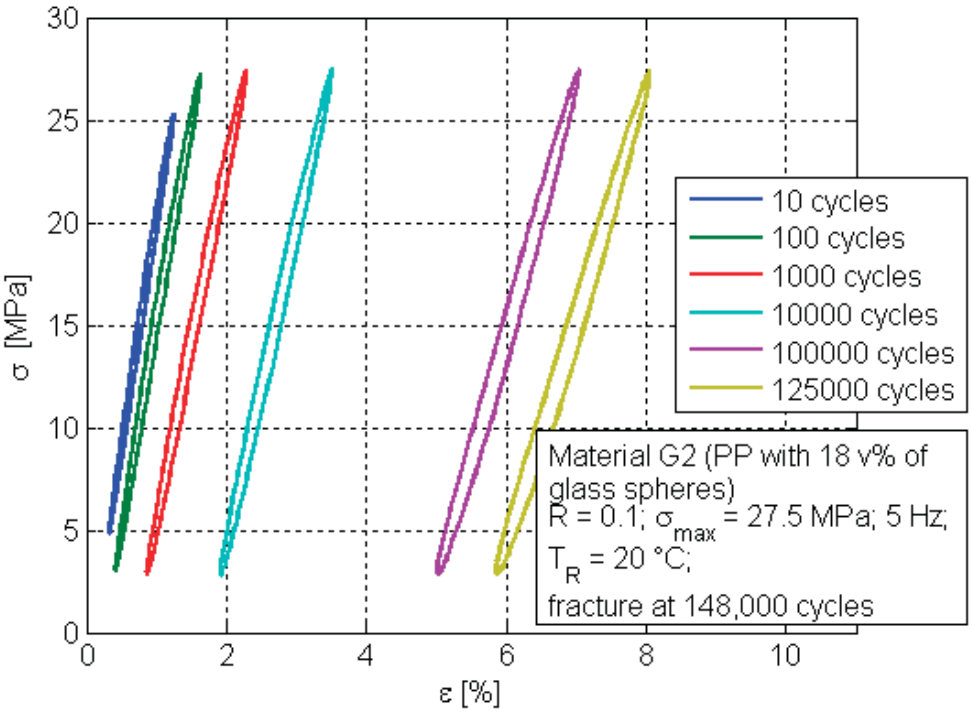

Figure 4.58: Development of the hysteresis at G2.

Figure 4.59 shows the development of the damping for the different materials at the same stress level of σ_{max} = 26.75 MPa. Among the filled materials, the stiffer materials show a higher damping rate. The pure PP lies in the region of the talc filled PP and above the PP filled with glass spheres. The damping increases among the filled materials with increasing stiffness of their composition. A different picture can be seen from a comparison of the heat generated during the fatigue tests (Figure 4.60). In this case the difference in the modulus plays an important role. As can be seen, the materials with the lowest modulus show the highest value of generated heat. The heat generated is represented by the area in the stress-strain hysteresis and if the modulus decreases, Δε increases in the stress controlled test and with the increase of Δε the area inside of the hysteresis also increases. The generated heat increases with an increasing cycle number in all cases.

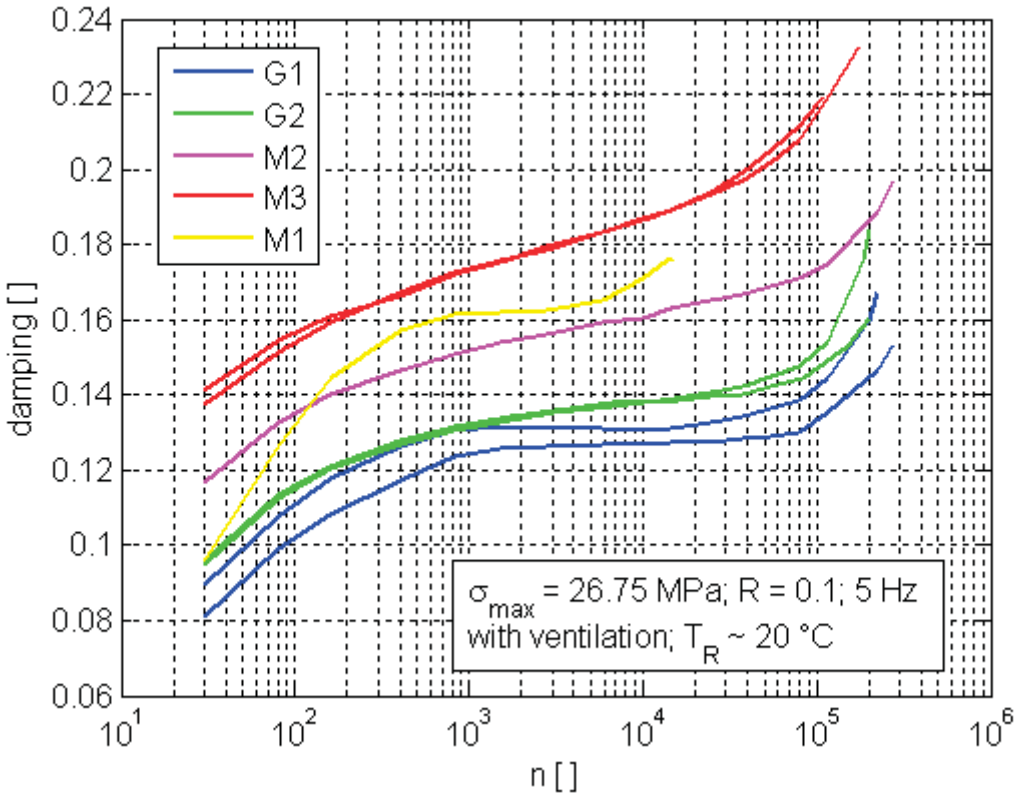

Figure 4.59: Development of the damping for different materials.

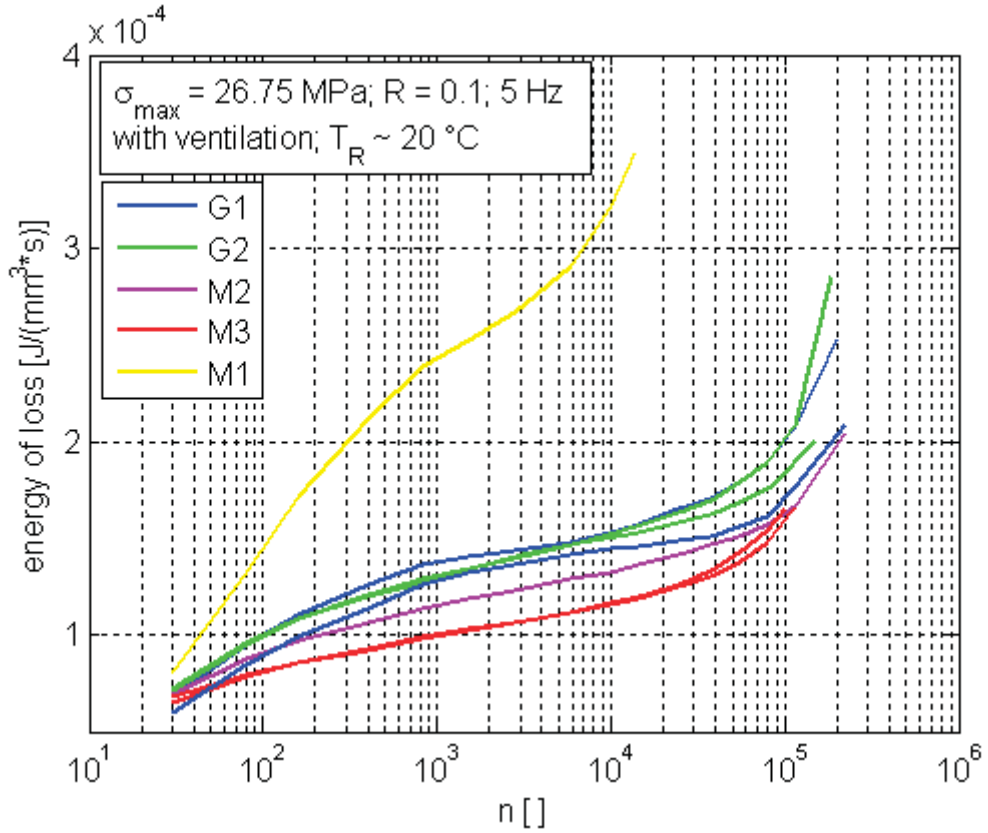

Figure 4.60: Development of the energy of loss for different materials.

4.3.3 Phase shift and deformed hysteresis

A change of the hysteresis form during the test was found during/after data evaluation of the tests. In particular, the bending of the Hysteresis seems to change with increasing fatigue with some materials (especially for the PP filled with strengthening particles). A short investigation was conducted on this topic to compare these changes and to get an idea of the regularities of this behaviour.

The hystereses are caused by a phase shift between stress and strain. The phase shift can be calculated by evaluating the mean stress $\sigma_{mean,}$ the mean strain ε_{mean}, and a comparison of the time of occurrence. With this calculation method there are differences between the rising edge and the falling edge. This difference seems to be dependent on the progress of the fatigue. In the case of the materials tested in this work, undamaged materials show a higher phase shift at the rising edge than at the falling edge. This seems to be caused by the falling modulus with rising load (non linear viscoelastic region). The other possible case is that the stiffness at the top of the hysteresis (at high stresses) is higher than at the bottom. This causes a flattening of the strain signal at high strain. A possible example for this case is shown schematically in Figure 4.61.

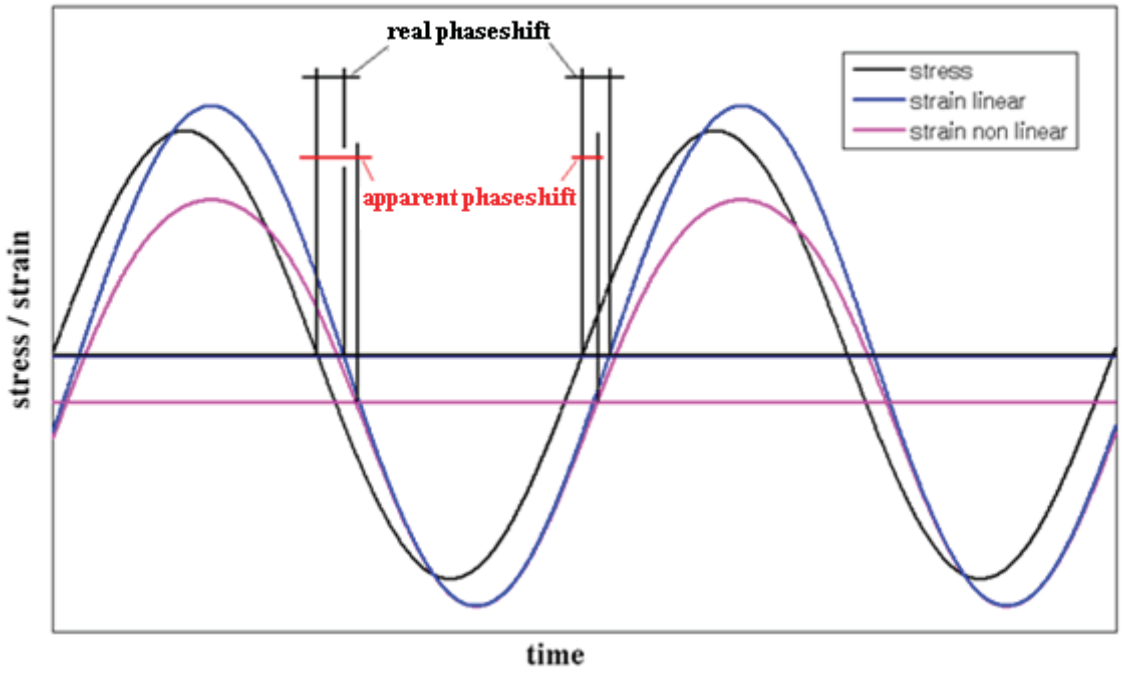

Figure 4.61: Apparent phase-shift caused by non linear elastic behaviour of the material during cyclic fatigue loading.

This behaviour seems to occur especially with damaged materials. If the phase shift is calculated at the medial strain, the flattening of the strain signal leads to a change of the phase shift. This “apparent phase shift” is different for the falling and the rising edge. This difference in the phase shift can also be seen at the hysteresis. The hystereses show a bending to a lower modulus in the upper load regions at the beginning of the test. With an increasing cycle number the bending reaches a neutral state, and after that the hysteresis starts to bend in the other direction (compare Figure 4.62).

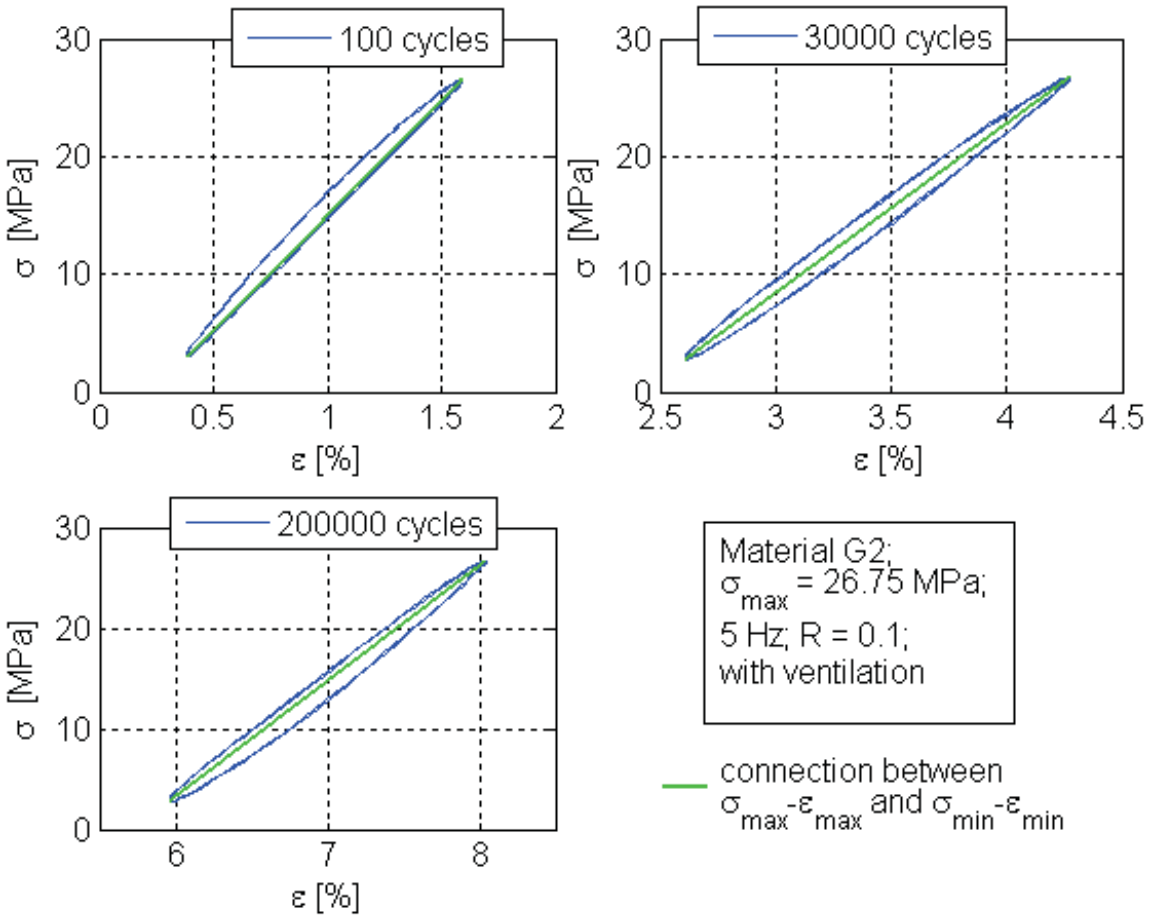

Figure 4.62: Development of the hysteresis shape during the fatigue test.

In Figure 4.62 the form of the hysteresis after different numbers of cycles can be seen. The green line is the direct connection between the points σ_{max}-ε_{max} and σ_{min}-ε_{min} and is drawn to enable better visibility of the bending of the hysteresis. While the slope of the hysteresis decreases at the top of the hysteresis (high stress) for low cycle numbers, which means a decrease of the modulus, the slope is higher at the top of the hysteresis compared to the bottom at higher cycle

numbers (after fatigue damage). The definition of falling edge and rising edge can be seen in Figure 4.63. Figure 4.64 shows the development of the phase shift between σ and ε.

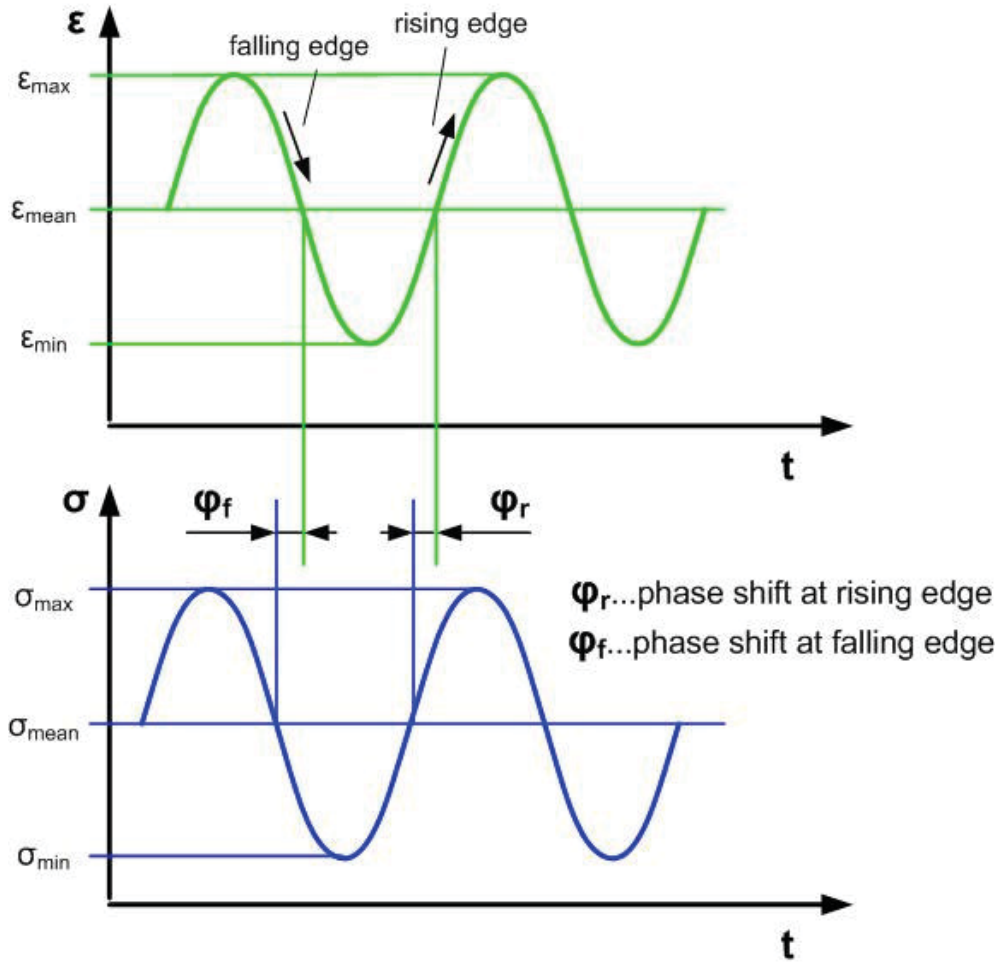

Figure 4.63: Definition of the phase shift between σ and ε at falling and rising edge.

The development of the phase shift at falling and rising edge for material G2 (19 w% of glass spheres) at a stress level of σ_{max} = 26.75 MPa can be seen in Figure 4.64. During the first 200 cycles (this time is need to reach the final stress level), both, φ_r and φ_f, are rising. After that the phase shift at the rising edge φ_r starts to decrease while the phase shift at the falling edge φ_f continues to increase. φ_{mean}. The medial between φ_r and φ_f, shows an increase during the whole fatigue test.

Another way to evaluate the form of the hysteresis is described in (Raue and Ehrenstein, 1999). There the modulus at the top of the hysteresis is compared with the modulus at the bottom. Raue and Ehrenstein (1999) do not describe the calculation method used to get the two moduli (at the top and at the bottom of the

hysteresis). An original way/method to calculate the two moduli is chosen in this work.

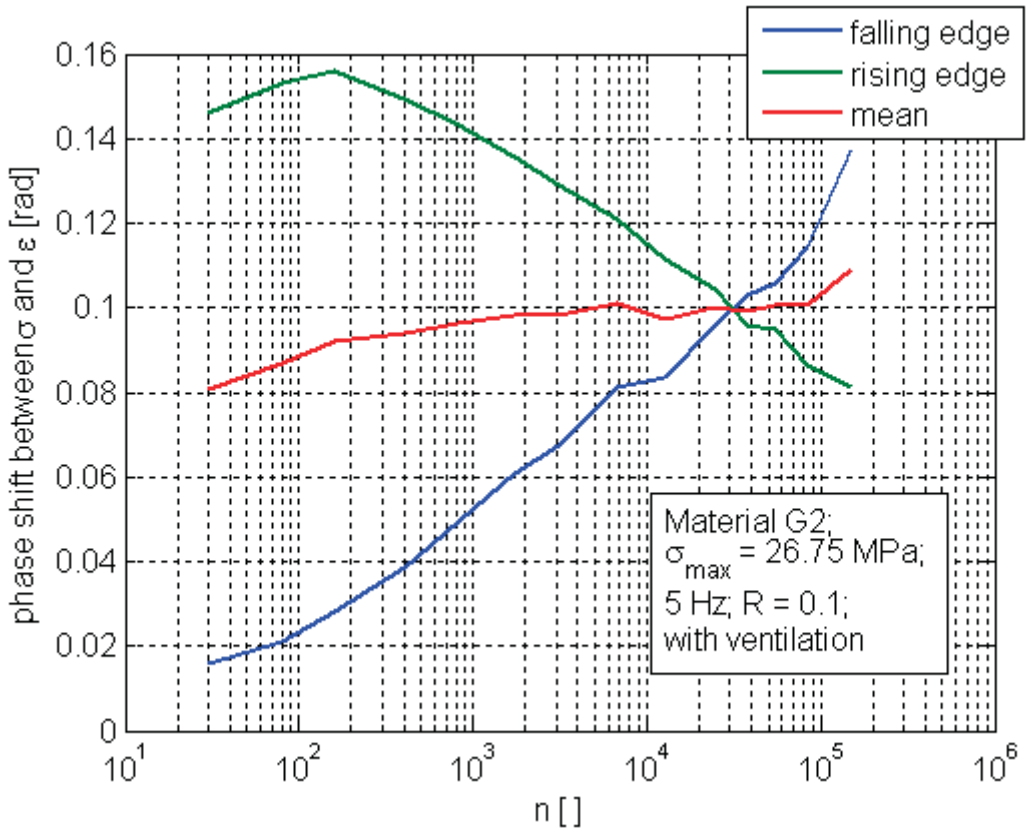

Figure 4.64: Development of the phase-shift between σ and ε at the rising and the falling edge.

The principle of calculation of the modulus is shown in Figure 4.65. For the calculation of the modulus at the bottom E_{bott} two data points of the hysteresis, one before and one after the point σ_{max}-ε_{max}, with the same distance from σ_{max}-ε_{max}, are connected with the point σ_{min}-ε_{min}. The slope of the line that is at the half angle between these two lines is defined as the modulus at bottom E_{bott} of the hysteresis (Figure 4.65). The same procedure at the top of the hysteresis leads to the modulus at the top E_{top} of the hysteresis. The graphic shows that the result of the evaluation of the modulus depends on the distance between the data points that are taken for the calculation. To get an idea regarding this influence, the difference of two different calculation distances is plotted in Figure 4.66.

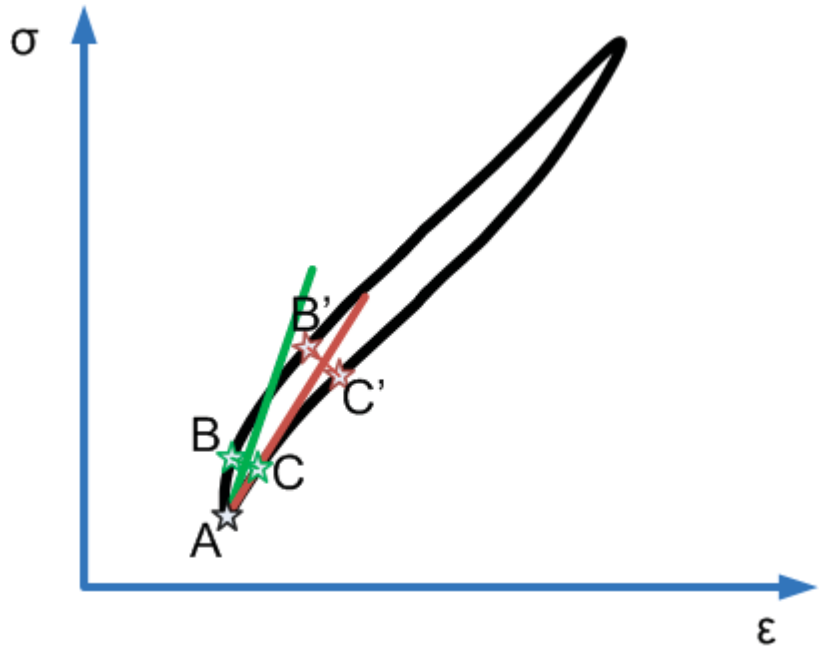

Figure 4.65: Calculation of the modulus at the bottom of the hysteresis; the result can vary depending on the distance of point B and C from A (calculation distance).

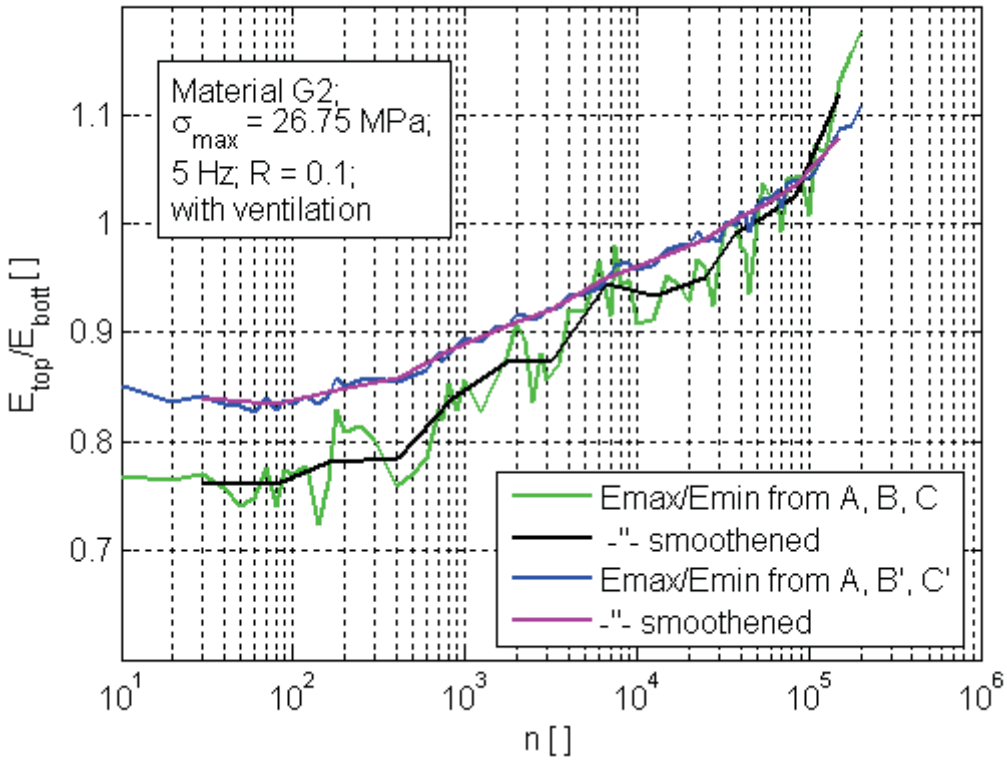

Figure 4.66: Development of the ratio E_{top}/E_{bott} during the fatigue test and dependence on the calculation.

The noise at the curves in Figure 4.66 is caused by fluctuations caused by the measuring tolerance (compare Figure 4.67). This noise decreases with an

increasing calculation distance. A disadvantage of a higher calculation distance is that the calculated modulus differs more and more from the real, local modulus at the bottom and at the top of the hysteresis. It is important for the comparison that all the compared curves result from the same calculation distance.

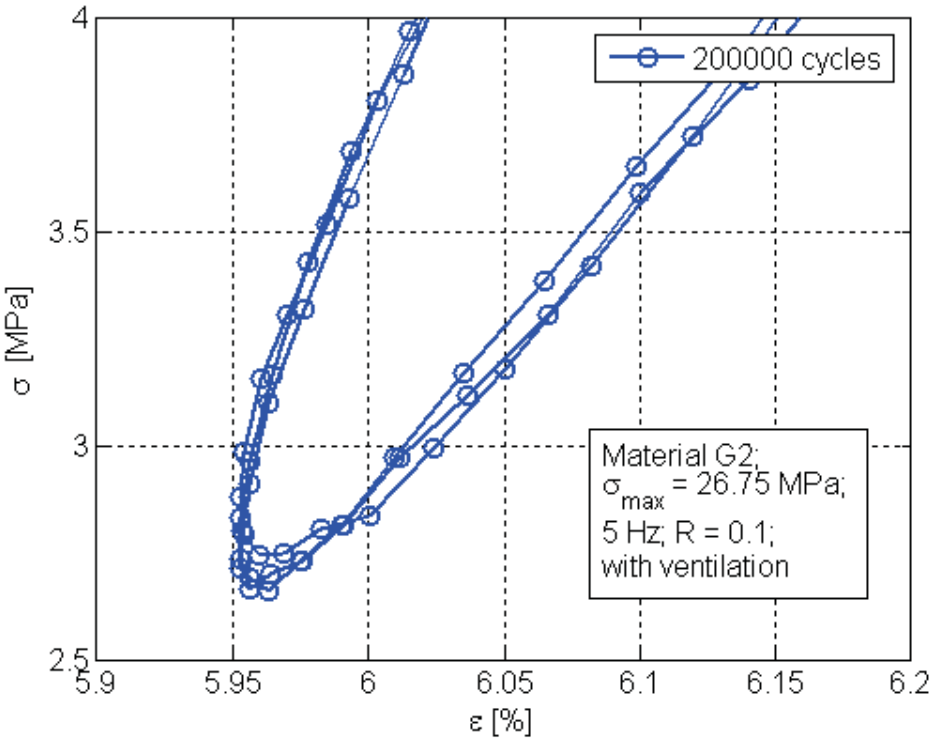

Figure 4.67: Zoom in on three following hystereses to see the fluctuations of the data points.

Figure 4.68 shows the development of the modulus at the top of the hystereses and at the bottom of the hystereses during the test on material G2 at a stress level of σ_{max} = 26.75 MPa. Both the modulus at the top and the modulus at the bottom of the hystereses decrease. At the start of the test the modulus at the top of the hystereses is lower than the modulus at the bottom. This means that the ratio E_{top}/E_{bott} is smaller than 1. During the testing the difference between these two moduli decreases, and at the end, the situation is inversed. The slower decrease of the modulus at the top of the hysteresis could be due to the existence of crazes. These crazes carry more when they are stretched, which means when the strain is in the upper regions (at the top of the hystereses). Thus they can cause a higher stiffness at higher strain.

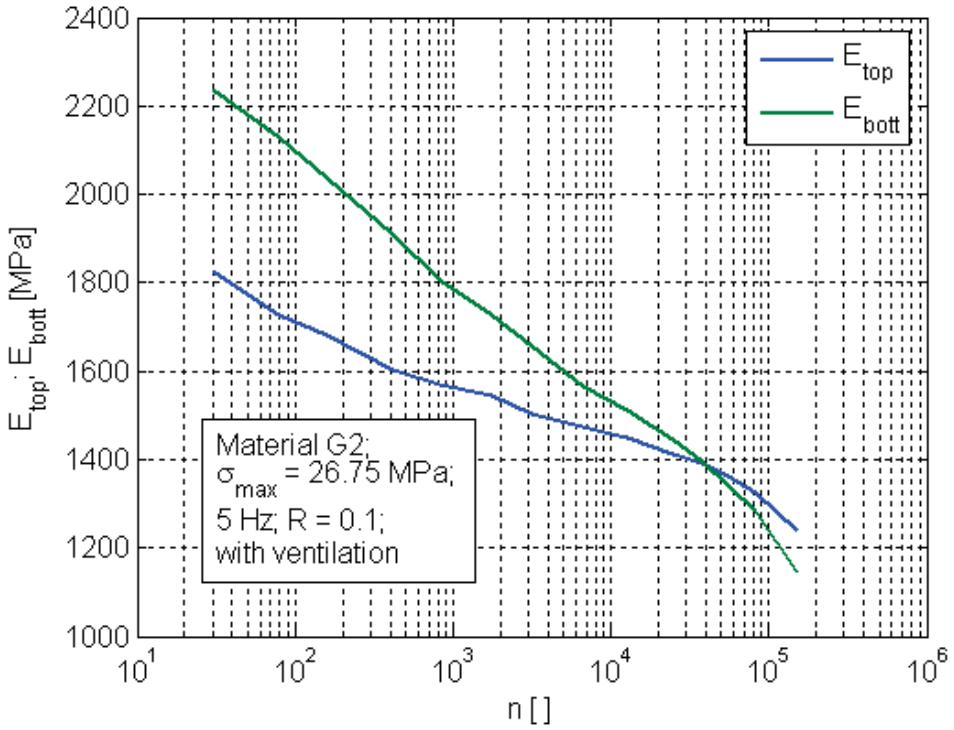

Figure 4.68: Development of Etop and Ebott during the fatigue test.

In Figure 4.69 the development of E_{top}/E_{bott} is plotted for different materials at the same stress level of σ_{max} = 26.75 MPa (exception: ER2 at σ_{max} = 21.25 MPa). The materials M1 (pure PP) and ER2 (PP filled with 7 w% of TPO) did not reach an equality of E_{top} and E_{bott}. This means that the shape of the hysteresis does not change in the same way or at least not to the same degree as with the reinforced materials. If the assumption is right, that the relative increase of the modulus at the top of the hysteresis (relative to the modulus at the bottom of the hysteresis) is caused by the crazes that are stretched at the bottom of the hysteresis and not stretched at the bottom of the hysteresis, the nearly constant E_{top}/E_{bott} at M1 and ER2 would mean that the materials either do not or hardly get damaged during the fatigue test by crazing. The different fracture modes at M1 and ER2 (ductile fracture) may also hint at this assumption.

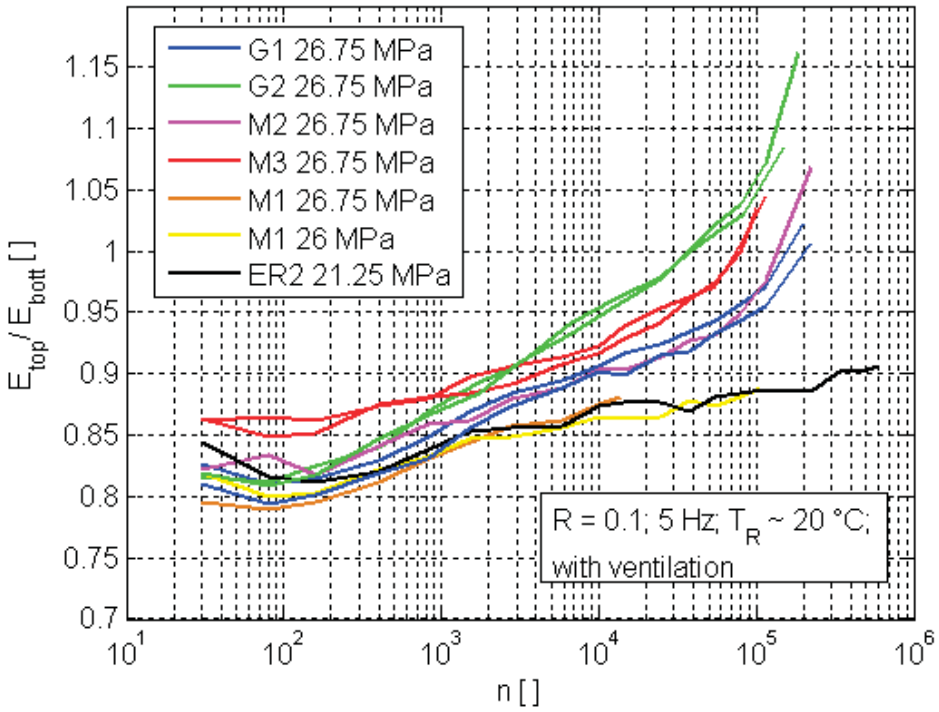

Figure 4.69: Development of E_{top}/E_{bott} for different materials during a fatigue test.

4.3.3.1 Correlation between the fracture cycle and the crossing cycle

A certain parameter for the hysteresis form is needed to get an idea about the correlation between the development of the hysteresis form and the material damage. This value could be the ratio between E_{top} and E_{bott}. In Figure 4.70 the cycle number at which the ratio E_{top}/E_{bott} is 1 ($E_{top} = E_{bott}$) n_{cr}, is plotted over the cycle number at fracture n. n and n_{cr} seems to show a certain correlation. A correlation was also found with material G1 (9 w% of glass spheres) between the fracture cycle N and the crossing cycle n_{cr}. Figure 4.71 shows the crossing cycle number and the fracture cycle number at different frequencies. A correlation can already be seen in this figure. A higher n means also a higher n_{cr}. An exception seems to be the tests at frequency 3 Hz. There the agglomerations that were found on some fracture surfaces seem to be an explanation. The three runs at 3 Hz show all a similar crossing cycle number whereas the fracture cycle numbers do not correlate. As already shown, the specimen that showed a fracture after around 150,000 cycles showed filler agglomerations on the fracture surface. These agglomerations seem to decrease the lifetime but do not influence the crossing

cycle number because they are a local phenomenon and the crossing cycle number is a result of strain data that is measured by an extensometer with a gauge length of 25 mm.

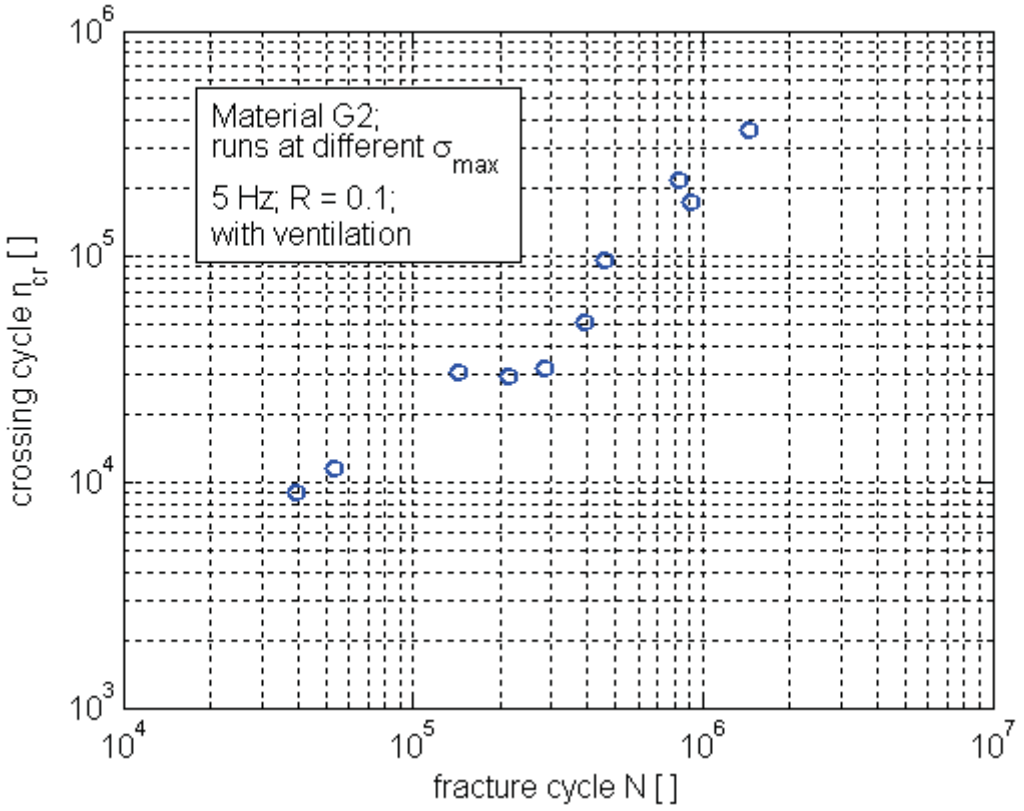

Figure 4.70: Cycle number at E_{top} = E_{bott} over cycle number at fracture.

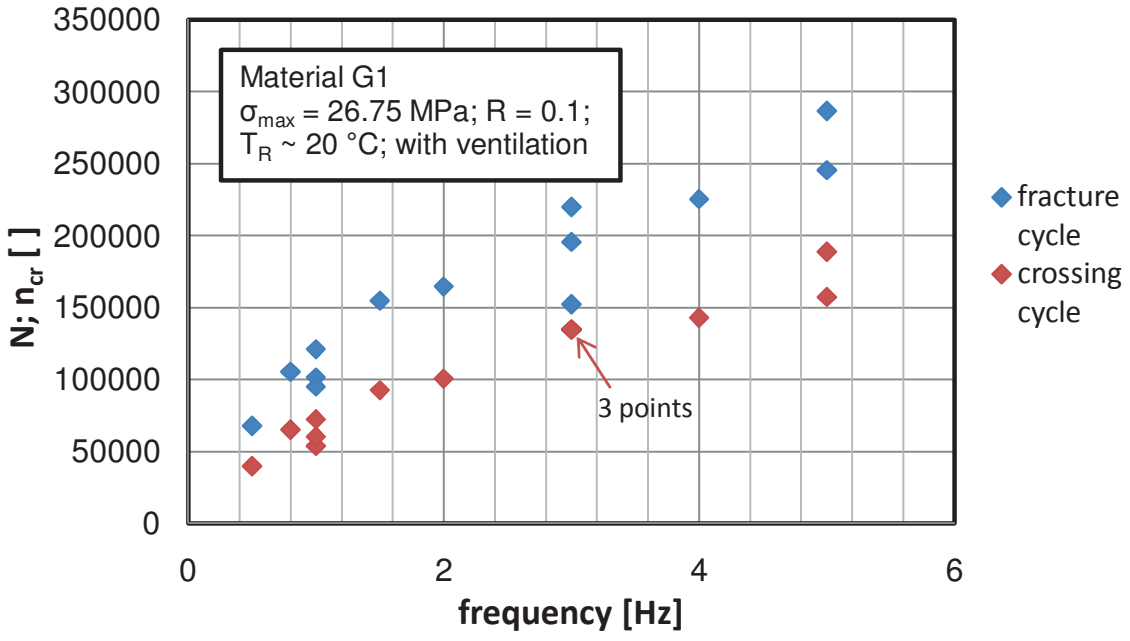

Figure 4.71: Crossing cycle n_{cr} and fracture cycle N at different frequencies.

Figure 4.72 shows the relation between the fracture cycle N and the crossing cycle n_{cr} at G1 (9 w% of glass spheres) at different frequencies and G2 (18 w% of glass spheres) at different stress levels. The correlation between the crossing cycle and the fracture cycle is clear in both cases.

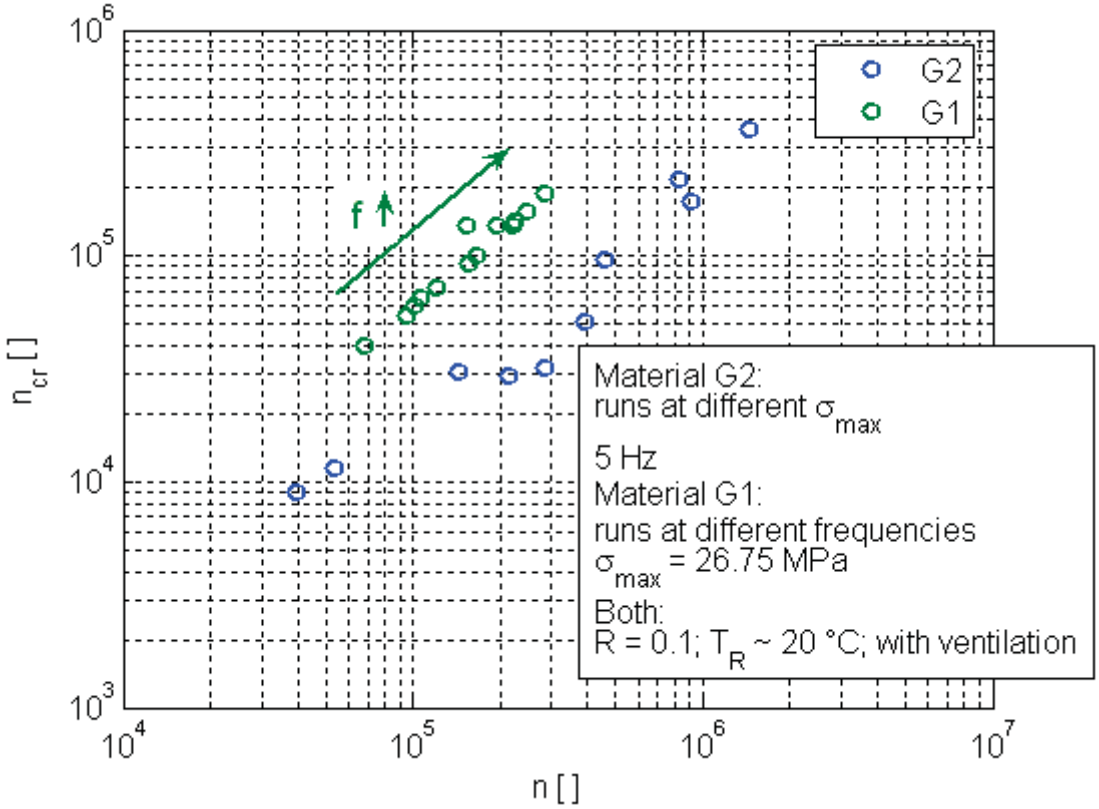

Figure 4.72: Crossing cycle n_{cr} over fracture cycle n for materials G1 (different frequencies) and G2 (different stress levels).

This relation shows that there might be a possibility to predict the fracture cycle by observing the development of the hysteresis form.

4.3.4 Fracture surface analysis by SEM

4.3.4.1 Fracture surface at material G2

The fracture surface of G2 (fracture after high cycle fatigue load, with a test frequency of 5 Hz, R = 0.1 and under ventilated conditions) shows different types of failure characteristics (Figure 4.73):

1. A crazed microstructure with a fine fibrillation is visible in the centre (Figure 4.74). This crazing in the centre might already start at low cycle numbers and might also be responsible for the stress whitening that can be seen

during the fatigue test. This stress whitening starts from the centre of the specimen and grows during the fatigue run.

2. This region is surrounded by a region of a craze microstructure with a course fibrillation (Figure 4.75). This course fibrillation seems to start a short time before fracture, due to the increased local stress and the increased temperature.

3. The borders of the fracture surface show a quasi-brittle rest break (Figure 4.76) that occurs at the areas of the specimen that are lying on the borders and are under a state of plane stress.

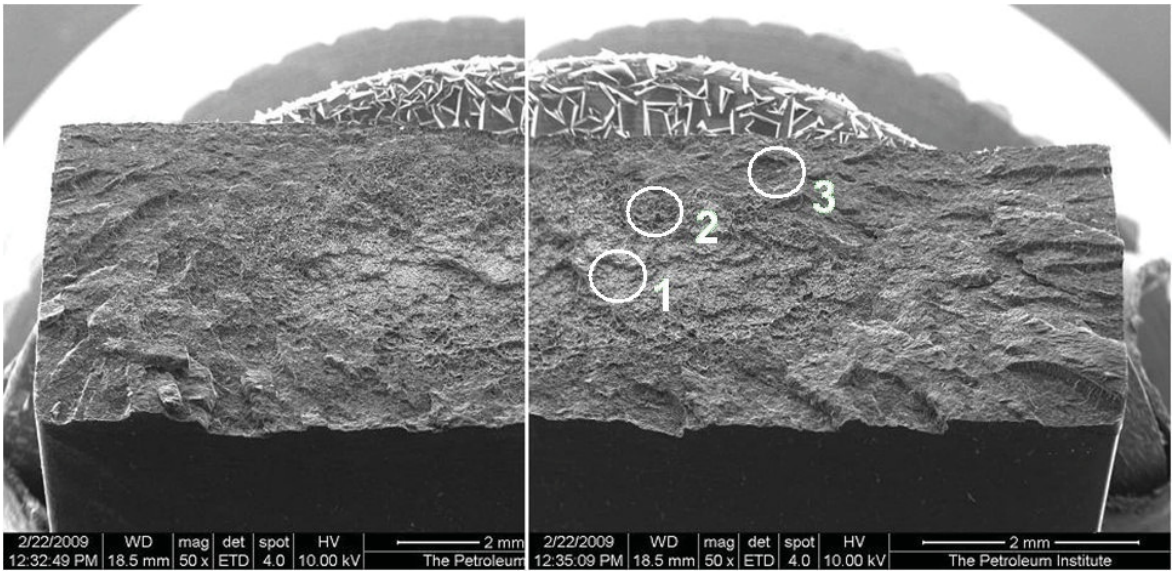

Figure 4.73: Fracture surface of G2, load 26.75 MPa; R = 0.1; 5 Hz; with ventilation; Three regions with different fracture characteristics; compare Figure 4.74 (region 1), Figure 4.75 (region 2) and Figure 4.76 (region 3).

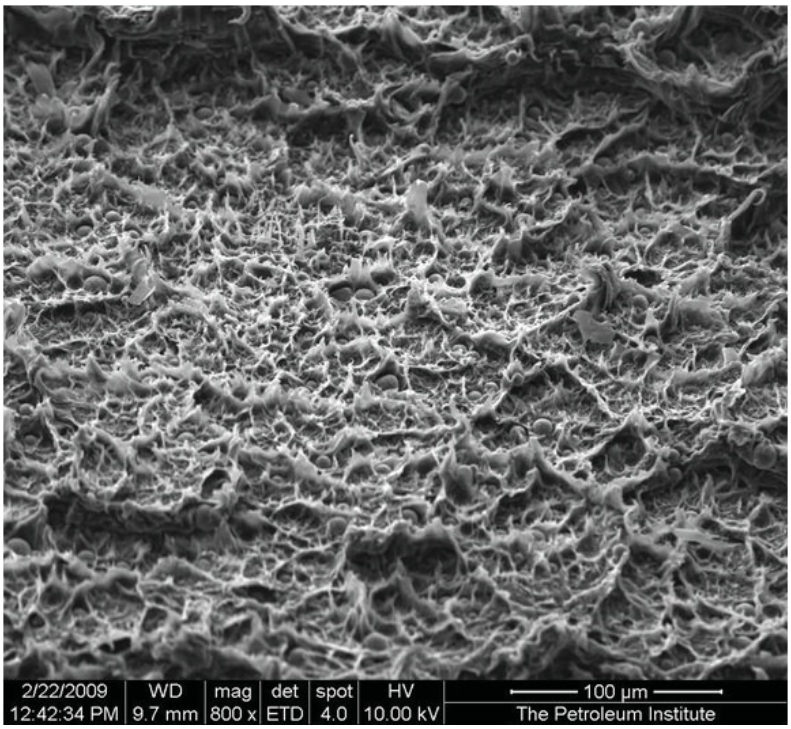

Figure 4.74: Zoom in of region 1 of Figure 4.73; Craze microstructure with a fine fibrillation in the centre of the fracture-surface.

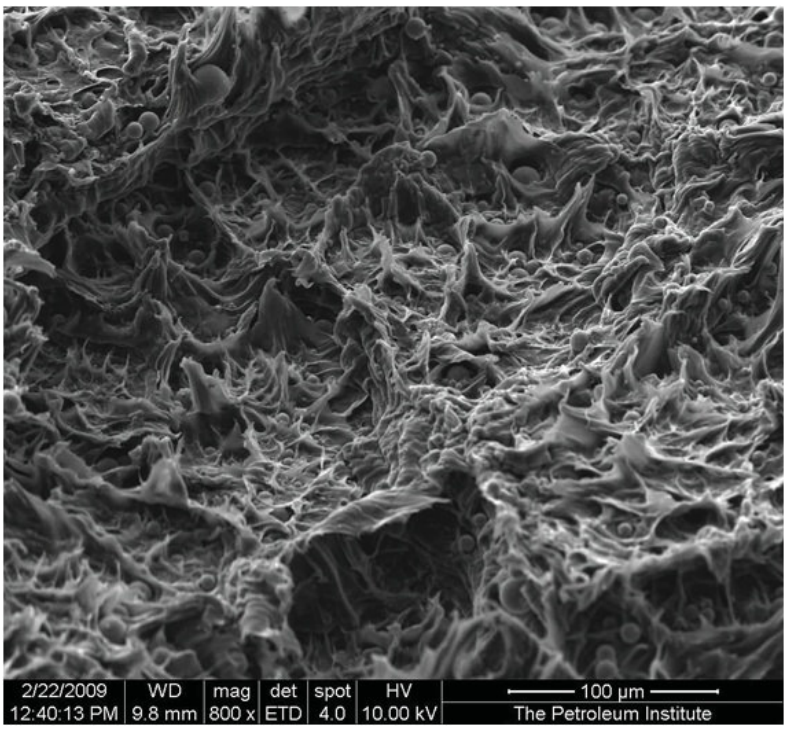

Figure 4.75: Zoom in of region 2 of Figure 4.73; Craze microstructure with a course fibrillation around the region with the fine fibrillation.

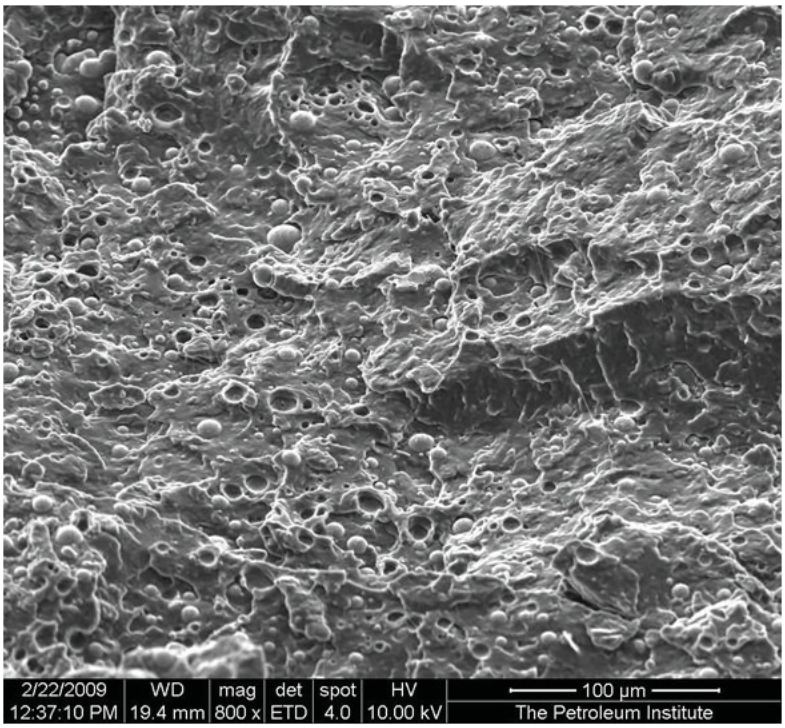

Figure 4.76: Zoom in of region 3 of Figure 4.73; Quasi brittle final fracture at the borders of the fracture surface.

To evaluate, if most of the crazes appear a short time before the final fracture or already earlier during the test, the specimen of G2 that was tested at 24.5 MPa and broke after 925,400 cycles was broken by sudden pull at another spot of the specimen. An SEM (Figure 4.77) shows some areas of craze on this new fracture surface. In Figure 4.77 and Figure 4.78 a relatively large particle of filler that seems to be the initiation of the craze is shown. The start seems to be an adhesive break between the polymer and the filler particle. This might cause a stress peak in the matrix around the particle and seems to cause the start of the craze. Figure 4.79 shows some craze areas with the sudden brittle rest break between them. All the crazes seem to start around a filler particle.

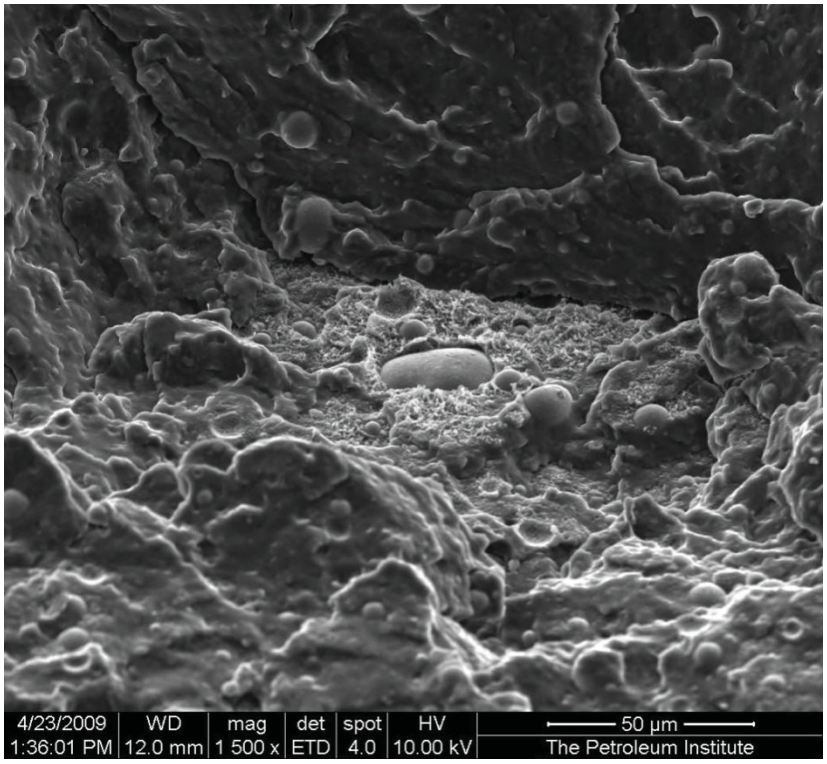

Figure 4.77: SEM of G2 at fracture by sudden pull after 925,400 cycles at 24.5 MPa; Craze started at a relatively large filler-particle and surrounding sudden brittle break.

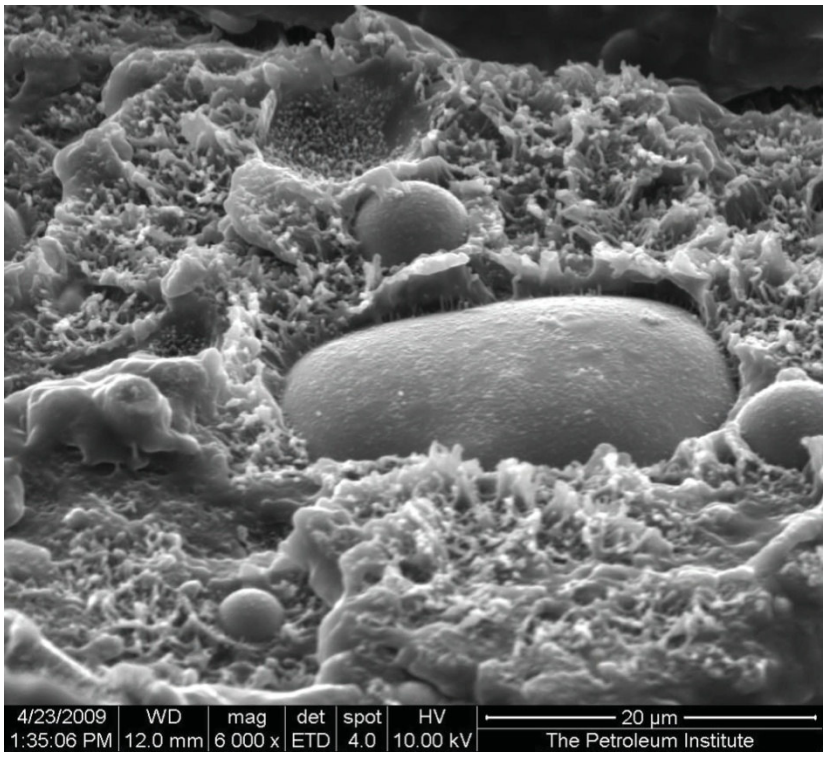

Figure 4.78: SEM of G2 at fracture by sudden pull after 925,400 cycles at 24.5 MPa; Craze started at a relatively large filler particle.

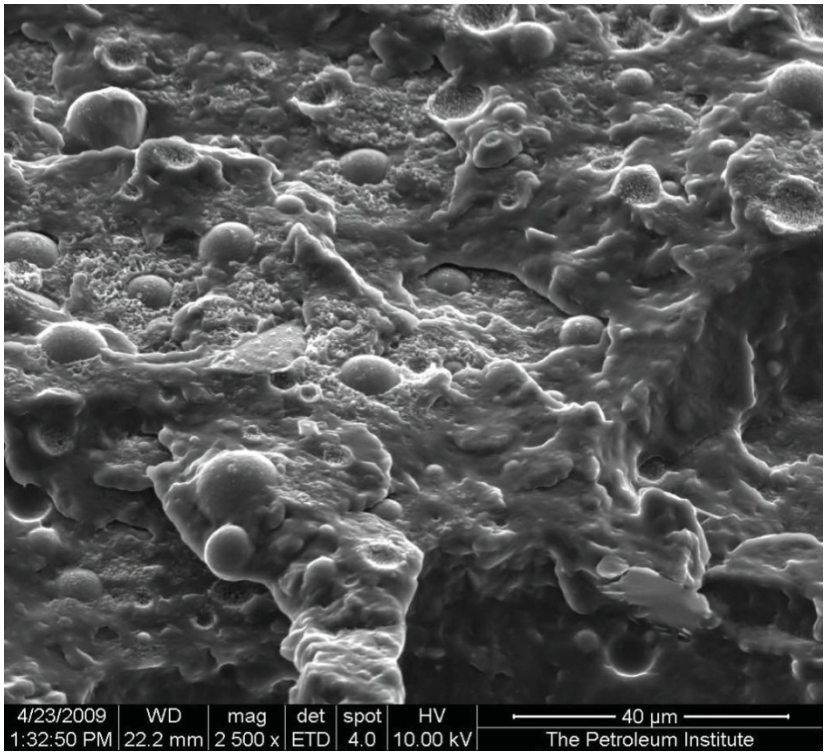

Figure 4.79: SEM of G2 at fracture by sudden pull after 925,400 cycles; Crazes and sudden brittle fracture between the crazes.

5 SUMMARY AND CONCLUSIONS

The fatigue behaviour of pure PP and PP with different fillers was investigated by S-N diagrams, hysteresis measurement and isocyclic stress-strain diagrams in this work. The materials were provided and moulded by Borealis. Two materials were PP filled with glass spheres (9 and 18 w%), two materials were filled with talc (10 and 20 w%) and one was filled with 7 w% of TPO. To evaluate the best testing conditions, tests were run with a PP filled with 30 w% of glass spheres. During these pre-tests the problem of hysteretic heating occurred and had a big influence on the test results. Some possibilities for avoiding the influence of hysteretic heating were tested. The reduction of the R-value ($\sigma_{min}/\sigma_{max}$) turned out to significantly reduce the hysteretic heating but increased the creep during the tests. The problem is a change in the fatigue behaviour due to an increase of R and an increase in the creep. Another possibility to decrease the hysteretic heating is a decrease of the test frequency. In our case of aspired cycle numbers of up to 10^6 cycles, a decrease in the frequency would mean a non-tolerable increase of test time. It turned out that cooling by ventilation was the best way to keep the specimen temperature within a certain limit.

The tests on the Borealis materials showed two different types of behaviour. While the pure PP and the material filled with TPO showed a ductile fracture with necking, the materials that were filled with reinforcing particles (glass spheres and talc) showed a brittle fracture. These two groups of different fracture types cannot be compared.

Among the reinforced PP types, no great influence could be found concerning the fatigue behaviour in the S-N curves. In the case of glass spheres, no big difference in the fatigue behaviour was expected, due to the results from the tensile tests. Therefore only two reference runs were performed for the PP with 9 w% of glass spheres. These two runs showed no significant difference with the results of the runs with the PP filled with 18 w% of glass spheres. A comparison between the two PP types filled with talc showed a slightly better performance of the PP with the lower talc content (10 w%). Significant differences could be found in the isocyclic stress strain diagrams and by hysteresis measurement. The stiffness of M3 (filled with 20 w% of talc) was higher compared to M2 (filled with 10 w% of talc)

during the whole range of the test. The relative decrease of the modulus was quite similar.

Regarding talc and glass spheres used as filler, no significant difference in lifetime could be found in the case of 9 w% of glass spheres compared with 10 w% of talc (3.5 v% of filler in both cases). In the isocyclic stress-strain diagrams the difference in the modulus was found/detected during the whole range of testing. The dynamic modulus of both materials decreased during the runs with increasing fatigue damage. The relative decrease shows slight differences between the differently strengthened materials.

To evaluate the influence of the frequency on the lifetime of the specimen, a series of runs were made at different frequencies between 0.5 and 5 Hz with the PP filled with 9 w% of glass spheres. In this range of frequencies it turned out that the lifetime in numbers of cycles increases with increasing frequency while the lifetime in hours decreases.

Voids were found on the fracture surface on some specimens. In the PP filled with 20 w% of talc, cavities in the centre of the specimen were found on the fracture surface of some specimens. These cavities decreased the lifetime significantly. In the PP filled with 9 w% of glass spheres, agglomerations of the filler particles caused a significant lower lifetime in some specimens. Thus inhomogeneities seem to be a factor that can negatively influence the fatigue behaviour.

During the fatigue, the shape of the hysteresis seems to change. This change seems to be dependent on the filler. While the strengthened materials showed a strong change in the shape, the unfilled PP and the PP with TPO barely changed the shape of the hysteresis during the fatigue run. This might be an indication of a different fracture behaviour concerning the affinity to crazing.

6 LITERATURE

Bolotin V.V. (1999), Mechanics of Fatigue, CRC Press

Kultural S.E., Eryurek I.B. (2005), Fatigue behaviour of calcium carbonate filled polypropylene under high frequency loading

Moore D.R. (2004), The Application of Fracture Mechanics to Polymers, Elsevier

Mai Y.W. (1981), Journal of applied Polymer Science, Vol 26 PP 3947 – 53, Cyclic Fatigue and Thermal Softening of Polypropylene

Moet A., Aglan H. (2005), Fatigue Failure Mechanism, Characterization and Failure Analysis of Plastics, ASM International, The Materials Information Society PP 249-258

Naranjo A.C., Noriega M.E., Osswald T.A., Roldan-Alzate A., Sierra J.D. (2008), Plastics Testing and Characterisation, Carl Hanser Verlag Munich

Osswald T.A., Menges G. (2003), Materials Science of Polymers for Engineers, 2nd Edition, Hanser

Pinter G., Ladstaetter E., Billinger W., Lang R.W. (2006), Characterisation of the tensile fatigue behaviour of RTM-laminates by isocyclic stress-strain-diagrams

Raue F., Ehrenstein G.W. (1999), Macromolecular Symposia ISSN 1022-1999 PP 229-240, Characterization of the Dynamic Properties of Binary Polypropylene Blends via the Hysteresis Measuerement Method

Raue F., Ehrenstein G.W. (1998), The static and dynamic behaviour of PP/EPDM- and PP/POE- and PP/POE-blends using the hysteresis measurement method; ANTEC

Roesler J., Harders H., Baeker M. (2007), Mechanical Behaviour of Engineering Materials (Springer Berlin Heidelberg New York), Page 364

Ren W. (2001), Creep behaviour of a continuous strand, swirl mat reinforced polymeric composite in simulated automotive environments for durability investigations, Material Science and Engineering A334 (2002) 312-219

Sapuan S.M., Maleque M.A., Hameedullah M., Suddin M.N., Ismail N. (2002), A note on the comceptual design of polymeric compsite automotive bumper system, Journal of Materials Processing Technology 159 (2005) 145-151

Schulte K. (1993), Damage monitoring in polymer matrix structures; JOURNAL DE PHYSIQUE, Volume 3, Nov. 1993

Talib A.R.A., Ali A., Goudah G., Lah N.A.C., Golestaheh A.F. (2009), Developing a composite based elliptic spring for automotive applications, Materials and Design 31 (2010) 475-484

Wypych G. (1999), Handbook of Fillers, ChemTec Publishing

Zahnt B.A. (2003), Fatigue Behaviour of discontinuous glassfiber reinforced Plastics, Montanistic University of Leoben, Austria

Zhou Y., Mallick P.K. (2005), Fatigue Performance of an Injection Molded Talc-Filled Polypropylene; Center of Lightweighting Automotive Materials and Processing, University of Michigan-Dearborn